

**Tattoo Pigments: Biodistribution and Toxicity of
Corresponding Laser Induced Decomposition Products**

**Inaugural-Dissertation
to obtain the academic degree
Doctor rerum naturalium (Dr. rer. nat.)**

**submitted to the Department of Biology, Chemistry and Pharmacy
of Freie Universität Berlin**

**by
Ines Schreiver
from Rostock**

2017

This thesis was carried out at the Federal Institute for Risk Assessment (BfR) in Berlin from June 2013 to June 2017 under the supervision of Prof. Dr. Dr. Andreas Luch.

1st Reviewer: Prof. Dr. Dr. Andreas Luch

2nd Reviewer: Prof. Dr. Günther Weindl

Date of defense: **21.02.2018**

Erklärung

Hiermit versichere ich, dass ich die vorliegende Dissertation mit dem Tittel "Tattoo Pigments: Biodistribution and Toxicity of Corresponding Laser Induced Decomposition Products" ohne Benutzung anderer als der zugelassenen Hilfsmittel selbstständig angefertigt zu haben. Alle angeführten Zitate sind als solche kenntlich gemacht. Die vorliegende Arbeit wurde in keinem früheren Promotionsverfahren angenommen oder als ungenügend beurteilt.

Berlin, den 16.10.2017

Ines Schreiber

Die Dissertation wurde in englischer Sprache verfasst.

Danksagung

Ich möchte mich auf diesem Wege bei Prof. Dr. Dr. Luch für die Möglichkeit, meine Doktorarbeit am BfR auf dem Thema Tätowiermittel in seiner Abteilung durchzuführen, bedanken. Herr Luch hat mich stets unterstützt innerhalb und außerhalb des Institutes Kooperationen zu initiieren, mir genügend Freiraum gegeben neue Projekte durchzuführen, mich weiterzuentwickeln, zu lernen, und so im Laufe meiner Doktorarbeit als Wissenschaftlerin zu wachsen.

Herrn Prof. Dr. Weindl danke ich für die Übernahme des Zweitgutachtens meiner Dissertation und seiner Unterstützung weiterer Projekte.

Einen großen Dank möchte ich Herrn Dr. Hutzler aussprechen, der mich mit viel Geduld die gaschromatographische Analytik gelehrt hat und auch sonst immer mit Rat zur Seite stand. Ohne ihn wäre das Projekt besonders in der Anfangsphase nicht so erfolgreich verlaufen.

Herrn Dr. Laux danke ich für die Initiierung vielerlei Kontakte in die Forschungsgemeinschaft der Tätowiermittel, die schon mit der Organisation des BfR-Symposiums zu Tätowiermitteln begann, sowie für die Unterstützung bei der Durchführung der Arbeit.

Auch für die Hilfe beim Erstellen der Publikationen und der Arbeit möchte ich mich bei Dr. Hutzler und Dr. Laux bedanken.

Diese Arbeit wäre ohne Kooperation mit anderen Wissenschaftlern und Forschungseinrichtungen nicht so erfolgreich verlaufen. Daher danke ich Prof. Berlien für sein Engagement, Enthusiasmus und wissenschaftlichen Drang aus dem heraus er seine limitierte Zeit aufgebracht hat, um mit mir bis nach Sonnenuntergang Pigmente zu bestrahlen. Auch außerhalb der Arbeit hat mich seine Herzlichkeit und sein Teamgeist inspiriert.

Dr. Hesse, Dr. Seim und Dr. Castillo-Michel möchte für die vielen schönen und spannenden Stunden in und um die „Maschine“ danken – abseits von Sonnenlicht und Zeitgefühl – sowie die intensive Zeit der Nachbereitung.

Dr. Hauri und Dr. Bäumler danke ich für viele nette fachliche Gespräche, ihre Unterstützung und Tatendrang.

Nadine Dreiack und Nils Dommershausen danke ich für die Hilfe im Labor sowie der gesamten Abteilung 7 für die gute Zusammenarbeit, viele hilfreicher Diskussionen und der schönen Zeit innerhalb und außerhalb des Labors.

Dabei geht ein besonderer Dank an das gesamte GZSZ-Büro in all seinen Besetzungen - auch durch euch habe ich mehr gute als schlechte Zeiten gehabt, mit dem besten Raumklima in dem wahrscheinlich pflanzenreichsten Büro des Institutes. Nicht zu vergessen sind auch die Masterstudentinnen, mit denen ich während meiner Doktorarbeit zusammen gearbeitet habe: Sarah, Maria, Nadine und Lisa-Marie haben in der Zusammenarbeit den Spaß an der Wissenschaft auch für mich gesteigert. Auch Henrik und Markus, die mit mir nun dieses Projekt weiterführen, danke ich für ihre wertvolle Arbeit und ihren Esprit.

Zu guter Letzt war außerhalb der Wissenschaft auch meine Familie immer für mich da. Eure Unterstützung bedeutet mir sehr viel.

Lieber Marcel, auch wenn ich nie alle Arten deiner Unterstützung in den Jahren meiner Doktorarbeit auflisten könnte, danke ich dir für jeden menschlichen und wissenschaftlichen Rat, die Pflege, Verpflegung, dein Verständnis und deine schier unerschöpfliche Geduld.

Table of contents

Abstract	7
Zusammenfassung	8
Abbreviations	10
1. Introduction	12
1.1. Past and present: Human history of tattooing	12
1.2. The tattooing procedure	13
1.3. Biodistribution of tattoo ingredients	15
1.4. Tattoo regulation and its shortcomings in Germany	16
1.5. Composition of tattoo inks	18
1.6. Toxic substances in tattoo inks	21
1.6.1 Impurities derived from ink manufacturing	21
1.6.2 Toxic substances resulting from the degradation processes	22
1.6.3 Other toxic tattoo ink ingredients	22
1.7. Health risks related to tattoos	24
1.7.1 Infectious diseases	24
1.7.2 Granulomatous reactions, sarcoidosis and allergies.....	24
1.7.3 Photosensitivity	26
1.8. Current methods of tattoo removal	27
1.8.1 Surgical and abrasive procedures.....	27
1.8.2 Chemical removal	27
1.8.3 Laser removal	28
1.9. Aim of this thesis	30
2. Results	31
2.1. Identification and hazard prediction of tattoo pigments by means of pyrolysis—gas chromatography/mass spectrometry	31

2.2.	Formation of highly toxic hydrogen cyanide upon ruby laser irradiation of the tattoo pigment phthalocyanine blue	44
2.3.	Tattoo laser removal releases carcinogens and sensitizers from organic pigments.....	55
2.4.	Synchrotron-based v-XRF mapping and μ -FTIR microscopy enable to look into the fate and effects of tattoo pigments in human skin	77
3.	Discussion.....	90
3.1.	Photothermolysis of organic pigments	90
3.1.1	Extrapolation of decomposition patterns to other pigments and sunlight exposure.....	90
3.1.2	Toxicological risks of major laser decomposition products	92
3.2.	Biokinetics of tattoo ink ingredients.....	95
3.3.	Tissue-particle interactions	98
3.4.	“Whitelist” for tattoo ink regulation: Scrutiny of the six organic pigments investigated	101
3.4.1	Cu-phthalocyanine P.B.15	102
3.4.2	Quinophthalone P.Y.138	103
3.4.3	Quinacridone P.V.19.....	104
3.4.4	Diketopyrrolopyrrole P.R.254.....	105
3.4.5	Azo-naphthol pigment P.R.170.....	105
3.4.6	Diazo pigment P.O.13	105
4.	Conclusion and Outlook	107
5.	References.....	109
6.	List of publications	119
Annex I	122
Annex II	137
Annex III	142

Abstract

Due to the continuous popularity of tattoos in Germany and other countries one fifth to a quarter of the population is already carrying this permanent body decoration. Despite this high incidence, numerous toxicological endpoints, especially in the case of the color giving pigments, are missing for an adequate risk assessment of tattoo inks. In this thesis, photostability and biokinetics are investigated as two of the key elements of tattoo pigment pharmacokinetics.

The light-induced decomposition of six organic pigments was investigated using laser irradiation, which is commonly used for tattoo removal. Decomposition products were analyzed using gas chromatographic separation coupled to mass spectrometric detection. Additionally, the photothermal decomposition as occurring with laser irradiation was mimicked by pyrolysis.

Data for pigment biokinetics could only be obtained by analysis of human samples since animal testing for tattoo applications was declined in Germany. Here, pigment and element distribution in skin and lymph nodes, as well as other peripheral organs, were assessed using mass spectrometric devices and synchrotron x-ray fluorescence techniques.

Upon laser irradiation, all organic pigments were cleaved into benzene and hydrogen cyanide. Also, potentially carcinogenic and sensitizing compounds were found for each pigment specifically. The same decomposition products were also found in pigment pyrolysis. In *in vitro* cytotoxicity tests, hydrogen cyanide showed an impairment of the skin cell metabolism in the expected concentrations.

The analysis of skin and lymph node samples revealed a preferential transport of smaller particles of organic and inorganic pigments. Associated to tattoo pigments, potentially carcinogenic and sensitizing elements like Ni, Cr and Cd are transported to the draining lymph nodes. No increased element concentrations were detected in other peripheral organs investigated so far.

The data obtained from laser irradiation and pyrolysis in combination with information from other publications allow an extrapolation of the decomposition of non-investigated pigments of the same chemical classes. This facilitates the exclusion of pigments degrading into toxins out of the several hundred potentially used in tattoo inks.

The data on distribution of tattoo inks do not display a full data set for biokinetics under the given circumstances but confirm life-long exposition to potentially harmful material in the lymph nodes. Since the distribution of other insoluble pigments including white titanium dioxide is well described in literature upon subcutaneous and intradermal application, this data might be used to extrapolate the distribution of tattoo pigments.

Zusammenfassung

Durch die anhaltende Beliebtheit von Tätowierungen tragen in Deutschland und anderen Ländern zwischen einem Fünftel und einem Viertel aller Menschen diesen permanenten Körperschmuck. Trotz dieser hohen Inzidenz stehen viele toxikologische Daten für eine ausreichende Risikobewertung der Inhaltstoffe von Tätowiermitteln, insbesondere der Pigmente, nicht zur Verfügung.

In dieser Arbeit wurden zwei Kernelemente der Pharmakokinetik von Tätowiermittelpigmenten, die Stabilität unter Lichteinfluss und die Biokinetik, untersucht.

Die lichtinduzierte Zersetzung von sechs organischen Pigmenten unter Laserbestrahlung, welche zur Entfernung von Tätowierungen eingesetzt wird, wurde mit Hilfe von Gaschromatographie mit massenspektrometrischer Detektion untersucht. Zudem wurde die photothermische Zersetzung unter Laserbestrahlung durch Pyrolyse simuliert.

Biokinetische Daten konnten nur durch die Analyse humaner Proben erhoben werden, da Tierversuche für diesen Anwendungsbereich in Deutschland nicht genehmigt wurden. Hier wurde die Verteilung von organischen Pigmenten und Elementen in Haut und Lymphknoten, sowie anderen peripheren Organen mit Hilfe massenspektrometrischer Methoden und Synchrotron-Röntgenfluoreszenz analysiert.

In den Laserversuchen konnte gezeigt werden, dass generell aus allen untersuchten organischen Pigmenten Benzol und Blausäure freigesetzt werden können. Zudem entstehen pigmentspezifisch potentiell krebserregende und allergieauslösende Substanzen. Die gleichen Zersetzungsprodukte zeigten sich ebenfalls durch Pyrolyse der Pigmente. *In vitro* Zytotoxizitätstests konnten zeigen, dass der Hautzellmetabolismus durch Blausäure in den zu erwartenden Konzentrationen eingeschränkt wird.

Die Analysen der Haut und Lymphknotenproben zeigten einen bevorzugten Transport von kleinen Partikeln organischer und anorganischer Pigmente. Zusammen mit diesen Pigmenten gelangen auch potentiell krebserregende und allergieauslösende Elementverunreinigung wie Ni, Cr und Cd in die Lymphknoten. In peripheren Organen konnten noch keine Pigmente oder erhöhte Elementgehalte festgestellt werden.

Durch die gewonnenen Daten der Laserbestrahlung, Pyrolyse und anhand der Literatur lassen sich für einzelne chemische Pigmentklassen auch die Zersetzungsprodukte nicht untersuchter Pigmente extrapolieren. Die Daten können dazu genutzt werden, unter Hunderten verfügbaren Pigmenten diejenigen mit toxischen Zersetzungsprodukten zu identifizieren und für die Anwendung in Tätowiermitteln auszuschließen.

Die unter den gegebenen Umständen gewonnenen Daten in Bezug auf die Verteilung von Tätowiermittelpigmenten im Körper stellen keine vollständige Biokinetik dar, belegen jedoch die

lebenslange Exposition gegenüber potentiell gesundheitsschädlichen Stoffen in den Lymphknoten. Da die Verteilung anderer unlöslicher Partikel, inklusive dem Weißpigment Titandioxid, auch in subkutaner und intradermaler Applikation in der Literatur gut beschrieben ist, können diese Daten ebenfalls zur Extrapolation der Verteilung von Tätowiermittelpigmenten herangezogen werden.

Abbreviations

All abbreviations occurring in the text, except for those used in the articles in Chapter 2, are listed in the following table.

ADME	administration, distribution, metabolism and secretion
ALARA	as low as reasonably achievable
BfR	Federal Institute for Risk Assessment (German: Bundesinstitut für Risikobewertung)
BVL	Federal Office of Consumer Protection and Food Safety (German: Bundesamt für Verbraucherschutz und Lebensmittelsicherheit)
BTEX	benzene, toluene, ethylbenzene, xylene
C.I.	color index
CYP	cytochrome P450
DNEL	Derived No-Effect Level
ECHA	European Chemicals Agency
EU	European Union
GC-MS	gas chromatography coupled to mass spectrometry
GHS	Globally Harmonized System of Classification and Labelling of Chemicals
HCB	hexachlorobenzene
IARC	International Agency for Research on Cancer
i.d.	intradermal
IPL	intense pulsed light
i.p.	intraperitoneal
i.v.	intravenous
LC-MS	liquid chromatography coupled to mass spectrometry
LFGB	German Food and Feed Code (German: Lebensmittelfuttergesetzbuch)
LOAEL	lowest-observed-adverse-effect level
MALDI-ToF-MS	matrix-assisted laser desorption/ionization time-of-flight mass spectrometry
MAK	Maximum workplace concentration (German: Maximale Arbeitsplatz-Konzentration)

NMR	nuclear magnetic resonance
OECD	Organization for Economic Co-operation and Development
PAA	primary aromatic amines
PAH	polycyclic aromatic hydrocarbons
PEG	polyethylene glycol
P.B.	pigment blue
P.G.	pigment green
P.O.	pigment orange
P.R.	pigment red
P.V.	pigment violet
P.Y.	pigment yellow
py-GC-MS	pyrolysis-gas chromatography-mass spectrometry
QSAR	Quantitative Structure-Activity Relationship
Q-switched	quality-switched
RAPEX	Rapid Alert System for dangerous non-food products
ReSaP(2008)1	Resolution on requirements and criteria for the safety of tattoos and permanent make-up
ROS	reactive oxygen species
s.c.	subcutaneous
TiO ₂	titanium dioxide
TätoV	tattoo products regulation (German: Tätowiermittelverordnung)
UV	ultra violet

1. Introduction

1.1. Past and present: Human history of tattooing

The permanent depositing of pigments in the skin—which is nowadays referred to as tattooing—reaches back to the beginning of modern humanity. Not only did „Ötzi“, the oldest European iceman mummy dating back to 3370–3100 BC, have 61 tattoos spread all over his body¹, but tattoos found on early mummies from Peru, Egypt and Russia imply that tattooing was a worldwide phenomenon². Tools discovered at archeological sites, which were used to create tattoos, even date the beginnings of tattooing back to the Upper Paleolithic³. During history, it has not lost any of its appeal to the present day and has consistently existed to the present day².

In the recent decades, there has been a massive increase in tattooing. In Germany a total of 9.1% of the population is tattooed, in the age group of 25–34 years the figure is 22.3%⁴. A comparison of multiple studies from Europe, Australia and the USA showed similar values with the highest prevalence of 38% in the 30–39 year age group in the USA⁵.

Over the centuries, the techniques used to perform this body modification have evolved and improved. The first tattoos were probably made by simply rubbing charcoal into the skin after it had been punctured with primitive tools such as thorns, sharpened bone or flintstone knives⁶. More sophisticated methods included sewing and needles hammered into the skin in the arctic and Polynesia⁷. Even today, these techniques still find devoted communities around the globe and are also practiced traditionally in some countries.

During the industrialization and electrification of Western societies, more advanced tattooing methods came into being. In 1891, Samuel O’Reilly and Thomas Riley patented the first electrical driven rotary and single coil tattoo machines, respectively^{8,9}. Modern tattoo machines are technologically refined descendants of this technology.

1.2. The tattooing procedure

Irrespective of the various techniques available to obtain a permanent skin colorization, the physiological process remains the same. Insoluble pigment particles are inserted into the dermal layer of the skin (Fig. 1). If deposited into the upper epidermis, the fast regeneration and dispensing of dead cells towards the skin surface would lead to a rapid fading of the tattoo within weeks. It should be mentioned, that the latter is attempted in the case of so-called “bio-tattoos” and permanent make-up which should resolve or disappear after some time. However, the epidermis is a relatively thin cell layer varying from 50–1500 μm in thickness that even an experienced tattoo artist using modern tattoo machines struggles to exclusively hit the epidermis. Therefore, a semi-vanished tattoo might even remain in the person’s skin in case of “bio-tattoos”. With permanent make-up, the outer border of lips, eye-lids and the shape of the eyebrows are highlighted with a tattooing procedure, which is intended to vanish after a certain time. Even if the depth of the needles is not controllable in a satisfactory manner, most permanent-make up colorations disappear. Presumably, permanent make-up vanishes because facial skin has a faster turn over, a thick corneal layer around the lips prevents deeper dermal injection or because less ink is injected. In terms of the eye brows, an exceedingly high number of case reports can be found in literature on laser removal of no-longer wanted coloration. Often because these inks tend to undergo color changes already before or after laser-removal^{10,11}. Since the procedure of permanent make-up is comparable to the tattooing process, the following work will use the term “tattoo” implicitly including permanent make-up.

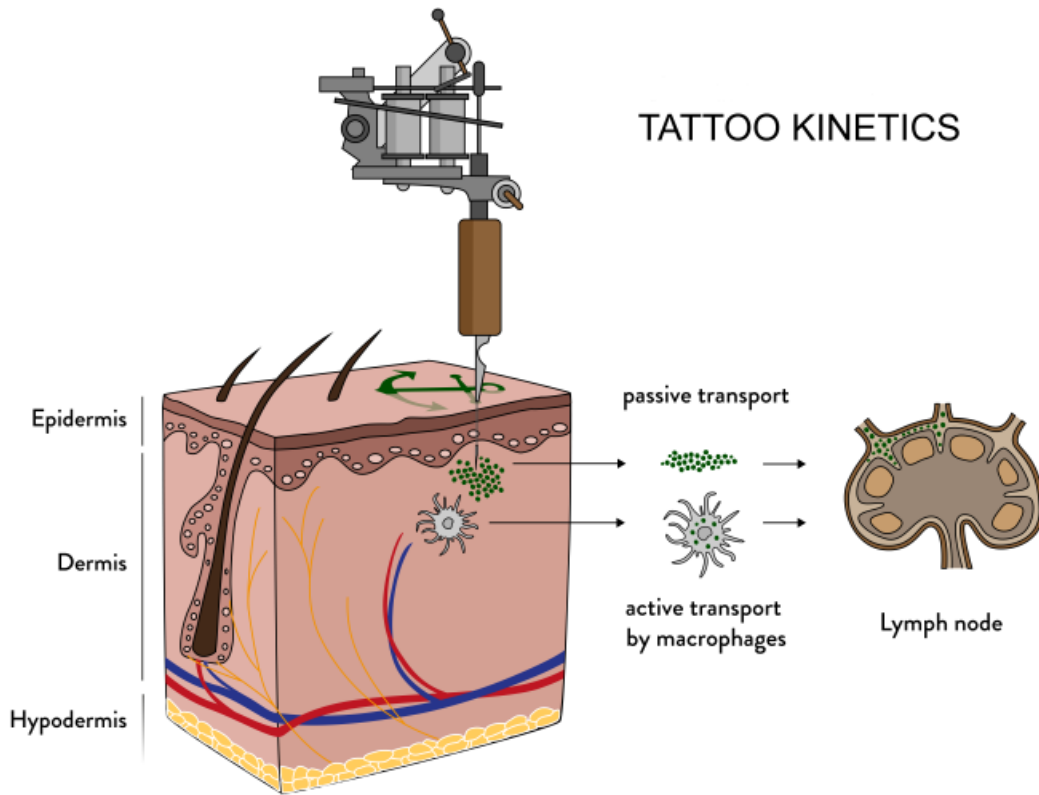


Figure 1: Translocation mechanism of tattoo particles from skin to lymph nodes. Upon injection of tattoo inks, particles can either be passively transported via blood and lymph fluid or phagocytized by immune cells and subsequently deposited in regional lymph nodes. When the wound has completely healed, particles are present in the dermis and in the sinusoids of the draining lymph nodes (from Schreiver *et al.* 2017, Chapter 2.4).

1.3. Biodistribution of tattoo ingredients

Once injected into the dermis, all tattoo ink ingredients are in contact with either lymph fluid, blood or both. Therefore, a full bioavailability of all ingredients is given. Pigments are actively and passively transported to the draining lymph nodes of that body area¹²⁻¹⁵(Fig. 1). This transport is macroscopically visible by the massive amounts of pigments that can be found in the lymph nodes of tattooed individuals¹². In the dermis, the pigments will be either phagocytized by fibroblasts or macrophages¹⁶ or stay in the extra-cellular matrix¹⁷⁻¹⁹. Whether pigments travel beyond the lymph nodes is part of ongoing research. Despite the observations in human and animal studies, the pigment translocation to the lymph nodes has not been characterized in terms of chemical composition or size so far. One study conducted on cadaveric black lymph node tissue revealed the storage of polycyclic aromatic hydrocarbons (PAH) inside the carbon particles²⁰. Colloidal carbon particles can be found in the draining lymph vessels and the ipsilateral para-aortic lymph nodes as quickly as 3–6 minutes after injection into hamstring muscles of the leg in Wistar rats¹⁶. Pigment titanium dioxide (TiO₂) was found in liver, lymph nodes, spleen, and lung after subcutaneous (s.c.) and intraperitoneal (i.p.) injection²¹⁻²³.

With regard to soluble components of tattoo ink, rapid biodistribution via the blood and lymph stream followed by excretion is to be expected. Other polymeric structures or pigments residing in skin might become distributed after degradation.

The biokinetics of tattoo inks therefore underlie different phases and mechanisms. Firstly, an immediate passive distribution of particles and soluble substances will occur at the time of the tattooing procedure. Secondly, phagocytizing cells will actively translocate particles to the draining lymph nodes until wound healing is complete. As a third step, cell metabolism, sunlight exposure and removal procedures can release degradation products from pigments or residual large polymers.

1.4. Tattoo regulation and its shortcomings in Germany

Before 2009, tattoo inks were regulated under the German Food and Feed Code (German: Lebens- und Futtermittelgesetzbuch, LFGB). As defined by this law, products must be safe and shall not harm human health. It is the manufacturer's responsibility to ensure the safety of products. The LFGB does not contain specific requirements for tattoo inks. On European level, a first resolution on requirements of tattoo safety was established in 2003 and renewed in 2008 (ResAP(2008)1)²⁴. It was translated into German law in 2009 (German: Tätowiermittelverordnung, TätöV)²⁵. The TätöV bans pigments from use in tattoo inks which are forbidden or restricted in their area of application according to Annexes II and IV of the European Union (EU) cosmetics regulation. Additionally, the TätöV contains a list of carcinogenic aromatic amines which are not to be released from pigments upon reductive cleavage. Still to this day, no health-related risk assessment of ingredients used in tattoo inks has been considered in this legislation. The main criticism of the current regulation is, that by providing a list of forbidden pigments, all non-listed pigments can potentially be used. Since more than 10.000 pigments and dyes have been listed in the color index (C.I.) to date, a large number of non-tested pigments with unknown toxicological effects exist for legal use in tattoo inks. The TätöV also does not cover other ingredients used in the multi-component ink mixture, e.g. element impurities, PAHs or preservatives.

Therefore, the BfR recommends the establishment of a "whitelist" of less harmful substances. However, this is a long-term goal due to the current lack of data for risk assessment. In an opinion letter, the BfR listed necessary steps for a health-based risk assessment. Besides the characterization of physico-chemical and toxicological properties of the ingredients, the biokinetics of pigments after *in vivo* subcutaneous application are also required²⁶. This opinion is shared by the broad majority of the tattoo research community²⁷.

On the one hand, the compliance of inks with legislation needs to be monitored by official authorities. Past investigations by the federal state laboratories reveal deficits in the microbiological and chemical state of the analyzed inks^{28,29}. On the other hand, no validated method for pigment identification is available to date. Thus, German state laboratories often rely on labelling as an indication of the pigments used. A Swiss study showed that nearly half of the inks caused complaints due to false declarations and that one third contained non-compliant pigments³⁰. Since threshold levels for impurities are missing, federal state laboratories have difficulties in banning substances found at increased levels if these are not explicitly listed in the annex II or IV of the EU regulations of cosmetics. Any complaints for Ni and PAHs, for example, are therefore based on the assumption that they can harm human health in the concentrations found. In general, the state laboratories probe tattoo inks from distributors, as well as

tattoo parlors, regarding microbial contamination and other ingredients. If an ink fails the test, manufacturers are informed about the non-compliance of their products. If inks are believed to pose a serious risk to the health and safety of consumers, the products are submitted to RAPEX (the European Rapid Alert System for dangerous non-food products)³¹. This allows consumers and tattoo parlors to inform themselves about potentially harmful inks.

In general, tattoo inks do not need to be approved before market entry, e.g. by submitting safety dossiers for the products to legal authorities. Only trade names and ingredients have to be sent to the Federal Office for Consumer Protection and Food Safety (German: Bundesamt für Verbraucherschutz und Lebensmittelsicherheit (BVL)).

1.5. Composition of tattoo inks

Color giving pigments certainly represent the most essential ingredient of tattoo inks. In the past, traditional tattoo inks were self-mixed by the tattooist from black soot of varying origin³² and some inks are still prepared this way today. Before the time of professional manufacturing of dedicated tattoo inks, it can be assumed that people used colored ingredients of all kinds for injection into the skin. In personal communication, people reported red bricks, plant leaves and household paints being used for tattooing. Even today, some professional and home-tattooists use Indian ink intended for calligraphic use³³.

The professionalization of the production of tattoo inks does not directly imply safe use, even if some manufacturers nowadays try to avoid certain ingredients to the best of available knowledge. The main qualities of a good tattoo ink from an artist's point of view is good suspension of the maximum possible amount of pigment in a watery consistency, immediate usability and ink that does not dry out too quickly. Therefore, the solvents used (e.g. water, ethyl alcohol or isopropanol) need to be mixed with stabilizers. Often surfactants and dispersants (e.g. glycols and polymers) known from the cosmetics and paint industries are used³⁴. Additionally, preservatives might be added to avoid microbial growth after opening of the ink containers. Furthermore, some ink formulations contain ingredients with a questionable purpose. These include fragrances such as eucalyptol and menthol, as well as plant extracts such as witch hazel.

The pigments can either be of organic or inorganic nature. Some decades ago, mostly inorganic salts and metal oxides were used^{35,36}. Black iron oxides have since mainly been replaced by carbon black due to its darker color. Also, other inorganic pigments have been replaced due to the increasing use of more brilliant organic pigments. The former are still favored in permanent make-up applications and when more earth-like tones are desired. In 2011, the inorganic pigments manganese violet (C.I. 77742), iron oxides red, yellow and black were only found in 1–4% of all tattoo inks according to content declarations³⁰. The most used inorganic pigment is white TiO₂ with an occurrence of 36% in all inks tested in the survey³⁰. It is needed to generate certain color shades and is sometimes replaced with white barium sulfate³⁴. Pigments are synthesized as particles and have a polydisperse primary size from two-digit nano to micrometer ranges.

The organic pigments used in tattoo inks are manufactured for the cosmetic and paint industry. The currently used chemical structures can be assigned to a few major families (Fig. 2).

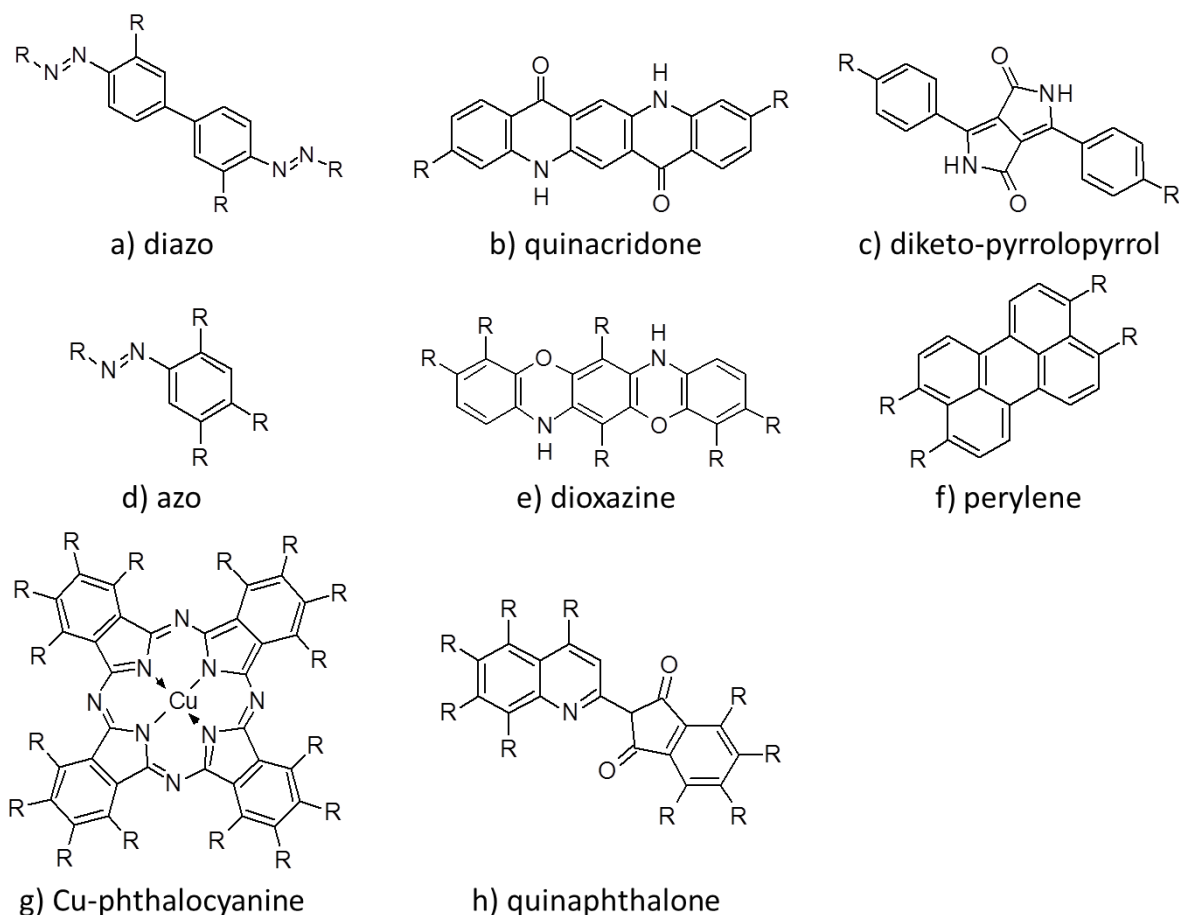


Figure 2: Common chemical structures used in tattoo inks. a)-h) Most organic pigments used in tattoo inks today belong to the displayed chemical classes. Their photostability varies dependent on the number of weak bonds in their structure. a,d) Azo pigments potentially release primary aromatic amines (PAAs) by cleavage of the azo bond leading to the formation of an amine. They account for most yellow, orange and red pigments currently used. b) Quinacridone pigments have a reddish to bluish pink appearance and are highly light-fast pigments. c) The most famous diketopyrrolopyrrole is better known as “Ferrari red”. These pigments are highly light-fast and give orange to red color tones. e) Dioxazine pigments are violet and their stability is dependent on the corresponding residues. f) The light-fast perylene pigments give a dark red, brown or black color. To date, these have not been frequently found in tattoo inks. g) Cu-phthalocyanines represent the only blue and green organic pigments found in tattoo inks today. h) Only one quinaphthalone yellow, highly chlorinated pigment has been used in tattoo inks to date. It has advantageous features in terms of light stability compared to azo pigments.

The surface of pigment particles is often modified to facilitate proper suspension with regard to their dedicated use in combination with specific solvents and dispersants. These so-called coatings can be proprietary and therefore unknown to the ink manufacturers. But similar to the surface of biomaterials,

coatings might have a crucial role in biocompatibility of the pigments³⁷. TiO₂, for example, is treated with aluminum silicates to reduce photoactivity. Organic surface coatings might be composed of polyethylenoxide, dioctylphthalate, 3-isobutoxypropylamine or polydimethylsiloxane³⁸.

In order to achieve the proper suspension of the pigments, glycerol, propylene glycol, polyethylene glycol (PEG), dimethyl siloxanes, polyvinylpyrrolidone, shellac or acryl-containing block co-polymers are used as auxiliary substances in tattoo inks^{34,38}. A market survey from 2011 revealed the use of the surfactants β -naphthol ethoxylates, octylphenol ethoxylate (better known as Triton X-100), nonylphenol ethoxylates and diethylenglycol in tattoo ink³⁰. Also 2,4,7,9-tetramethyl-5-decin-4,7-diol and cyclosiloxanes were identified in various inks (unpublished data).

The higher the water content of an ink, the more likely it is that microorganisms can grow in the products. If an ink is produced with a water activity value below 0.6, it might be produced without preservatives to reduce risks of allergic reactions³⁴. Since many inks contain high amounts of various alcohols as solvents, the antimicrobial properties of these make preservatives unnecessary. Nonetheless, some inks contain preservatives such as phenol, isothiazolinones, phenoxyethanol, glyoxal, benzoic acid and formaldehyde^{29,30}.

1.6. Toxic substances in tattoo inks

1.6.1 Impurities derived from ink manufacturing

Depending on the manufacturing process of the raw pigments, different purity grades at different costs are available on the market. Since most inorganic iron pigments are made from mining products, they commonly contain Ni, Cr, Cu or Co—amongst other elements³⁹. Ni might also be used as a catalyst in pigment synthesis e.g. for phthalocyanines. Especially pigment impurities with sensitizing properties are considered problematic. Ni, for example, is one of the most common contact allergens⁴⁰ and therefore people with known sensitivities should take into consideration that tattooing might trigger an unwanted allergic reaction. The ResAP(2008)1 and the BfR recommend the restriction of Ni in tattoo inks by the ALARA-principle (“as low as reasonably achievable”). However, this gives no absolute threshold level that can be applied by responsible surveillance laboratories or manufactures to declare inks as compliant with legislation²⁴. Also, there is currently a deficit of information as to which concentrations can be considered reasonably achievable for the different kinds of pigments.

Other impurities might derive from organic pigments either as residues of their chemical building blocks or solvents from wet-synthesis. These include carcinogenic PAAs and carcinogenic nitrosamines^{28,41}. For some PAAs an increased risk of bladder cancer was found, other substances such as 3,3'-dichlorobenzidine (DCBD) might cause cancer in a variety of tissues⁴². Solvents used during the manufacturing process that can still be detected in the inks are toluene, xylene, ethylbenzene and styrene (unpublished data). These volatiles partly belong to the BTEX (benzene, toluene, ethylbenzene, xylene) group of chemicals known to cause acute and chronic toxic effects to the liver and the nervous system⁴³. Moreover, styrene is also mutagenic⁴⁴.

Carbon black contains various amounts of PAHs, dependent on the manufacturing process used. A contamination with PAHs cannot be fully avoided, even if highly purified products exist. They are known carcinogens and frequently found in tattoo inks²⁰. PAHs are constant contaminants in our daily life wherever combustion takes place, e.g. in open fires or food processing, as well as in mineral oil based products. Still, carbon black tattoos can display an additional chronic exposure to PAHs with unknown health effects. However, a recent study conducted in naked mice suggests that at least in skin, black tattoos have a protective effect regarding the development of skin cancer due to the light absorptive properties of the pigment⁴⁵.

1.6.2 Toxic substances resulting from the degradation processes

Degradation products of organic pigments are increasingly recognized as a potential health threat. Toxic and carcinogenic substances may be released from the pigments after exposure to ultra-violet (UV) or visible light irradiation⁴⁶. This has been shown for various mono azo pigments using sunlight simulation (pigment red (P.R.)22, pigment yellow (P.Y.)74, P.R.112, P.R.170). Also, the frequency doubled quality-switched (Q-switched) Nd:YAG laser, as used in tattoo laser removal, has been shown to cleave azo pigments (P.Y.97, P.R.9, P.R.22, P.R.112)^{15,46-49}. In the case of diazo pigments, decomposition into the carcinogen DCBD has been shown in sunlight, laser irradiation or both for P.Y.14, P.Y.83, pigment orange(P.O.)13 and P.O.34^{50,51}. The diazo P.O.16 released 3,3'-dimethoxydiphenyl upon sunlight simulation^{50,51}. The quinacridone P.R.202 is the only non-azo pigment for which a cleavage product, namely the carcinogen 4-chloroaniline, has been described in literature⁴⁹. To prevent this light-induced degradation, colorful tattoos should be protected from sunlight either by applying sunscreen or textiles. Also, the metabolization of pigments is a subject of intense discussion. In general, pigments are thought to be inert due to their insolubility and therefore considered not accessible to degrading enzymes. However, the metabolization of the azo compound P.Y.74 by liver cells has been verified *in vitro*⁵². The degradation of pigments is accompanied by a higher solubility of the evolving substances. As in the case of the impurities mentioned above, these can therefore be distributed throughout the body.

1.6.3 Other toxic tattoo ink ingredients

Indian ink sometimes used for tattooing was mentioned in clinical case reports as causing allergies³³. Some studies report carmine dyes as possible tattoo ingredient⁵³. The usage of these lice-derived dyes is critical for two reasons: first, they are light sensitive and will decay and thus vanish from the tattoo over time, and second because they have been reported to cause severe allergies even leading to systemic anaphylaxis⁵³. Preservatives are mostly of concern due to their sensitizing effects⁵⁴. Since their use is not restricted in Germany, preservatives that have been banned or restricted for cosmetic products may be used in tattoo inks and are frequently found in market surveys (cf. Chapter 1.4). The toxicity of polymers used to disperse the pigments in tattoo inks might be induced by their metabolization in the human body. For example, toxic acidification can be induced by metabolism of PEG into its hydroxy acid and diacid derivatives and the monomer ethylene glycol^{55,56}. Also, phthalates were identified in black tattoo inks^{41,57}. The toxicity of dibutyl phthalate in particular on the reproductive system is of special concern.

The genotoxicity of the commonly used white pigment TiO_2 shown in alveolar cells *in vitro*⁵⁸ and carcinogenicity in animal studies *in vivo*^{59,60} is currently the subject of much debate. Based on the available data, the French Agency for Food, Environmental and Occupational Health & Safety (ANSES) proposed harmonized classification of TiO_2 under carcinogenicity category 1B according to the GHS (Globally Harmonized System of Classification and Labelling of Chemicals) with the hazard statement H350i “may cause cancer upon inhalation”. However, in view of epidemiological data, the International Agency for Research on Cancer (IARC) working group concluded that only inadequate evidence exists for the carcinogenicity of TiO_2 in humans⁶⁰. Currently, no hazards have been classified regarding TiO_2 in the substance information portal of the European Chemicals Agency (ECHA). However, the ECHA’s Committee for Risk Assessment concluded that TiO_2 can be classified as suspected of causing cancer (category 2, through the inhalation route) but the final decision of the European Commission is still pending.

Other ingredients that might exhibit toxic properties are contained in UV-active tattoo inks. These “glow-in-the-dark” inks are described as polymethylmethacrylate microspheres containing 2.5% fluorescent dye⁶¹. Some sources claim the use of phosphate based inks⁶² which will glow even in the absence of a UV light source. The glow in the dark feature will probably vanish after a short period of time. However, no scientific sources or chemical analyses can be found in literature. No survey indicates how many people have had these kinds of tattoos, but it most likely accounts only for a minority. One case report on these inks showed severe granulomatous dermatitis due to a foreign material including lymphocyte infiltration and formation of giant cells⁶³.

1.7. Health risks related to tattoos

The most frequently reported side effects of tattoos are infectious diseases (151) followed by allergic/foreign body reactions (96) and tumor growth at the site of the tattoo (33), as reported in a review by Wenzel *et al.* in 2013⁶⁴. A survey among 448 French tattooists revealed that 42.5% percent had experienced adverse reactions to at least one of their tattoos. The most reported tattoo reactions were transient itching, swelling and sunlight sensitivity (23–57%) followed by “allergy” with 8%⁶⁵. A study by Klügl *et al.* reported that 67.5% of tattooed people exhibit health issues directly after tattooing of which 1.8% were graded as intense to very intense. 7.7% occurred after 4 weeks and 6% had persistent problems in their skin⁶⁶. Similar observations were made in a survey in New York but with a slightly increased percentage of reactions to red tattoos normalized to their overall use as tattoo color⁶⁷. After laser treatment, 5% of patients reported persistent side effects still present after 30 weeks⁶⁸.

1.7.1 Infectious diseases

Infections of the tattooed skin areas appearing shortly after tattooing are a major complication. These can be caused by bacteria (e.g. *streptococcus*, *staphylococcus*, *mycobacteria*), viruses (e.g. papilloma, herpes, hepatitis) or fungi (e.g. *candida*, mold fungi). The infection can be introduced by non-sterile tattoo inks, improper handling and storage after opening of the inks, a lack of hygiene during or after the tattooing process or by contaminated ink—independent of sterility claims on the label⁶⁹.

The transmission of viral, fungal or bacterial infections by tattooing can be easily avoided by preventive procedures. Nonetheless, case reports of small epidemics can still be found in current literature. For example, contaminated water used to dilute the ink or non-sterile ink bottles used for multiple customers were reported to have caused an outbreak of mycobacteria infections^{70,71}.

1.7.2 Granulomatous reactions, sarcoidosis and allergies

Non-infectious inflammations in skin can have multiple causes and diverse manifestations. Allergies can occur as hyperkeratosis, lichenoid reactions, granuloma or plaque elevation. In cases of strong allergy, progression towards autoimmunity can lead to an ulcero-necrotic pattern where the full thickness of the skin and ultimately also non-tattooed regions are affected. In a case of a tattooed man, multiple amputations of one leg had to be carried out due to an allergic response⁷².

Allergies can arise as a reaction to different substances. If no immediate onset of the reaction has been observed, soluble substances like preservatives and soluble elements that will be quickly removed from the site of the tattoo are not thought to be the cause of these reactions. However, these immediate

allergic reactions in sensitized individuals exist and mild forms might be confused with prolonged wound healing and will resolve as the trigger substance vanishes⁷³.

In terms of pigment related allergies, most case reports identify Cr as a source of element-related allergies occurring with tattoos⁷⁴. Additionally, allergic responses due to the presence of Hg¹⁹, Co³⁶ and Ni⁷⁵, which are frequent contaminants in inorganic pigments, were reported. The presence of the aforementioned metals was confirmed by chemical analysis of the tattoo. Positive patch tests of the identified elements on the corresponding patients confirmed a sensitization of the patient and appear to be the plausible cause of the tattoo allergy. In contrast, a causative relationship of allergic reactions to tattoos and the use of certain organic pigments is somewhat debated. In reports of allergies to the quinacridone pigments violet (P.V.)19 and P.R.122, the identity of the pigments was not verified by chemical analysis but deduced only from the declaration of contents. Subsequent patch tests with the used inks failed to induce an allergic reaction^{76,77}. Only undiluted ink containing P.R.210 provoked an allergic reaction in a patch test at day 7, but not in prick testing⁷⁷. However, since the patch test was conducted with the ink formulation and not the pigment alone, other ingredients might be the cause for the allergic reaction observed. The most commonly used pigment phthalocyanine blue was connected to an allergic reaction to gloves in one case report⁷⁸. But since the pigment was not further characterized, free Cu ions, Ni or other unknown coatings might have been present and therefore could have been the actual cause of the sensitivity.

Wenzel *et al.* were able to conclusively show that allergic reactions to permanent make-up were caused by the thioindigo-derivative P.R.181⁷⁹. In their study, prick tests revealed papule formation after 2 days. Tamaro *et al.* also reported a Cu and Disperse Blue 3 or 124 (not clearly specified) hypersensitivity as a cause of a reaction without specifying the color of the tattoo⁸⁰.

The often observed failure to link the emergence of allergic reactions to insoluble organic pigment by patch or prick testing might indicate that the formation of hapten might take place after pigment metabolization or degradation processes⁸¹. This is supported by the observation that allergic reactions occur frequently after laser irradiation^{77,82}.

Besides allergic reactions, foreign body reactions can also occur. These are characterized by granuloma formation either due to pigment overload or as part of a systemic sarcoidosis reaction⁸³. This can also be induced by Intense Pulsed Light (IPL) treatments for hair removal if the patient is already susceptible to sarcoidosis⁸⁴. Rorsman *et al.* reported a simultaneous development of granuloma and eye inflammation (uveitis) as a manifestation of a systemic sarcoidal reaction³⁶. The granuloma formation in a tattoo was linked to the aluminum contained in the ink in one case report⁸⁵. The causes for foreign body reactions

probably include distinct surface properties of the pigments leading to agglomeration and reduced biocompatibility^{37,86}.

However, differentiating between the aforementioned skin reactions caused by tattoos might be challenging for the diagnosing physician since chemical induced granuloma, delayed hypersensitivity and granulomatous hypersensitivity might coexist⁷⁴.

1.7.3 Photosensitivity

Another common side effect of tattoos, is an increased photosensitivity. 21.5% of tattooed people have complaints related to solar radiation such as swelling, itching, stinging, pain and redness of the skin⁸⁷. These reactions are not necessarily related to specific color shades but can occur in all kinds of tattoos. One possible explanation for this phenomenon is the formation of reactive oxygen species (ROS) on the particle surface as observed in carbon black pigments²⁰. In white tattoos, rutile or anatase TiO₂ pigments are frequently used. The latter is known to be a photocatalyst and could also increase photosensitivity in patients. In a study of Wamer *et al.* the occurrence of anatase TiO₂ in permanent make-up and its phototoxicity *in vitro* were positively correlated⁸⁸.

In the analysis of red tattoo reactions by Sowden *et al.*, seven of 18 patients noticed stronger inflammation of their tattoo upon sunlight exposure and three of them reported sunlight exposure as the initial cause of the onset of their reaction¹⁹.

1.8. Current methods of tattoo removal

In parallel to the rising popularity of tattoos, the number of people desperate for removal is increasing. The wish can be triggered by changes in life and work circumstances that do not comply with the position or message of the tattoo. Other reasons are artistically poorly executed tattoos or a change in taste. The psychological strain for the patient that leads to the urge for tattoo removal may vary dependent on the illustration and its position⁸⁹.

However, each method of removal bears its own risks and sometimes entails a high financial burden which must be well considered before starting the procedure. Due to the continuous development of new removal procedures, no complete list of all methods employed is available.

Less widely used methods such as IPL⁶⁸ and strong ultrasound will not be discussed here due to their limited success on pigment removal. Nevertheless, non-professional use of these techniques can lead to skin burning, scarring, inflammatory reactions and pigmentary abnormalities⁸⁴.

1.8.1 Surgical and abrasive procedures

Excision of unwanted tattoos using knives or other sharp objects was a form of removal practiced by tattooed individuals themselves before other methods were developed. Surgical removal or skin grafts by physicians are mostly carried out as complete excision of the tattoo and are therefore only applicable for a certain, smaller, size of tattoo⁹⁰. Salt-abrasion is a form of removal also mentioned in literature⁸².

Dermabrasion of the upper dermis until the pigmented layer is removed is more advantageous especially with patients suffering from allergies and other side effects. It may result in partial scarring which is dependent on the depth of the removed layer. The recovery of the epidermal layer is facilitated by stem cells residing in hair follicles and glands⁹¹.

1.8.2 Chemical removal

On August 1st, 2011, the BfR published an opinion regarding lactic acid tattoo removal. Concentrated lactic acid is considered critical because of its irritating properties on the skin. It can lead to heavy inflammation and scarring after intradermal (i.d.) application⁹². The first report of using acids for tattoo removal date back to the Greek Aetius in the year 543⁹³. The success of the procedure is based on introducing a lactic acid solution with a tattoo machine thereby perforating the epidermis. The inflammatory response induced by the lactic acid leads to excretion of the pigment particles through the epidermis. The strong inflammatory reaction and the open wound pose an increased risk of an infectious

reaction. Therefore, the BfR recommends this procedure only be carried out by trained professionals under strict hygienic conditions⁹⁴.

Other removal methods make use of trichloroacetic acid which leads to a major chemical burn at the treated site⁹⁵. Other suppliers sell removing paste containing zinc oxide, magnesium oxide, calcium oxide, triethanolamine, isopropanol, and benzoic acid to be injected into the skin. These paste lead to dermal fibrosis and hypertrophic scarring developed as a result of a large inflammatory response⁹⁶.

1.8.3 Laser removal

The first lasers used in an attempt to remove tattoos were carbon dioxide lasers. This technique is based on the thermal coagulation and removal of superficial skin followed by excretion of the tattoo pigments and are therefore related to surgical removal⁸². Similarly, the usage of non-pulsed argon lasers leads to tissue disruption due to heating and thus inevitably causes scarring of the treated site. Modern laser treatments involve Q-switched lasers of different wavelengths, which emit photons in a nanosecond pulse that are well absorbed by the ink particles. These lasers are able to cause selective photothermolysis⁹⁷. It is disputed whether the mechanical disruption of the tattoo pigment is followed by site clearance due to macrophages, or if the chemical cleavage of organic pigments with simultaneous loss of the chromophore leads to the fading of the tattoo⁹⁸. Also, the alteration of the fine structure of carbon particles leading to transparency is a further possible explanation for the bleaching of the visible pigments¹⁷.

The use of lasers equipped with pigment specific wavelengths and short pulse durations leads to less risk of scarring. However, due to the light absorption of melanin over a broad range of visible and infrared-light wavelengths, hypo- or hyperpigmentation and skin injury can occur when treating tanned individuals or darker skin types⁸².

Even if side effects are less likely with laser removal compared to all other methods of tattoo removal, they can still occur. In a survey, 24% of participants reported slight and 8% more profound scarring of the skin after laser removal⁶⁸. In particular, badly trained laser operators and an increase in laser power pose a greater risk of scarring⁹⁹.

Another risk factor is color change of the pigment into darker shades, which possibly occurs due to the laser procedure¹⁰⁰. This phenomenon is thought to be caused by iron oxides or TiO₂ being transferred into a different state of oxidation^{18,101}. From observations made in one of our publications, a carbonization reaction of the organic pigment also appears to be plausible (cf. Chapter 2.3). However, further studies are needed to prove any of these theories. If the removal of the pigments from the skin is

successful, hypo- or hyperpigmentation can remain at the treated site¹⁰². Full removal of the tattoo often cannot be achieved; especially when it comes to yellow and orange tattoos. Violet, green and blue inks might also prove challenging¹⁰³. More recently, application of lasers with a pulse duration in the pico-second range, have also been found suitable for removing yellow tattoos⁹⁹.

1.9. Aim of this thesis

In the recent years, tattoos have become increasingly popular around the globe. The variety of pigments used in tattoo inks has moved towards the use of highly light-fast organic pigments. Yet, current legislation in Germany only forbids the use of a portion of available pigments. This leaves all remaining pigments free to use despite them never being tested for this route of application. The increase in people having a tattoo automatically leads to an increase in people seeking tattoo removal—with Q-switched laser removal still being the most widely applied method.

In the face of the increasingly recognized toxicity of organic pigments, especially after chemical decomposition, a central aim of my work was to further investigate the degradation processes of common pigments used in tattoo inks upon laser irradiation.

Since laser irradiation leads to thermolysis of organic pigments in the skin, pyrolysis was used to mimic this heat dependent decomposition. The work was aimed at identifying the decomposition products and their potential hazards for tattooed individuals (Chapter 2.1). The feasibility of pigment identification based on their specific degradation pattern during pyrolysis was investigated in order to broaden the spectrum of methods able to detect already forbidden pigments (Chapter 2.1).

Subsequently, we aimed to prove the release of the substances found in pyrolysis under laser removal conditions. Since animal studies for tattoo research are forbidden in Germany, a suitable alternative to mimic laser removal was needed. In this thesis, aqueous suspensions (Chapter 2.2) and *postmortem* tattooed pig skin were used to mimic the *in vivo* laser removal of organic pigments (Chapter 2.3). To estimate exposure to the corresponding substances, quantitative methods were applied. Cleavage patterns of each chemical pigment family obtained from pyrolysis and laser irradiation shall be evaluated for their ability to manually predict hazard decomposition products in pigments not investigated.

A second objective of this thesis was to investigate the biodistribution of pigments and elemental contaminants from the inks after tattooing. Therefore, identity and chemical characteristics of pigments in skin and regional lymph nodes of the same individual, as well as the alteration of bio-molecules in surrounding areas, were targeted in this study (Chapter 2.4).

The results obtained during the course of my thesis should help develop improved tattoo ink regulation with the ultimate goal of a whitelist containing less-harmful pigments for this application.

2. Results

Publications are displayed non-chronologically to ease understanding through a logical order. The publications in Chapter 2.2–2.4 contain a section “author contributions” to distinguish individual involvement in the manuscripts.

The resulting chapters each feature independent units. Therefore, abbreviations and references are defined within each chapter.

2.1. Identification and hazard prediction of tattoo pigments by means of pyrolysis—gas chromatography/mass spectrometry

Ines Schreiber, Christoph Hutzler, Sarah Andree, Peter Laux, Andreas Luch

This chapter was published online on 21. May 2016 in:

Archives of Toxicology 90(7):1639–1650 (2016).

DOI: 10.1007/s00204-016-1739-2

Link: <https://doi.org/10.1007/s00204-016-1739-2>

Involvement of the author within this publication: Project planning (80%), project execution (95%), data analysis (95%), writing of the manuscript (90%).

Supplementary materials for the following publication are detailed in Annex I.

2.2. Formation of highly toxic hydrogen cyanide upon ruby laser irradiation of the tattoo pigment phthalocyanine blue

Ines Schreiver, Christoph Hutzler, Peter Laux, Hans-Peter Berlien, Andreas Luch

This chapter was published online on 5. August 2015 in:

Scientific Reports 5, 12915 (2015).

DOI: 10.1038/srep12915

Link: <https://doi.org/10.1038/srep12915>

Involvement of the author within this publication: Project planning (65%), project execution (95%), data analysis (95%), writing of the manuscript (80%).

SCIENTIFIC REPORTS

OPEN Formation of highly toxic hydrogen cyanide upon ruby laser irradiation of the tattoo pigment phthalocyanine blue

Received: 20 March 2015

Accepted: 14 July 2015

Published: 05 August 2015

Ines Schreiber¹, Christoph Hutzler¹, Peter Laux¹, Hans-Peter Berlien² & Andreas Luch¹

Since laser treatment of tattoos is the favored method for the removing of no longer wanted permanent skin paintings, analytical, biokinetics and toxicological data on the fragmentation pattern of commonly used pigments are urgently required for health safety reasons. Applying dynamic headspace—gas chromatography with mass spectrometric detection (DHS—GC/MS) and comprehensive two-dimensional gas chromatography coupled to time-of-flight mass spectrometry (GCxGC—ToF-MS), we identified 1,2-benzene dicarbonitrile, benzonitrile, benzene, and the poisonous gas hydrogen cyanide (HCN) as main fragmentation products emerging dose-dependently upon ruby laser irradiation of the popular blue pigment copper phthalocyanine in suspension. Skin cell viability was found to be significantly compromised at cyanide levels of ≥ 1 mM liberated during ruby laser irradiation of >1.5 mg/ml phthalocyanine blue. Further, for the first time we introduce pyrolysis-GC/MS as method suitable to simulate pigment fragmentation that may occur spontaneously or during laser removal of organic pigments in the living skin of tattooed people. According to the literature such regular tattoos hold up to 9 mg pigment/cm² skin.

Inserting inorganic or organic pigments into the dermis for the purpose of tattooing or permanent make-up represents an unbroken modern trend world-wide^{1,2}. At the same time, dramatically increasing numbers of tattooed people result in a similarly increasing demand for laser removal of tattoo pictures and designs that occasionally become subject of embarrassment and deepest regret later in life^{1,3}. In this regard the potential risk for pigment cleavage into toxic or carcinogenic fragments upon tattoo laser treatment or even just during the exposure of skin to regular light (e.g. while sunbathing) are increasingly recognized as a serious health-related issue^{1,4-7}. Due to insufficient research, the identity of the possible chemical descendants and their long term effects when being released into systemic distribution throughout the human body remains unclear. Data on laser decomposition of pigments used in tattoo inks are available for a few azo dyes only⁵⁻⁸. On the other hand, there is a complete lack of data that would look into the decomposition and fate of rather lightfast molecule species such as phthalocyanines, in particular when it comes to the irradiation of cutaneous pigment deposits with medical lasers.

To the best of our knowledge copper phthalocyanine (also called phthalocyanine blue or pigment B15:3) is the only blue organic pigment currently used in tattoo inks on the European market⁹. Yet data regarding its safety as tattoo pigment and its decomposition behavior are presently not available. At the least, a most recent review cited two unpublished studies (PhD theses) that failed to detect any fragmentation of highly lightfast pigments including copper phthalocyanine upon irradiation with ultraviolet (UV) or visible (VIS) light¹⁰. In contrast to the well-known UV/VIS-induced photolysis of azo

¹German Federal Institute for Risk Assessment (BfR), Department of Chemical and Product Safety, Max-Dohrn-Strasse 8-10, 10589 Berlin, Germany. ²Evangelical Elisabeth Hospital, Department of Laser Medicine, Lützowstrasse 24-26, 10785 Berlin, Germany. Correspondence and requests for materials should be addressed to A.L. (email: Andreas.Luch@bfr.bund.de or luch@mit.edu)

dyes, color fading upon laser irradiation of tattoo pigments is therefore assumed to be rather the result of heat-dependent chemical decomposition (photothermolysis) and the breakup of particles followed by cellular clearance (i.e. phagocytosis by macrophages)⁶. Since laser irradiation of tattoo pigments can produce local temperatures exceeding 1,000 °C, the fracturing of the particles by steam-carbon reactions will be induced^{11,12}. All of these assumptions are supported by the observation that only empty tissue vacuoles can be found in upper dermal layers directly after laser irradiation, whereas smaller fragmented particles remain in the mid dermal layers accompanied by mild infiltration of macrophages¹³. Hence chemical decomposition toward atomization is thought to be the main cause of pigment fading in laser treatments¹³.

In clinical dermatology amongst others ruby lasers are commonly used for the irradiation of colored tattoos¹⁴. Since they are particularly effective in the treatment of blue pigments, marked heat-dependent decomposition is likely to occur. To achieve the required high temperatures selectively inside the pigment deposits and—at the same time—preventing any major heat transfer to the surrounding tissue, short pulsed q-switched or the newly developed picosecond lasers are now common practice^{15,16}.

In our study we applied pyrolysis conditions to mimic the laser-induced and temperature-dependent decomposition of the blue pigment copper phthalocyanine. Online coupling to gas chromatographic (GC) separation of the occurring fragmentation products and subsequent mass spectrometric (MS) analyses enabled us to identify all emerging volatile descendants based on available mass spectra libraries. To prove the relevance of the detected decomposition product pattern of copper phthalocyanine, we conducted q-switched ruby and neodymium-doped yttrium aluminium garnet (Nd:YAG) laser irradiation experiments, the latter of which is also used in dermatology for the purpose of tattoo removal¹⁴. Since pyrolysis-GC/MS (Py-GC/MS) analyses also provided evidence for the occurrence of very volatile and highly toxic compounds such as hydrogen cyanide (HCN) and benzene, we further developed a dynamic headspace (DHS) method to avoid any significant loss of the volatile compounds during work-up and analysis. By applying DHS along with two-dimensional gas chromatography coupled to time-of-flight mass spectrometry (GCxGC—ToF-MS) we were then able to sensitively and specifically address all of the expected compounds irrespective of their tendency to vaporize.

The detection and unambiguous identification of the highly toxic gas HCN further prompted us to investigate whether its level released via laser decomposition of copper phthalocyanine would be high enough to induce cellular toxicity. To this end we applied cyanide (CN⁻) concentrations that corresponded to the range of HCN released upon laser cleavage of pigment B15:3 and measured the inhibition of the mitochondrial electron transport chain via declining ATP levels in HaCaT cells *in vitro*. In summary the present work is the first that proves the occurrence of hazardous compounds upon laser-induced decomposition of the lightfast tattoo pigment copper phthalocyanine at concentrations high enough to produce cellular harm.

Results

Pyrolysis-GC/MS of copper phthalocyanine blue. Using an online coupling to GC/MS we identified HCN, 1,2-benzene dicarbonitrile (BDCN), benzonitrile (BCN), and 2-butanone as the four main cleavage products of pigment B15:3 upon pyrolysis at ≥ 800 °C (Fig. 1a). Since the latter is often added as solvent its presence is likely a remainder from pigment synthesis. In addition, some traces of benzene also emerged in the pyrograms at temperatures > 800 °C. In contrast to 2-butanone, levels of HCN, BDCN, BCN and benzene were increasing with pyrolysis temperature, thus confirming their occurrence as specific degradation products (Fig. 1b–d). Commercially available standards for HCN (including its isotopes) and BDCN were used for the identification of pyrolysis-dependent descendants of the pigment. Further, retention times and mass spectra were identical to those peaks identified as HCN and BDCN by library comparison. Whereas the decomposition of pigment B15:3 into BDCN has been already shown by a previous study¹⁷, additional formation of the lower molecular weight compounds BCN and benzene, and the gaseous HCN has remained undiscovered yet (Fig. 2).

Laser irradiation of copper phthalocyanine blue. To investigate whether the decomposition patterns are similar under various laser treatment scenarios applied in cosmetic dermatology, water-based pigment dispersions of pigment B15:3 were either treated with multiple quantities of ruby (5 J/cm², spot size 5 mm, 694 nm) or Nd:YAG (5 J/cm², spot size 3 mm, at 1,064 nm or 532 nm) laser pulses. Subsequent to laser irradiations quantitative analysis of both volatiles HCN and benzene was carried out using a DHS-GC/MS method, whereas screening and quantification of the other fragments (i.e. BDCN, BCN) were carried out by extraction with ethyl acetate followed by GCxGC-ToF-MS analysis. So, HCN, BCN and BDCN levels were all found increasing as a function of the number of ruby laser beams applied and the initial pigment concentrations (Fig. 3a–c). On the other hand, quantitative analysis of benzene revealed kind of challenging due to its occurrence only in traces and the necessity for an adaptation of the analytics applied (which were intentionally optimized to target CN-containing compounds). Nevertheless we were able to detect 0.32 μ M (25.1 ng/ml) benzene after three ruby laser irradiation pulses applied to 1 mg pigment B15:3 per ml suspension (mean out of n = 3). With this we experimentally confirmed the occurrence of all intermediates in the degradation pathway of phthalocyanine blue according to theoretical and reasonable predictions (Fig. 2). We further demonstrated that the decomposition

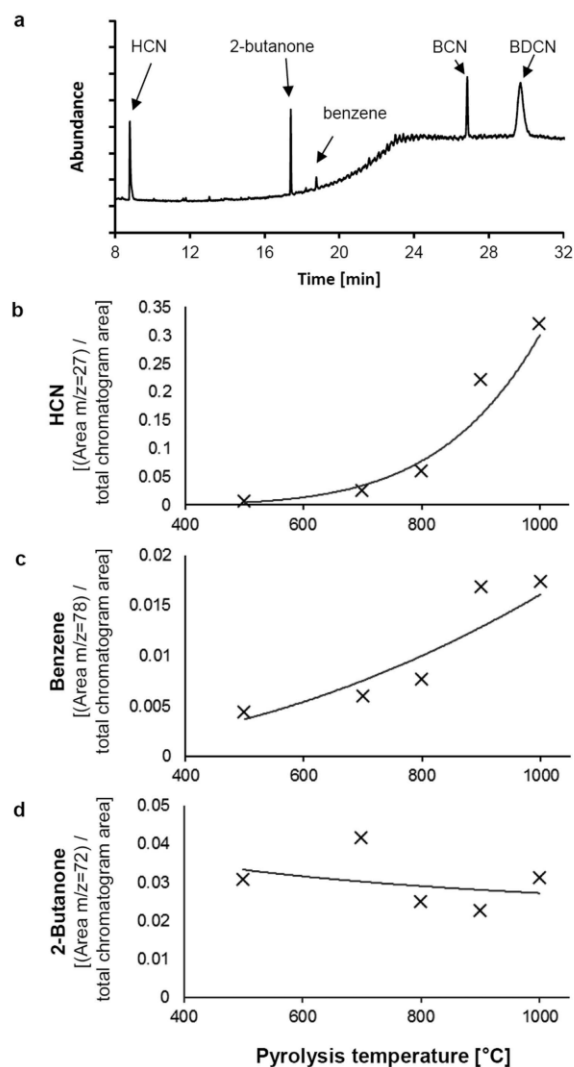


Figure 1. Phthalocyanine blue (pigment B15:3) is cleaved into BDCN, BCN and HCN upon pyrolysis. (a) Py-GC/MS chromatogram (1,000 °C) of pigment B15:3. BDCN, BCN, HCN, and 2-butanone represent the main compounds detected. Some tiny amounts of benzene were also detectable at temperatures > 800 °C. (b)–(c) Temperature-dependent formation of HCN and benzene during Py-GC/MS analysis of the pigment phthalocyanine blue (pigment B15:3). The values shown represent extracted ion areas of (b) HCN ($m/z = 27$), (c) benzene ($m/z = 78$), and (d) 2-butanone ($m/z = 72$) that have been normalized to the total chromatogram area. Therefore, absolute numbers do not correlate to peak areas of all ion fragments of the molecules included (cf. Fig. 1a). Similar as with BCN and BDCN (data not shown), HCN and benzene formation increases with pyrolysis temperature while levels of 2-butanone did not.

products in aqueous suspensions of pigment copper phthalocyanine upon ruby laser irradiation correlate well with those found in the corresponding Py-GC/MS analyses (cf. above).

By contrast, decomposition of pigment B15:3 was only low under Nd:YAG laser irradiation at both wavelengths applied (Fig. 3a–c). This can be explained in view of the absorption spectrum of pigment B15:3 which displays maxima in the visible spectrum at wavelengths between 550–800 nm (orange to red), thus being beyond the zone of coherent green light (532 nm) as emitted by the frequency doubled Nd:YAG laser (Fig. 4)^{18,19}. With regard to its absorption behavior at 1,064 nm there is repeated proof in the literature that the pigment copper phthalocyanine does not undergo molecular vibrations in the near-infrared and hence is unable to absorb significant amounts of light in this part of the spectrum^{20,21}.

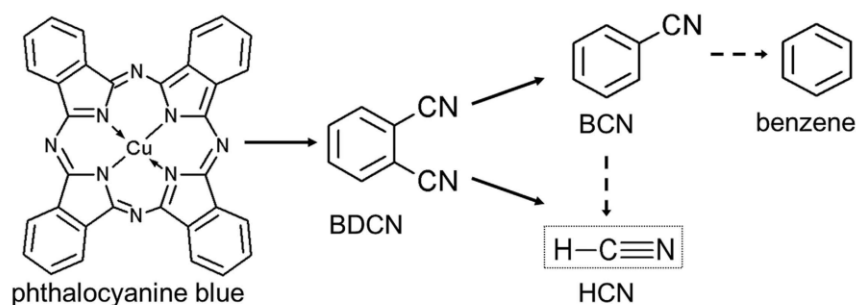


Figure 2. Decomposition pattern of phthalocyanine blue (pigment B15:3) based on the pyrolysis and laser irradiation data presented.

The observed non-linear increases (saturation) in the levels of decomposition products formed upon laser irradiation (Fig. 3d) were—at least in part—due to the visible carbonization of the UV/VIS cuvettes occurring after multiple laser pulses (Fig. 3e). Similar to the whitening of the skin that occurs during tattoo laser removal, the light is being scattered at the damaged cuvette surface, resulting in a reduced transmission of laser energy to the pigment suspension. On the other hand, the color intensity of treated samples was slightly increasing after multiple laser pulses (Fig. 3e), an observation most likely due to the reduction of particle sizes that is known to result in higher color brilliance²². Declining particle sizes upon laser irradiation have been previously described by Ferguson *et al.*¹³.

***In vitro* toxicity of HCN on human skin cells.** We further looked into the cellular toxicity of HCN and observed significantly decreasing amounts of ATP at CN^- concentrations that lay in the range of the HCN levels detected after ruby laser irradiation of concentrated (>1.5 mg/ml) pigment dispersions (cf. Fig. 3a with Fig. 5a). Compromised cellular ATP synthesis results from the high binding affinity of CN^- to trivalent iron ions (i.e. Fe^{3+}), which are part of the heme prosthetic group of cytochrome c oxidase in the mitochondrial electron transport chain and essentially required in the course of cellular ATP generation^{23,24}. To assess cellular toxicity human HaCaT cells were exposed to increasing concentrations of sodium cyanide (NaCN) in 96-well plates (note: NaCN completely dissolves into Na^+ and CN^- ions in aqueous solution). A significant decrease of cellular ATP levels was detected in cells treated with ≥ 1 mM CN^- when compared to controls (Fig. 5a). To verify the initial concentrations added and to rule out significant complexation of CN^- ions by Fe^{3+} in the media, samples were analyzed for HCN release upon acidification using DHS–GC/MS. Initial HCN concentrations quantified in the cell culture media at pH 7.4 nicely correlated to the added amounts of NaCN but were found subsequently depleted to 30–50% due to the outgassing of HCN during 30 min of incubation at 37 °C (Fig. 5b)²⁵. The reasoning for the assessment of cellular toxicity after 30 min of incubation was based on both practical considerations in the performance of the assay as well as the kinetics of HCN outgassing vs. its possible tissue distribution. So, 30 min was considered an appropriate time-point mimicking the *in vivo* situation where local HCN concentrations would be diluted throughout tissue layers. The reduction of HCN concentrations down to 50% due to outgassing was another factor to be considered. Yet it seemed likely that this value found in aqueous solution *in vitro* could be also much lower in cornified skin *in vivo*.

Discussion

Here we provide evidence for the suitability of Py–GC/MS analysis of tattoo pigments as reliable and predictive method for the generation and identification of chemical decomposition patterns that are likely to emerge upon laser irradiation of tattooed skin. Both q-switched ruby (694 nm) laser irradiation and pyrolysis-mediated fragmentation of the blue pigment copper phthalocyanine result in the same pattern of main cleavage products (i.e. benzene, BCN, BDCN, and HCN). Conversely, larger quantities of fragmentation products have neither been detected by applying the 1,064 nm nor the frequency-doubled 532 nm wavelength of an Nd:YAG laser. Since copper phthalocyanine is unable to absorb significant amounts of visible (green) light at 532 nm or infrared light at 1,064 nm^{20,21}, it does not come as surprise that Nd:YAG lasers at these wavelengths reveal ineffective in clinical dermatology when it comes to the removal of blue colored tattoos²⁶. While increasing concentrations of both benzene and HCN under ruby laser irradiation indicate the generation of temperatures in pigment deposits of at least 800 °C (cf. Fig. 1b,c), due to insufficient absorption Nd:YAG laser irradiation fails to generate temperatures high enough to cause particle fracturing¹¹.

Among all of the compounds emerging upon ruby laser irradiation of copper phthalocyanine, HCN is of particular relevance due to its strong cellular toxicity. It has long been known as colorless, rapidly acting highly toxic gas (*bp* 26 °C)^{27,28}. HCN was first prepared in 1782 by the Swedish chemist Carl Wilhelm Scheele from the dye “Prussian blue” (that is, “Berlin blue” or iron-III ferrocyanide: $[\text{Fe}_4[\text{Fe}(\text{CN})_6]_3]$)

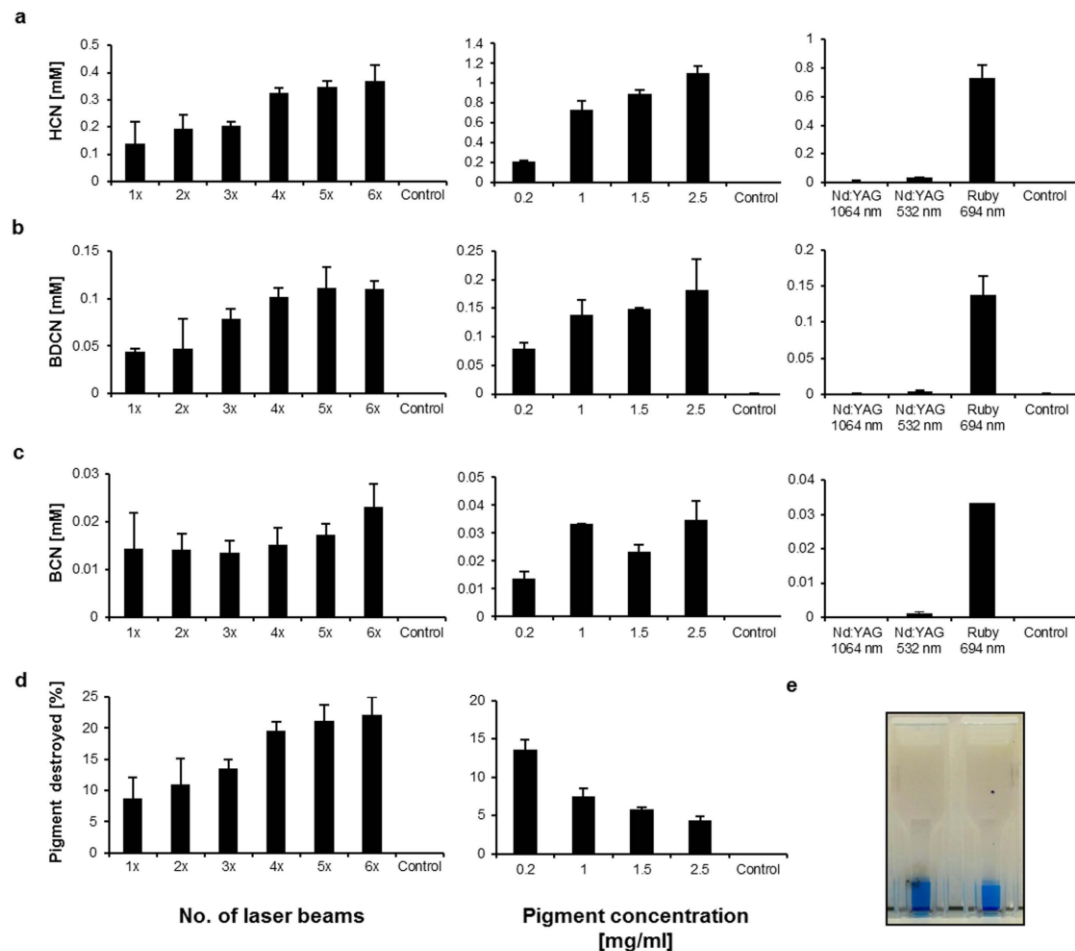


Figure 3. Phthalocyanine blue (pigment B15:3) is cleaved into BDCN, BCN and HCN upon laser irradiation. (a)–(c) left: Levels of BDCN, BCN and HCN depending on the number of applied ruby laser pulses (1× to 6×; initial pigment concentration used: 0.2 mg/ml; control = no laser beam). (a)–(c) middle: BDCN, BCN and HCN levels as function of the initial pigment concentration (0.2 mg/ml to 2.5 mg/ml; at each concentration 3 laser pulses applied; control = no pigment). (a)–(c) right: Only slightly increased fragment concentrations were found upon Nd:YAG laser irradiation when compared to ruby laser irradiation (3 laser pulses at 1 mg/ml pigment; control = no laser beam). (d) left: Fraction (in %) of pigment destroyed depending on the number of ruby laser pulses applied (1× to 6×; initial pigment concentration used: 0.2 mg/ml; control = no laser beam). (d) right: Fraction (in %) of pigment destroyed depending on the initial pigment concentration (0.2 mg/ml to 2.5 mg/ml; at each concentration 3 laser pulses applied; control = no pigment). (e) UV/VIS cuvette after 3 laser pulses (left) compared to an untreated sample (right) containing 0.2 mg/ml of pigment B15:3 each. The laser-treated sample is carbonized at the outer cuvette surface but appears more intensely blue colored (see text for further details). All values are displayed as mean ± SD (n = 3).

and therefore also named “prussic acid”²⁹. Depending on the concentration inhaled, it can cause toxic effects and death from cardiac arrest within seconds^{30,31}. The lethal dosage of HCN in most animal species is about 2 mg/kg body weight, and 50 ppm (0.005%) the concentration in air officially announced as “immediately dangerous to life or health” (IDLH) in humans³². From the toxicological point of view any possible emerging of HCN during laser removal of skin pigment deposits in tattooed individuals is thus to be regarded as health concern.

Here we demonstrate that the cell toxicity of HCN actually occurs in human skin cells *in vitro* at concentrations that lie in the range of the levels observed as result of ruby laser-mediated cleavage of copper phthalocyanine. According to the literature, minimum toxic concentrations of CN^- measured *in vitro*

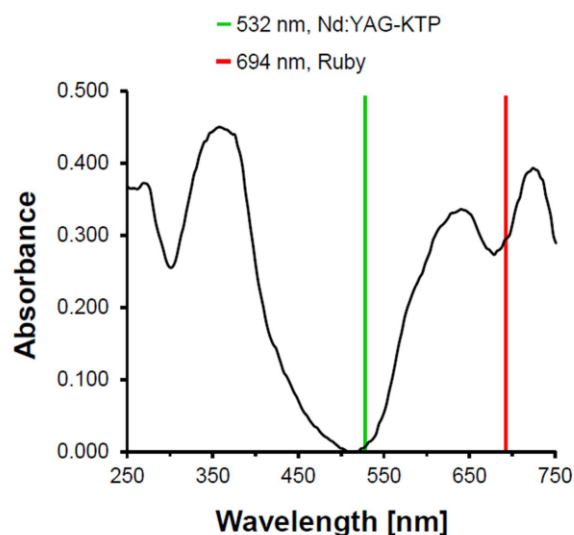


Figure 4. Absorption spectrum of pigment B15:3 at UV/VIS light. Wavelengths of ruby laser (694 nm) and the frequency doubled Nd:YAG (532 nm) are indicated by red and green lines, respectively.

range from 100 μM to 10 mM depending on the various experimental set-ups that may differ in their extent of HCN outgassing²⁵. Delhumeau and coworkers showed an inhibition of the cytochrome c oxidase at 250 μM potassium cyanide (KCN) in an activity test applying purified protein³³. So, the levels of about 0.2–1.1 mM HCN that were dose dependently formed upon ruby laser treatment of 0.2–2.5 mg/ml pigment in suspension lie well within and beyond the concentration range of this compound shown to exert cellular toxicity. In this regard it is to be noted that the average tattooed individual usually features 100–300 cm^2 of tattooed skin surface with pigment deposits that can range from 0.6 to 9.42 mg/ cm^2 , depending on the experience of the tattooist^{1,3}. (Note: The whole-body surface of an adult covers approximately 2 m^2). Thus, the levels of chemical hazards such as HCN emerging upon laser removal of tattoos in human skin *in vivo* may greatly vary as function of tattoo size, pigment concentration and localization, irradiation dose (fluence) and wavelength applied. Still, levels as high as 1.1 mM HCN, measured in our study upon irradiation of 2.5 mg/ml pigment dispersion *in vitro*, would correspond to 29.7 μg HCN per ml of volume. Although the most common ways of cyanide poisoning are ingestion and inhalation, percutaneous absorption has also been repeatedly described for injured skin^{34,35}, but also in non-injured skin³⁶. Given an estimated level of 5 $\mu\text{g}/\text{ml}$ cyanide in blood as lethal concentration³⁷, local concentrations of about 30 $\mu\text{g}/\text{ml}$ HCN that might be generated within tissue layers well supplied with blood vessels may trigger some concern, in particular when extremely large tattoos will be irradiated. Of course, the laser impact and its shattering efficiency on the pigments as well as the biokinetics of possibly emerging HCN in living skin tissue are currently unknown but certainly require urgent investigation in the future ahead.

Even though its concentrations measured upon ruby laser-induced pigment degradation were comparably low, the occurrence of the volatile aromatic hydrocarbon benzene further adds to these health concerns. According to U.S. EPA benzene is a “known human carcinogen by all routes of exposure”³⁸. Induction of acute non-lymphocytic leukemia and other blood disorders such as aplastic anemia have been sufficiently supported only in highly exposed human workers via the inhalation route though.

Altogether our findings suggest that, in the course of laser removal, lightfast organic pigments such as copper phthalocyanine might be cleaved into toxic fragments in quantities likely to be capable of harming the integrity of patients’ skin locally and potentially also other tissues in the body systemically. Further studies applying real human skin tissue specimens *ex vivo* are necessary and will be conducted to shed further light on the issue of emerging HCN and benzene levels as consequence of the laser irradiation of blue colored pigment deposits in real human skin. Modifying interactions with cell or tissue constituents are well be conceivable and might lead to alterations of the decomposition pattern qualitatively (chemical composition) as well as quantitatively. In any case, however, in view of the data presented the consideration of possible cleavage products of tattoo pigments in the frame of future tattoo ink regulation becomes mandatory.

Methods

Chemicals and reagents. All chemicals, analytical standards and solvents used were of analytical or LC–MS grade. Potassium cyanide-¹³C-¹⁵N (isotope purity 99% and 98%, respectively), sodium cyanide (NaCN), sodium hydroxide (NaOH), benzene, benzene- d_6 (isotope purity 97%), 1,2-benzene

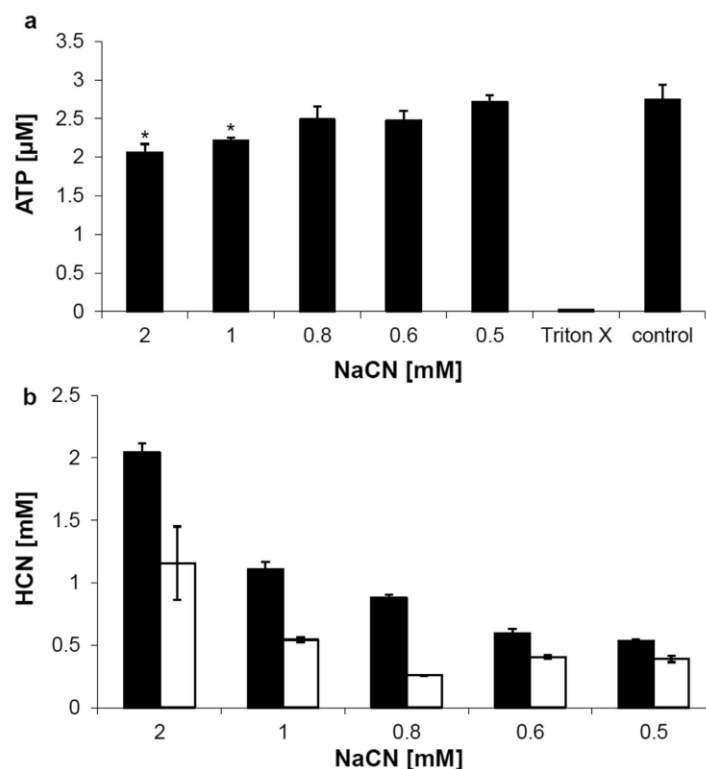


Figure 5. Toxicity of NaCN (respectively CN^- ions) in HaCaT cells *in vitro*. (a) ATP levels in cells treated with various doses of NaCN for 30 min in 96-well plates sealed with parafilm and compared to the control (that is, a 1:10 dilution of 5×10^{-6} N NaOH); Triton X was used as death control to verify depletion of ATP under toxic conditions. Values are displayed as mean \pm SD ($n=4$) for all groups except 0.6 mM NaCN ($n=3$). Average ranks in control cells and cells treated with 1 mM and 2 mM NaCN were 6.5 and 2.5, respectively (Mann-Whitney U-Test, $p=0.029$ two-tailed, $*p < 0.05$). Ranked, unequal variance *t*-test resulted in $p=0.005$ and $p=0.013$ for cells treated with 2 mM and 1 mM NaCN when compared to the controls, respectively. (b) HCN recovery from cell culture media before (black bars) and after 30 min of incubation at 37°C (light bars). Prior to incubation, varying doses of NaCN were added to the media as indicated. Values are displayed as mean \pm SD ($n=3$).

dicarbonitrile (BDCN), benzonitrile (BCN), benzylnitrile (BenzCN) and benzylalcohol (BenzOH) were obtained from Fluka/Sigma-Aldrich (Munich, Germany). Pigment B15:3 (C.I. 74160, m.w. 576.02; *mp* 600°C) was kindly provided from Clariant as trade name product PV Fast Blue (Frankfurt, Germany). Ethyl acetate was purchased from Merck (Darmstadt, Germany).

GC/MS. If not described differently, the Agilent 7890A gas chromatograph was coupled to an Agilent 5975C inert XL MSD with Triple-Axis Detector (Agilent Technologies, Santa Clara, CA, USA). Ionization was induced by an inert electron impact (EI) ion source at 70 eV and helium (purity of 99.999%) from Air Liquide (Düsseldorf, Germany) was used as carrier gas.

Pyrolysis–GC/MS of pigment B15:3. For Py–GC/MS analysis an HP-Plot/Q 30 m long column with a stationary phase of 0.32 mm thickness and 20 μm i.d. (Agilent Technologies, Santa Clara, CA, USA) was used. Small samples of pigment B15:3 were directly placed inside a glass tube which were then automatically inserted to the pyrolysis module at the thermal desorption unit (TDU) (both from Gerstel, Mühlheim, Germany) of the GC/MS inlet system. Pyrolysis was carried out at temperatures of 500–1,000°C for 6 s. The temperature of the cold injection system (CIS), TDU and transfer line was maintained at 260°C. The carrier gas flow rate was 1 ml/min using a split ratio of 1:30. The GC oven was kept at 50°C for 2 min and afterwards ramped at 10°C/min to 260°C which was then held for 10 more minutes. The mass range was scanned in full scan mode from 10 to 550 m/z. Fragments were identified using a library of standards (US-NIST – National Institute of Standards and Technology – 2011 MS Library). Match and rematch for HCN, BCN and BDCN were above 900 on a scale to 999 being

the best possible match. Data were analyzed using Enhanced ChemStation (E02.02.1431) from Agilent Technologies.

Pigment dispersion and laser irradiation. Varying amounts of pigment B15:3 per ml ultrapure water (18.2 M Ω -cm at 25 °C) containing 5×10^{-5} N NaOH were weighted into an ND18 20 ml brown glass vial (Neolab, Heidelberg, Germany). A pH of ≥ 10 was ensured to prevent premature outgassing of emerging HCN during laser irradiation. For analysis of benzene, 1 mg/ml pigment B15:3 were weighted in ultrapure water without addition of NaOH. The dispersions were shaken vigorously by hand and then placed into a sonorex digitec ultrasonic water bath with 50/60 Hz (Bandelin Electronic, Berlin, Germany) for 60 min for further dispersion. The vials were shaken repeatedly to ensure best dispersion of pigment agglomerates which tend to stick at the walls or the caps of the vials. Then 200 μ l of the dispersion was transferred into semi-micro UV/VIS cuvettes (Brand, Wertheim, Germany) and closed with polypropylene caps (Ratiolab, Dreieich, Germany). Samples were treated with multiple quantities of q-switched ruby (5 J/cm², spot size 5 mm, pulse duration 20 ns, 694 nm, Sinon, WaveLight, Erlangen, Germany) or Nd:YAG (5 J/cm², spot size 3 mm, pulse duration > 20 ns, at 1,064 nm or 532 nm, Revlight SI, Cynosure, Westford, MA, USA) laser pulses and then placed on ice until further processing.

DHS–GC/MS method for HCN and benzene quantification. NaCN standard substance was dissolved in aqueous 0.02 N NaOH to prevent outgassing. The basic solution was stored at -20 °C and freshly thawed right before usage. For further dilution, water containing 5×10^{-5} N NaOH was used to guarantee a pH value of 10. One ml of a standard solution or a 1:5 dilution of the laser sample was then transferred into an ND18 20 ml brown glass vial (Neolab, Heidelberg, Germany) and 10 μ l of a stock solution of 100 μ g/ml K¹³C¹⁵N were added as internal standard. The cap on top of the vial was screwed firmly and 50 μ l of 30% phosphoric acid was then added through the septum using a 100 μ l Hamilton syringe (Neolab, Heidelberg, Germany). The last step guaranteed protonation of dissolved cyanide ions to form gaseous HCN. Samples designated for benzene quantification were directly processed after laser irradiation. To this end, 200 μ l of the irradiated pigment dispersion was transferred into an ND18 brown glass vial (20 ml) containing 800 μ l of 5×10^{-5} N NaOH and screwed immediately. Benzene-d₆ was added as internal standard through the septum using a Hamilton syringe to achieve a final concentration of 5 ng/ml. Prior to the laser experiments the linearity of benzene quantification was confirmed within the range of 1 to 500 ng/ml, and a one-point calibration for the test samples was carried out. For subsequent DHS–GC/MS analysis of HCN and benzene an HP-Plot/Q system (Agilent Technologies, Santa Clara, CA, USA) was used (cf. above). Samples were incubated for 3 min at 30 °C before trapping the gas phase on a Carboxen B+X/Carboxen-1000 desorption liner (Gerstel, Mühlheim, Germany) with agitation. The trapping of samples was carried out with a volume of 100 ml N₂ gas and a flow rate of 50 ml/min. Analytes were desorbed from the liner in a TDU (Gerstel, Mühlheim, Germany) and cryofocused in a CIS at -50 °C. After 12 s the temperature of the CIS was increased to 40 °C and held for 5.5 min followed by a second increase to 240 °C which was held for additionally 5 min. TDU and transfer line were kept constant at 260 °C. Injections were carried out in splitless mode. The initial oven temperature of 40 °C was held for 0.5 min and then heated by 10 °C/min up to 260 °C which was held for 10 more minutes. The mass range was scanned in the scan/single ion mode (SIM) from 10 to 350 m/z with acquisition ions 27, 28, 78 and 84 with a dwell time of 40 ms, respectively.

Based on the overall amount of HCN, BCN and BDCN measured upon laser irradiation the percent fraction of pigment B15:3 destroyed has been calculated in relation to the maximum possible release of CN residues per molecule pigment (that is, $8 \times \text{CN}$; cf. Fig. 2).

GCxGC-ToF-MS. The Pegasus 4D GCxGC-ToF-MS system (Leco, Mönchengladbach, Germany) was used for analysis of the extracts of the laser experiments. Rxi[®]-5Sil MS (20 m, 0.25 mm, 0.25 μ m i.d.) and Rxi[®]-17Sil MS (1 m, 0.18 mm, 0.18 μ m i.d.) columns (Restek, PA, USA) were arranged as first and second dimension columns, respectively. The initial oven temperature was set to 70 °C and remained for 1 min followed by the first ramp with 15 °C/min to 120 °C, the second ramp with 8 °C/min to 150 °C, and the third ramp with 25 °C/min to 330 °C, which was finally held for 4 min. Secondary oven temperature and modulator oven temperature were 5 °C and 15 °C higher relative to the oven temperature, respectively. The modulator period was 3.5 s with a hot pulse time of 1 s and a cool time period between 0.75 s and 13 min of the GC program and elongated to 4 s with a hot pulse time of 1.5 s till the end of the run. The chiller was cooled to -80 °C. Front inlet flow was 1 ml/min. The temperatures of the ion source and transfer line were set to 250 °C and 295 °C, respectively. Mass spectra were collected with an acquisition rate of 200 Hz in a mass range of 35–500 m/z. BCN and BDCN were quantified by using BenzCN and BenzOH as internal standards. To this end, 4 μ l of a mixture containing equal parts of BenzOH (2 μ g/ml) and BenzCN (0.5 μ g/ml) were added to 196 μ l sample and capped in a 2 ml glass vial. After extraction with 200 μ l ethyl acetate for 1 hour while shaking, 1.5 μ l of the extract were analyzed using GCxGC-ToF-MS.

Cytotoxicity assay. HaCaT cells were grown in Dulbecco's modified Eagle medium (DMEM) with 1 g/l glucose plus 5% fetal bovine serum (FBS) supplemented with penicillin/streptomycin (10,000 U/ml; 10 mg/ml) and 5 ml of L-glutamine (200 mM) until they reached 50% density in 96-well plates. All

reagents were purchased from PAH Biotech (Aidenbach, Germany). Prior to the assay, cells were washed with phosphate buffered saline (PBS) and DMEM without FBS was added to the wells. From a stock solution of 1 mg/ml NaCN dissolved in 5×10^{-6} N NaOH aliquots of no more than 10 μ l were directly transferred into the well with a pipette (dilution of 1:10). As controls, 10 μ l of 5×10^{-6} N NaOH without NaCN or 2 μ l of 1:10 Triton X were added to the cells. Subsequently 96-well plates were sealed with parafilm (Pechiney Plastic Packaging Inc., Washington, NJ, USA) and incubated for 30 minutes.

For the determination of ATP levels cells were treated as follows: Cultures were rinsed with 100 μ l PBS first. Then 50 μ l of lysis buffer (ATP Bioluminescence Assay Kit HS II; Roche Diagnostics, Mannheim, Germany) were added to the wells and further incubated for 5 min at room temperature followed by 2 min at 99 °C. Afterwards, 50 μ l PBS were added and plates were frozen and stored at -20 °C until further processing. Cell debris was separated by centrifugation at 5,000 g for 10 min (Thermo Scientific Haeareus Multifuge 1s-r, MA, USA) and 40 μ l supernatant was transferred into a white 96-well plate. Luminescence was analyzed without filters for 10 s in each well after automated injection of 40 μ l luciferase reagent.

UV/VIS Absorbance. Spectral absorbance of pigment B15:3 (2 μ l of an 0.2 mg/ml aqueous pigment dispersion) was measured using the NanoDrop® 1000 spectrophotometer (Peqlab, Erlangen, Germany) according to manufacturer's instructions.

Statistics and calculations. The results are presented as the mean values (mean \pm standard deviation (SD)). Data analyses were performed using IBM SPSS Statistics (Version 21, Armonk, NY, USA). Due to small sample sizes data were regarded as non-normally distributed and unequal in variances. Statistical significance was therefore tested using the non-parametrical Mann-Whitney U-Test for two independent samples. The exact 2-tailed significance was used for group comparison. Additionally, a ranked, unequal variance *t*-test was carried out. A *p*-value of <0.05 was considered significant and marked with an asterisk.

References

1. Laux, P. *et al.* A medical-toxicological view of tattooing. *Lancet*, published online July 24, 2015 ([http://dx.doi.org/10.1016/S0140-6736\(15\)60215-X](http://dx.doi.org/10.1016/S0140-6736(15)60215-X)).
2. Koch, J. R., Roberts, A. E., Cannon, J. H., Armstrong, M. L. & Owen, D. C. College students, tattooing, and the health belief model: extending social psychological perspectives on youth culture and deviance. *Sociol. Spectr.* **25**, 79–102 (2005).
3. Klügl, I., Hiller, K. A., Landthaler, M. & Bäumler, W. Incidence of health problems associated with tattooed skin: a nation-wide survey in German-speaking countries. *Dermatology* **221**, 43–50 (2010).
4. Carlsen, K. H. & Serup, J. Photosensitivity and photodynamic events in black, red and blue tattoos are common: A 'Beach Study'. *J. Eur. Acad. Dermatol. Venereol.* **28**, 133–262 (2013).
5. Engel, E. *et al.* Photochemical cleavage of a tattoo pigment by UVB radiation or natural sunlight. *J. Dtsch. Dermatol. Ges.* **5**, 583–589 (2007).
6. Engel, E. *et al.* Tattooing of skin results in transportation and light-induced decomposition of tattoo pigments—a first quantification *in vivo* using a mouse model. *Exp. Dermatol.* **19**, 54–60 (2010).
7. Vasold, R. *et al.* Tattoo pigments are cleaved by laser light—the chemical analysis *in vitro* provide evidence for hazardous compounds. *Photochem. Photobiol.* **80**, 185–190 (2004).
8. Cui, Y. *et al.* Photodecomposition of pigment yellow 74, a pigment used in tattoo inks. *Photochem. Photobiol.* **80**, 175–184 (2004).
9. Hauri, U. *Tinten für Tattoos und Permanent Make-Up / Pigmente, Konservierungsstoffe, Aromatische Amine, Polyaromatische Kohlenwasserstoffe und Nitrosamine* (2015). (Report on inks used in tattoos and permanent make-up. Available in German only at: <http://www.gesundheitsschutz.bs.ch/konsum-umwelt/berichte.html>. (Accessed at May 19, 2015))
10. Hauri, U. & Hohl, C. in *Tattooed Skin and Health*. Vol. 48 (eds Serup, J., Kluger, N., Bäumler, W.) 164–169 (Karger, 2015).
11. Ho, D. D. M., London, R., Zimmerman, G. B. & Young, D. A. Laser-tattoo removal—a study of the mechanism and the optimal treatment strategy via computer simulations. *Laser Surg. Med.* **30**, 389–397 (2002).
12. Taylor, C. R., Anderson, R. R., Gange, R. W., Michaud, N. A. & Flotte, T. J. Light and electron microscopic analysis of tattoos treated by Q-switched ruby laser. *J. Invest. Dermatol.* **97**, 131–136 (1991).
13. Ferguson, J. E., Andrew, S. M., Jones, C. J. P. & August, P. J. The q-switched neodymium:YAG laser and tattoos: a microscopic analysis of laser-tattoo interactions. *Br. J. Dermatol.* **137**, 405–410 (1997).
14. Bernstein, E. F. Laser tattoo removal. *Semin. Plast. Surg.* **21**, 175–192 (2007).
15. Ross, E. V. *et al.* Comparison of responses of tattoos to picosecond and nanosecond Q-switched neodymium:YAG lasers. *Arch. Derm.* **134**, 167–171 (1998).
16. Brauer, J. A. *et al.* Successful and rapid treatment of blue and green tattoo pigment with a novel picosecond laser. *Arch. Derm.* **148**, 820–823 (2012).
17. Russell, J., Singer, B. W., Perry, J. J. & Bacon, A. The identification of synthetic organic pigments in modern paints and modern paintings using pyrolysis–gas chromatography–mass spectrometry. *Anal. Bioanal. Chem.* **400**, 1473–1491 (2011).
18. Beute, T. C., Miller, C. H., Timko, A. L. & Ross, E. V. *In vitro* spectral analysis of tattoo pigments. *Dermatol. Surg.* **34**, 508–515 (2008).
19. Bäumler, W. *et al.* Q-switch laser and tattoo pigments: first results of the chemical and photophysical analysis of 41 compounds. *Laser Surg. Med.* **26**, 23–21 (2000).
20. Farag, A. A. M. Optical absorption studies of copper phthalocyanine thin films. *Opt. Laser Technol.* **39**, 728–732 (2007).
21. Mali, S. S. *et al.* Electro-optical properties of copper phthalocyanines (CuPc) vacuum deposit thin films. *RSC Advances* **2**, 2100–2104 (2012).
22. Bermel, A. D. & Bugner, D. E. Particle size effects in pigmented ink jet inks. *J. Imag. Sci. Technol.* **43**, 320–324 (1999).
23. Wikstrom, M. K. Proton pump coupled to cytochrome c oxidase in mitochondria. *Nature* **266**, 271–273 (1977).
24. Cooper, C. E. & Brown, G. C. The inhibition of mitochondrial cytochrome oxidase by the gasses carbon monoxide, nitric oxide, hydrogen cyanide and hydrogen sulfide: chemical mechanism and physiological significance. *J. Bioenerg. Biomembr.* **40**, 533–539 (2008).

25. Arun, P. *et al.* Rapid sodium cyanide depletion in cell culture media: outgassing of hydrogen cyanide at physiological pH. *Anal. Biochem.* **339**, 282–289 (2005).
26. Kilmer, S. L. & Anderson, R. R. Clinical use of the Q-switched ruby and the Q-switched Nd:YAG (1064 nm and 532 nm) lasers for treatment of tattoos. *J. Dermatol. Surg. Oncol.* **19**, 330–8 (1993).
27. Way, J. L. Cyanide intoxication and its mechanism of antagonism. *Ann. Rev. Pharmacol. Toxicol.* **24**, 451–481 (1984).
28. Daniell, J. B. History of a case of poisoning by prussic acid. *Prov. Med. Surg. J.* **12**, 428–431 (1848).
29. Scheele, C. W. Experiment concerning the coloring substance in Berlin blue (article in Swedish). *Royal Swed. Acad. Sci. Proc.* **3**, 264–275 (1782).
30. Huzar, T. F., George, T. & Cross, J. M. Carbon monoxide and cyanide toxicity: etiology, patho-physiology and treatment in inhalation injury. *Expert Rev. Respir. Med.* **7**, 159–170 (2013).
31. Centers of Disease Control and Prevention (CDC). *Facts about cyanide*. Available at: <http://www.bt.cdc.gov/agent/cyanide/basics/facts.asp>. (Accessed at September 15, 2014).
32. Centers of Disease Control and Prevention (CDC). *Documentation for Immediately Dangerous To Life or Health Concentrations (IDLHs): Hydrogen Cyanide*. Available at: <http://www.cdc.gov/niosh/idlh/74908.html>. (Accessed at September 15, 2014).
33. Delhumeau, G., Cruz-Mendoza, A. M. & Lojero, C. G. Protection of cytochrome c oxidase against cyanide inhibition by pyruvate and α -ketoglutarate: effect of aeration *in vitro*. *Toxicol. Appl. Pharm.* **126**, 345–351 (1994).
34. Bonnichsen, R. & Maehly, A. C. Poisoning by volatile compounds 3. Hydrocyanic acid. *J. Forensic Sci.* **11**, 516–528 (1966).
35. Karhunen, P. J., Lukkari, I. & Vuori, E. High cyanide level in a homicide victim burned after death: evidence of *post-mortem* diffusion. *Forensic Sci. Int.* **49**, 179–183 (1991).
36. Seidl, S., Schwarze, B. & Betz, P. Lethal cyanide inhalation with *post-mortem* trans-cutaneous cyanide diffusion. *Leg. Med.* **5**, 238–241 (2003).
37. Chikasue, F. *et al.* Cyanide distribution in five fatal cyanide poisonings and the effect of storage conditions on cyanide concentration in tissue. *Forensic Sci. Int.* **38**, 173–183 (1988).
38. United States Environmental Protection Agency. *Carcinogenic effects of benzene: an update*. Available at: <http://cfpub.epa.gov/ncsa/cfm/recordisplay.cfm?deid=2806>. (Accessed at May 18, 2015).

Acknowledgements

This work was supported by the intramural research project (SFP No. 1322-536) at the German Federal Institute for Risk Assessment (BfR). Laser equipment was provided by the Evangelical Elisabeth Hospital in Berlin.

Author Contributions

C.H., I.S., P.L. and A.L. designed the study. I.S. and H.P.B. performed the experiments. I.S., C.H., P.L. and A.L. critically reviewed the data and wrote the manuscript. C.H. and A.L. supervised the entire study, including design, execution and interpretation of instrumental analytics and *in vitro* experiments.

Additional Information

Competing financial interests: The authors declare no competing financial interests.

How to cite this article: Schreiber, I. *et al.* Formation of highly toxic hydrogen cyanide upon ruby laser irradiation of the tattoo pigment phthalocyanine blue. *Sci. Rep.* **5**, 12915; doi: 10.1038/srep12915 (2015).



This work is licensed under a Creative Commons Attribution 4.0 International License. The images or other third party material in this article are included in the article's Creative Commons license, unless indicated otherwise in the credit line; if the material is not included under the Creative Commons license, users will need to obtain permission from the license holder to reproduce the material. To view a copy of this license, visit <http://creativecommons.org/licenses/by/4.0/>

2.3. Tattoo laser removal releases carcinogens and sensitizers from organic pigments.

Ines Schreiber, Nadine Röder, Maria Gebhardt, Christoph Hutzler, Hans-Peter Berlien, Peter Laux, Andreas Luch

This chapter has not yet been submitted for publication.

Involvement of the author within this publication: Project planning (70%), project execution (70%), data analysis (90%), writing of the manuscript (90%).

Supplementary materials for the following publication are detailed in Annex II.

Tattoo laser removal releases carcinogens and sensitizers from organic pigments

Ines Schreiver¹, Nadine Röder, Maria Gebhardt, Christoph Hutzler¹, Hans-Peter Berlien², Peter Laux¹, and Andreas Luch¹

¹German Federal Institute of Risk Assessment (BfR), Department of Chemical and Product Safety, Max-Dohrn-Strasse 8–10, 10589 Berlin, Germany

²Evangelical Elisabeth Hospital, Department of Laser Medicine, Luetzowstrasse 24–26, 10785 Berlin, Germany

Abstract

Laser treatment represents the state-of-the-art method for tattoo removal. Carcinogenic substances deriving from azo pigments used for tattooing feed the current discussion about an impact of the procedure on skin cancer incidence. Conversely, the liberation of carcinogens and other toxins from non-azo pigments upon laser irradiation are widely unknown.

We here irradiated aqueous suspensions and *postmortem* tattooed pig skin containing six common organic tattoo pigments of various chemical classes with medical ruby and Nd:YAG lasers. Decomposition products were quantified by gas chromatography coupled to mass spectrometric detection. All pigments released hydrogen cyanide and benzene upon laser irradiation. Other carcinogens and sensitizing compounds such as 3,3'-dichlorobenzidine (DCBD), aniline and hexachlorobenzene were also found. Additionally, mixing the organic pigments with TiO₂ and the evaporation of volatile compounds from the *postmortem* tattooed pig skin were shown to alter the quantity of decomposition products.

The data presented fills knowledge gaps concerning general decomposition patterns of organic pigments upon laser irradiation and provides quantitative data for this exposition scenario. Using this data, it may be possible to estimate the role of laser-induced decomposition products in cancer formation. The potential of the substances identified to cause allergic reactions may be further investigated in future.

Introduction

The ever-increasing number of tattooed people world-wide is accompanied with a higher demand for tattoo removal. Long-term health effects associated with tattoos prior and after their removal are largely unknown today¹. Nowadays, tattoo removal is mostly carried out with short-pulsed color-matched laser systems. Accurately executed laser procedures convey only low risks of causing directly occurring local or systemic side effects². Besides skin damage induced by the use of too high laser fluences, tattoo darkening and allergies are the most common side effects³⁻⁶. In addition to these visible complications, chemical decomposition and therefore the release of small-molecular toxins from organic tattoo pigments has been perceived as risk factors⁷.

The clearance of tattoo pigments by laser light is partly due to their breakup into smaller particles, which are subsequently transported towards the regional lymph nodes⁸. On the other hand, photothermolysis-mediated cleavage of organic molecules usually leads to the loss of chromophore moieties^{9,10}. Since the tattoo pigments are localized in the deeper dermal layers of the skin, cleavage products may become fully bioavailable and thus represent a potential risk to human health.

In previous investigations, we have shown that pyrolysis can mimic the thermal decomposition of organic pigments that likely occur during laser removal of tattoos¹¹. Among others, carcinogenic primary aromatic amines were shown to be pyrolytically released from azo pigments and have also been reported in laser experiments in relevant literature^{12,13}. In addition, the quinacridone pigment red 202 has been reported to liberate 4-chloroaniline upon exposure to different light sources¹⁴. In one of our previous investigations, we were able to prove the dose-dependent formation of benzene and hydrogen cyanide (HCN) upon laser irradiation of copper (Cu)-phthalocyanine blue in aqueous suspensions¹⁵. Such findings illustrate that the quantification of possible decomposition products of tattoo pigments would be crucial for any proper and reliable risk assessment as prerequisite to future tattoo ink regulation.

In the present study, we selected six chemical structures covering the most important classes of organic pigments used in tattooing today. In addition to aqueous suspensions, pigments were irradiated in *postmortem* tattooed pig skin to mimic a more *in vivo*-like situation. Aqueous pigment suspensions enable the irradiation of reproducible quantities of pigments in a defined environment. Tattooed pig skin was chosen to examine the influence of the skin matrix on the decomposition patterns of pigments. We applied Q-switched lasers at three common wavelengths in different intensities that are regularly used for tattoo removal in humans. A short-term *in vivo* pig study was conducted to extrapolate differences of healed skin compared to our *postmortem* tattooed pig skin model. Additionally, the influence of TiO₂ on pigment decomposition was investigated.

Table 1: Laser decomposition products display different toxic properties upon skin exposure.

pigment	substance	comment	quantified	Toxicity (GHS)[#]	
all	HCN		yes	* Acute toxicity, Cat. 1, dermal	
	benzene		yes	* Carcinogenicity, Cat. 1A * Germ cell mutagenicity, Cat. 1B * Skin irritation, Cat. 2	
P.B.15	1,2-benzenedicarbonitrile		yes	* Acute toxicity, Cat. 2, oral	
	benzotrile		yes	* Acute toxicity, Cat. 4, dermal	
	phthalimide (m/z 147)	impurity		* -	
	1,3-benzenedicarbonitrile (m/z 128)			* Acute toxicity, Cat. 4, oral	
	benzenetricarbonitrile (m/z 153)			n.a.	
	biphenyldicarbonitrile (m/z 204)			n.a.	
P.Y.138	1,2,3,4-tetrachlorobenzene		yes	* Acute toxicity, Cat. 4, oral	
	pentachlorobenzene		yes	* Acute toxicity, Cat. 4, oral	
	xylene		yes	* Skin irritation, Cat. 2 * Acute toxicity, Cat. 4, dermal	
	HCB		yes	* Carcinogenicity, Cat. 1B	
	benzotrile		yes	* Acute toxicity, Cat. 4, dermal	
	unknown product (m/z 426)	also in control		* n.a.	
P.O.13	DCBD		yes	* Skin sensitizer, Cat. 1 * Carcinogenicity, Cat. 1B * Acute toxicity, Cat. 4, dermal	
	benzotrile		yes	* Acute toxicity, Cat. 4, dermal	
	aniline		yes	* Skin sensitizer, Cat. 1 * Carcinogenicity, Cat. 2 * Germ cell mutagenicity, Cat. 2 * Acute toxicity, Cat. 3, dermal	
	phenylisocyanate		yes	* Skin sensitizer, Cat. 1 * Skin corrosion, Cat. 1B * Acute toxicity, Cat. 4, oral	
	2-aminobenzotrile		yes	* Skin sensitizer, Cat. 1 * Skin irritation, Cat. 2 * Acute toxicity, Cat. 4, dermal	
	biphenyl		yes	* Skin irritation, Cat. 2	
	chlorobenzene		yes	* Skin irritation, Cat. 2 * Acute toxicity, Cat. 4, inhalation	
	PCB No. 11		yes	* -	
	2-chloroaniline		yes	* Acute toxicity Cat. 3, dermal	
	1-phenyl-3-methyl-5-pyrazolone (m/z 174)			* Skin irritation, Cat. 2 * Acute toxicity, Cat. 4, oral	
		3,3-dichlorobiphenyl-4-amine (m/z 237)		* n.a.	
	P.R.254	4-chlorobenzotrile		yes	* Skin irritation, Cat. 2 * Acute toxicity, Cat. 4, oral
		benzotrile		yes	* Acute toxicity, Cat. 4, dermal
		chlorobenzene		yes	* Skin irritation, Cat. 2 * Acute toxicity, Cat. 4, inhalation
3-chlorobenzamide			yes	* Skin sensitizer, Cat. 1 * Acute toxicity, Cat. 4, oral	
3-chlorobenzotrile			yes	-	
	4-chlorostyrene (m/z 136)			* -	
P.R.170	benzamide		yes	* Germ cell mutagenicity, Cat. 2 * Acute toxicity, Cat. 4, oral	
	4-aminobenzamide		yes	* Skin irritation, Cat. 2 * Acute toxicity, Cat. 4, oral	
	<i>o</i> -phenetidine (m/z 137)	also in control		* Acute toxicity, Cat. 3, dermal	
	benzotrile		yes	* Acute toxicity, Cat. 4, dermal	
	aniline		yes	* Skin sensitizer, Cat. 1 * Carcinogenicity, Cat. 2 * Germ cell mutagenicity, Cat. 2	

			Acute toxicity, Cat. 3, dermal
	1-cyanonaphthalene	yes	Skin irritation, Cat. 2 Acute toxicity, Cat. 4, dermal
	2-ethoxyphenylisocyanate (m/z 163)	also in control	* Skin irritation, Cat. 2 Acute toxicity Cat. 4, dermal
P.V.19	benzotrile	yes	Acute toxicity Cat. 4, dermal
	biphenyl	yes	Skin irritation, Cat. 2
	1-cyanonaphthalene	yes	Skin irritation, Cat. 2 Acute toxicity, Cat. 4, dermal
	aniline	yes	Skin sensitizer, Cat. 1 Carcinogenicity, Cat. 2 Germ cell mutagenicity, Cat. 2 Acute toxicity, Cat. 3, dermal
	2-amino-9-oxo-9,10-dihydroacridine-3-carbaldehyde (m/z 238)	also in control	* n.a.

*pyrolysis product¹¹

[#]Toxicity categories (cat.) listed according to the Globally Harmonized System of Classification and Labelling of Chemicals (GHS) most relevant to laser irradiation of pigments in skin

Abbreviations: n.a.= no data available

Results

Skin toxins evolve during laser irradiation of organic pigments

In order to determine the potential hazards due to laser tattoo removal, we selected six organic pigments based on their use in tattoo inks and by covering the most common chemical pigment classes. Selection for quantification of decomposition products was made dependent on their hazard potential for skin irritation, corrosion, sensitization, mutagenicity and carcinogenicity (Table 1). Additionally, some less toxic substances representing common products of pigment decomposition were quantified.

We applied Q-switched ruby as well as frequency-doubled and fundamental Nd:YAG lasers with wavelengths of 694 nm, 532 nm, and 1064 nm, respectively. These lasers are commonly used for tattoo removal and their success is partly dependent on the absorbance of the coherent laser light by the pigment (cf. Fig. 1a). In accordance to their absorbance spectra, pigment red (P.R.), orange (P.O.) and yellow (P.Y.) were primarily cleaved at 532 nm (Supplementary Tables 1-4). Pigment blue (P.B.) 15 was most effectively fragmented using the ruby laser and pigment violet (P.V.) 19 with both ruby and 532 nm Nd:YAG lasers (Supplementary Tables 5,6).

For all pigments investigated, we were able to confirm cleavage into the same main products regardless of whether pigments were placed in pig skin or suspended in water (Figure 1b, Supplementary Tables 1-6). The pigments used in our investigation were not quantified due to their lack of solubility and volatility, preventing an estimation of pigment clearance and the amounts tattooed into the pig skin. Only in the case of P.B.15, was it possible to assess the total content of pigment in pig skin prior to irradiation by means of Cu quantification, since it is the pigment's core element. Upon irradiation, 250 μ l of an aqueous suspension of P.B.15 contained 4–5 times more Cu compared to the pig skin biopsies of 4 mm thickness (Supplementary Fig. 1). The amount of pigment injected cannot be adequately monitored and therefore cannot be extrapolated with regard to the other pigments investigated. The pig skin sections in this investigation showed, that particularly the amount of P.V.19 in skin was much lower (Fig. 2).

Figure 1: Scheme of the six investigated organic pigments.

a) Absorption spectra of the investigated pigments recorded with a NanoDrop 1000 spectrophotometer (Peqlab, Erlangen, Germany). b) Cleavage patterns may be used to predict the decomposition of non-tested organic pigments with structural similarities.

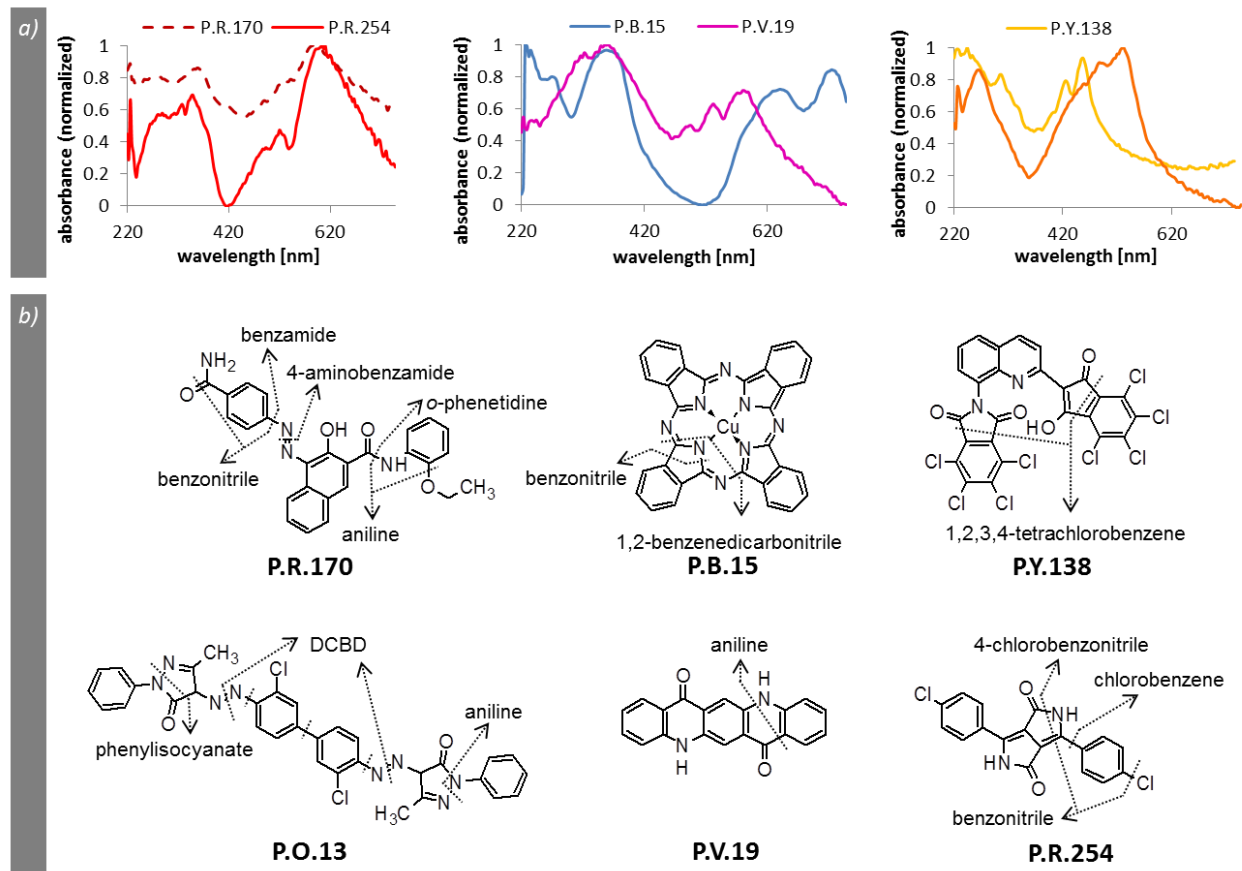
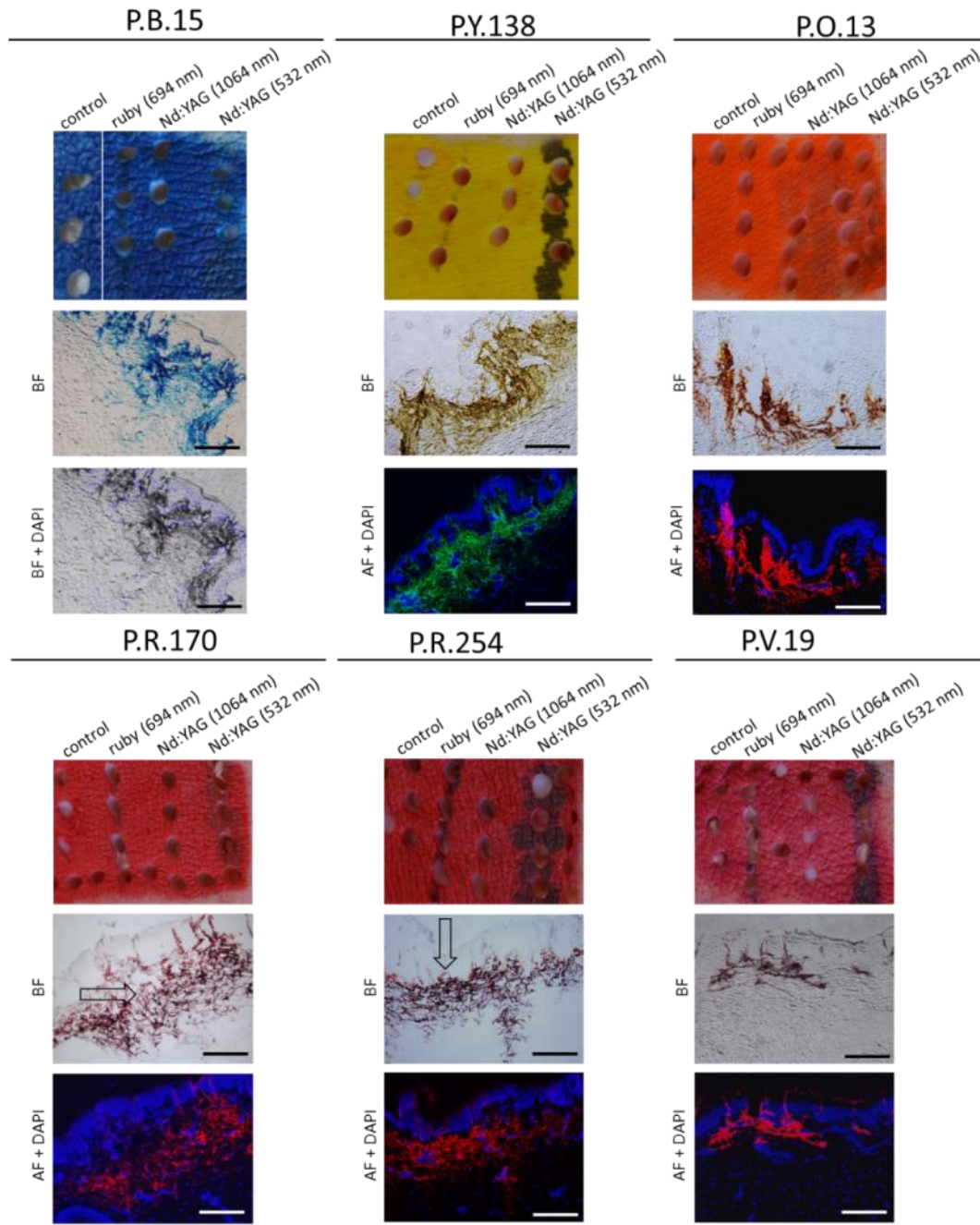


Figure 2: Laser irradiation of *postmortem* tattooed pig skin leads to visible carbonization.

Macroscopic pictures of the *postmortem* tattooed pig skins of different organic pigments were obtained after removal of biopsies for decomposition analysis. Thin sections presented are taken from biopsies after laser irradiation with either ruby laser (P.B.15) or the 532 nm wavelength of the Nd:YAG laser (all other pigments). Sections are displayed as bright field (BF) or DAPI staining of the cell nuclei in overlay with BF or autofluorescence (AF)(scale bar= 100 μ m). The quantity of injected ink varied with different pigments. Pigment discoloration towards the skin surface is indicated by arrows with P.R.170 and P.R.254.



Despite differences in original pigment content, most of the liberated non-volatile compounds were found in a similar quantity in suspensions and skin samples for each of the six pigments tested. In the following, major differences are presented. In P.R.170, 4-aminobenzamide and the germ-cell mutant benzamide were increased 10- to 18-fold in pig skin. Upon irradiation of P.Y.138, pentachlorobenzene and the carcinogen hexachlorobenzene (HCB) concentrations were reduced by half in the skin matrix. With irradiation of P.O.13 in pig skin, biphenyl, chlorobenzene and 3,3'-dichlorobiphenyl (PCB No.11) increased by the factor 2-3 but the corrosive and sensitizing compound phenylisocyanate decreased by the factor 100.

In contrast to non-volatile compounds, the volatiles HCN and benzene decreased 2- to 10-fold in pig skin compared to the aqueous suspensions of P.B.15 and other pigments. Only in the case of P.Y.138 and P.V.19, were the amounts of benzene higher after irradiation in pig skin. Although HCN and benzene were found evolving from all pigments, the release of benzene was highest after irradiation of P.O.13. The highest quantity of HCN was released after irradiation of aqueous P.B.15 suspensions.

In most pigments, one or several of the carcinogens HCB, DCBD, aniline and benzene were identified. Additionally, P.R.170 released benzamide, which is classified as a category 2 germ cell mutagen (GHS, Table 1). In addition to possible carcinogens, a multitude of substances were identified that are categorized as possibly causing allergic skin reactions—among them DCBD, aniline, 2-aminobenzonitrile, phenylisocyanate and 3-chlorobenzamide. Phenylisocyanate also causes skin corrosion.

From decomposition products found in this investigation (besides HCN and benzene) cleavage sites in the parent molecules can be assumed (Fig. 1b). To test these cleavage patterns, we qualitatively assessed the main decomposition products of two additional phthalocyanines and four azo pigments and found them to be cleaved at the same main bonds—namely amide, azo and other secondary or tertiary amines and next to phenyl rings (Table 2). With azo pigments, most potential cleavage products also occur as residues from pigment synthesis. In general, bonds with low dissociation energies display main cleavage sites. The quinacridone P.R.122 did not reveal any decomposition products. Accordingly, in the case of quinacridone P.V.19, only minor amounts of the only specific cleavage product aniline were found (Supplementary Table 6).

In pig skin, the levels of cleavage products of P.B.15 also increased with laser energy fluence, with the exception of benzene (Supplementary Table 7). Hence, the extent of pigment fragmentation most probably depends on the amounts of pigment located in the focus of the laser beam.

Table 2: Non-quantified decomposition products of pigments with similar chemical structure after liquid extraction.

pigment	laser	substance [#]	m/z	comment
P.G.7	ruby	tetrachloroisophthalonitrile	266	* not in control
		pentachlorobenzonitrile	273	* not in control
P.G.36	ruby	tetrachloroisophthalonitrile	266	* not in control
		1,2-benzenedicarbonitrile [+1Br, +3Cl]	310	* not in control
		1,2-benzenedicarbonitrile [+2Br, +2Cl]	354	* not in control
		benzonitrile [+2Br, +3Cl]	365	* not in control
		1,2-benzenedicarbonitrile [+3Br, +1Cl]	400	* not in control
		1,2-benzenedicarbonitrile [+4Br]	444	* not in control
P.R.112	Nd:YAG (532nm)	<i>o</i> -toluidine	106	* peak area > control
		1-isocyanato-2-methylbenzene	133	* peak area ≈ control
		1,3,5-trichlorobenzene	182	* peak area ≈ control
		3,4,5-trichlorobenzenamine	195	* peak area > control
		unknown product	375	* not in control
P.R.122	Nd:YAG (532nm)	-	-	-
P.Y.74	Nd:YAG (532nm)	2-methoxyphenylisocyanate	149	* peak area > control
		2-methoxy-4-nitrobenzenamine	168	* peak area > control
P.Y.1	Nd:YAG (532nm)	aniline	93	* peak area ≈ control
		isocyanatobenzene	119	* peak area ≈ control
		4-methyl-2-nitrobenzenamine	152	* peak area ≈ control
P.V.23	Nd:YAG (532nm)	1,3-dichlorobenzene	146	* peak area ≈ control
		9 <i>H</i> -carbazol	167	* peak area ≈ control
P.R.5	Nd:YAG (532nm)	2-chloro-4,6-dimethoxyaniline	187	* peak area ≈ control
		2-methoxyphenyl-5-sulfonic acid diethylamide	243	* peak area > control
		2-methoxyaniline-5-sulfonic acid diethylamide	258	* peak area > control

*pyrolysis product¹¹[#]benzene and HCN have not been evaluated

Titanium dioxide alters the decomposition of organic pigments

Since most tattoo inks contain a mixture of color-brilliant organic pigments and white titanium dioxide (TiO₂), we investigated the effect of rutile TiO₂ on pigment decomposition. Experiments were carried out in suspensions in order to achieve defined amounts of pigments in each sample. Upon irradiation of samples containing TiO₂, a much higher splashing of the liquid was noticed.

After irradiation of P.O.13 with TiO₂, DCBD, HCN, 2-chloroaniline and benzene were notably decreased (Supplementary Table 4). For the other pigments, semi-volatile compounds in the suspensions with TiO₂ after laser irradiation were analyzed (Supplementary Tables 1-3,5,6). In P.R.254 and P.B.15, main decomposition products increased with the addition of TiO₂, whereas chlorinated benzenes decreased in mixtures of P.Y.138 and TiO₂. Upon irradiation of P.R.170 and P.V.19 with TiO₂, some decomposition products were below the limit of quantification. *O*-phenetidine cleaved from P.R.170, is highly unstable when exposed to light or air and was therefore not quantified further in pig skin. Its content was also reduced by the addition of TiO₂.

Healed skin traps volatile decomposition products

Laser irradiation causes temperatures of several hundred degrees inside the pigment particle, leading to the formation of combustion products such as HCN and benzene and is therefore also referred to as photothermolysis. *In vivo*, a so-called whitening effect is caused by the trapping of steam from the combustion (Fig. 3a). In contrast, carbonization of the pig skin samples was visible in our approach (Fig. 2). In our *postmortem* tattooed pig skin, the epidermis was still perforated by the needle injection channels at the time of laser irradiation (Fig. 3b). Hence, the gaseous compounds formed could exhaust from the skin with no occurrence of whitening. The exhausted substances therefore might lead to an underestimation of the exposition to volatile compounds such as HCN and benzene.

To investigate a possible loss of volatile compounds, we conducted a short term *in vivo* pig study alongside a medical training exercise. Here, an anaesthetized pig was tattooed and allowed to heal for 3 h. Laser irradiation took place with biopsies of the excised skin taken at a later point in time. As a second approach, the so-called trans-ice method was used. Here, the skin is compressed by a clear ice-cube and the laser is applied through it. This ensures index matching from the ice cube to the skin, a cooling effect, as well as buffering of the mechanical stress caused by the shock wave in the skin and thus less bursting of the skin. A possible reduction of evaporation by lower temperatures caused by the ice cube was counter-checked using skin samples cooled with dry ice.

The initial wound healing in the 3 h pig study already increased the concentration of volatile decomposition products following *postmortem* ruby laser irradiation compared to the non-healed control (Fig. 3d). Using the trans-ice method on our *postmortem* tattooed pig skin, we also detected higher amounts of volatile decomposition products (Fig. 3d). Hence, we conclude that by covering the skin, fewer volatiles can escape through the injection holes still present in the epidermis (Fig. 3b). In the dry-ice cooled samples, no difference to the non-cooled samples was seen. The concentration of pigments estimated by Cu-quantification did not significantly differ in the *postmortem* tattooed pig skin compared to the *in vivo* tattoo (Fig. 3e).

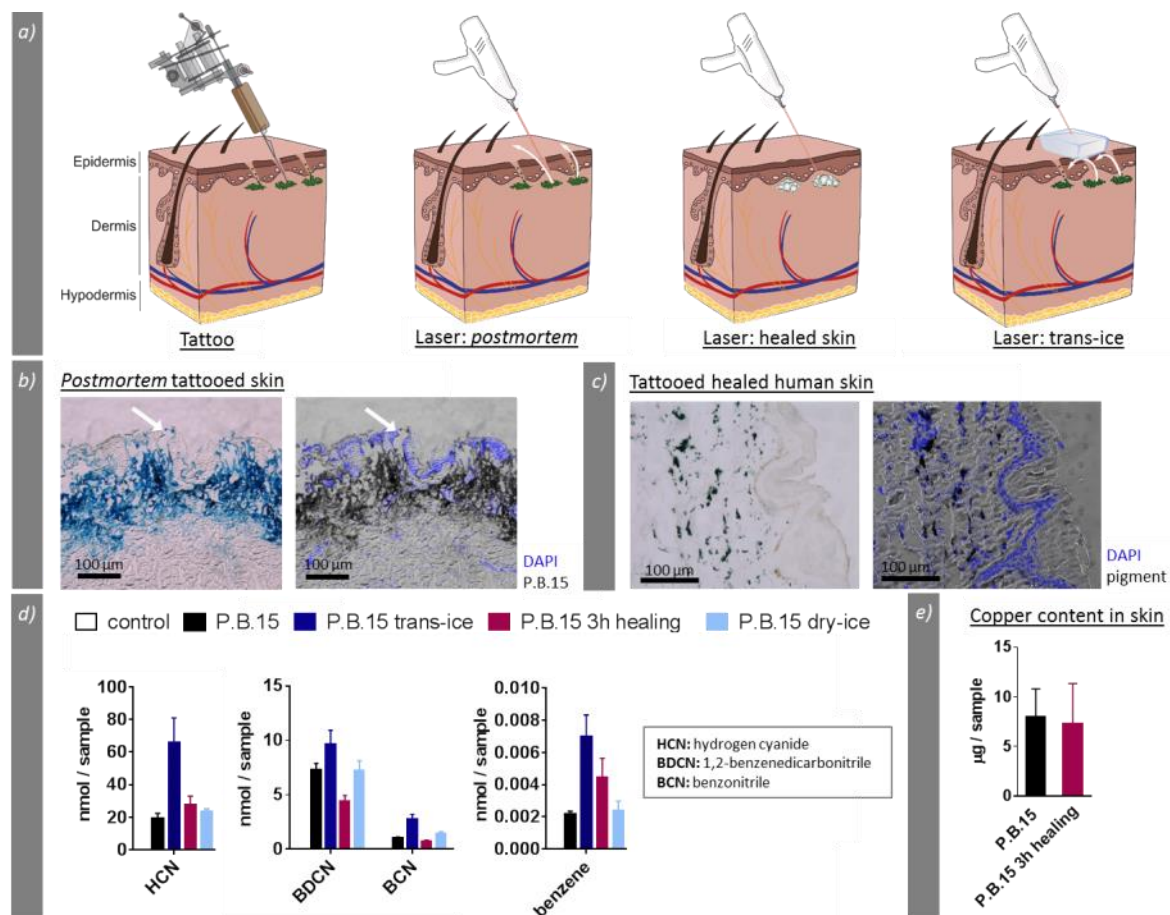


Figure 3: Highly volatile decomposition products evaporate from *postmortem* tattooed pig skin.

Decomposition of P.B.15 in *postmortem* tattooed pig skin with and without trans-ice irradiation or pre-cooling by dry-ice were compared to *in vivo* tattooed pig skin with 3 h primary wound healing (referred to as 3 h healing). a) Scheme of the compared laser irradiation scenarios. Volatiles can evaporate from injection channels in the epidermis during laser irradiation of *postmortem* tattooed skin but are captured inside the skin after healing of the epidermis or by covering with ice (white arrows). b) Tissue sections of *postmortem* tattooed skin with needle injection channels (white arrows). Color image (left) and DAPI staining (right) verify the dermal deposit of the pigment. c) Section of a healed human skin biopsy of a tattoo is displayed for comparison of pigment distribution *in vivo*. d) Pig skin samples were irradiated with a ruby laser (data is displayed as mean \pm SD of four replicates).

e) Injected P.B.15 in *postmortem* and *in vivo* tattooed pig skin was quantified by its core element Cu in 4 mm skin biopsies (data is displayed as mean \pm SD of four replicates).

Discussion

Tattoo pigment decomposition in different matrices

Here we demonstrated the general suitability of aqueous suspension and *postmortem* pig skin to serve as models for fragmentation studies of organic pigments upon laser irradiation. Our data supports the assumption that all organic pigments will undergo cleavage upon laser irradiation since temperatures of more than 600°C can be expected during the treatment^{8,16}. Therefore, common combustion fragments such as HCN and benzene will occur in all organic pigments, but to varying degrees. Since the methods used in our investigation are only suitable for volatile and GC-suitable decomposition products, other fragments may also occur.

Presumably, only those pigments present at the uppermost layer of skin or the boundary surface in aqueous suspensions, will have been reached and destroyed by the laser beam. Such an assumption is supported by histological sections of the skin after laser irradiation (Fig. 2). Here, we found color changes solely in the superficial pigment layers when tattooed with either P.R.170 or P.R.254.

We observed similar amounts of most decomposition products in aqueous suspensions and pig skin, yet the quantity of certain decomposition products differed. Phenylisocyanate evolving from P.O.13 was greatly reduced in pig skin compared to in aqueous suspension (Supplementary Table 4). It is known, that isocyanates can either be hydrolyzed to amines with water or react directly with amines to form urea compounds¹⁷. Though, the quantity of aniline after laser irradiation of P.O.13 is also reduced in pig skin, indicating reactivity with amines rather than decay by hydrolyzation with water.

After laser irradiation of the highly chlorinated P.Y.138, penta- and hexachlorobenzene were formed in addition to the cleavage product tetrachlorobenzene. Most likely, the high energy absorbed by the pigment leads to the formation of halogen radicals and therefore to halogenation¹⁸. This effect was more pronounced in aqueous suspensions (Supplementary Table 1).

Translation of pigment decomposition to human exposure

With regard to the pigment content used in our investigation, we expect no overestimation of pigment decomposition. Calculated from the Cu-content, a pigment concentration of 0.398 mg/cm² in skin can be assumed for P.B.15 (c.f. Fig. 3e), which is lower than the average of 0.6 mg/cm² red azo pigment injected by a professional tattooist in another study¹⁹. However, the amount of pigment injected cannot be adequately monitored. The tattooist normally injects ink until the desired color intensity is achieved. Therefore, the color brilliance strongly influences how much pigment is needed for the desired tone. The pig skin sections in this investigation showed that in particular the amount of P.V.19 in skin was much lower (Fig. 2). In addition, the mixing pigments with TiO₂ can alter decomposition to a greater or lesser extent presumably through light scattering. The scattering effects of rutile TiO₂ pigments (250 nm

diameter) is known to cause a higher energy transfer to dyes when irradiated with a 532 nm Nd:YAG laser²⁰. Regarding the irradiation of P.O.13 with TiO₂, possible further DCBD decomposition products, such as hydrogen chloride and nitrogen oxides were not monitored²¹.

Also, aqueous suspensions containing TiO₂ show increased splashing upon laser irradiation from rapid local heating, which results in mechanical energy—visible as a shock wave¹⁰.

In literature, inhibitory effects of TiO₂ on tattoo clearance by laser irradiation are described^{4,22}.

When extrapolating the quantities of decomposition products observed in this investigation with regard to *in vivo* tattoo removal, a possible underestimation of volatile compounds should be considered. Our short-term healing study on a pig and the trans-ice experiments (Fig. 3) revealed increased amounts of HCN and benzene compared to *postmortem* skin without further occlusion. Therefore, the maximum amounts observed in aqueous suspension or pig skin should be used for a worst-case scenario risk assessment. The whitening effect occurring *in vivo* most likely derives from a multitude of volatile compounds induced by the steam carbon effect¹⁶. The absolute amounts of semi-volatile azo cleavage compounds in our investigation were in the same range of decomposition products found after laser irradiation of a red azo pigment in healed mouse skin as part of an *in vivo* study (0.1 µg 4-nitrotoluene in a 5 mm biopsy equal 0.73 nmol)²³. Since the quantities of decomposition products were comparable to the *in vivo* mouse study, we also believe that the occurring carbonization of the pig skin will not lead to a major difference in pigment destruction. *In vivo*, this color change upon tattoo removal is only rarely observed^{3,24}. It should also be noted, that only slight pigment clearance in pig skin was achieved in our investigation. Laser dermatologist often report the persistence of modern tattoos²⁵, probably containing smaller pigment agglomerates, which make the use of pico-second lasers more appropriate^{16,26}. Older and non-professional tattoos are easier to remove²⁷. The fine spread of ink in the *postmortem* tattooed pig skin compared to more agglomerated healed tattoos might explain the poor clearance (Fig. 3b,c). Similar to our model, pigment density in tattoos, as well as size and depth of pigments^{19,27} in the skin, vary widely and a representative exposure is hard to estimate.

Conclusion

The data presented in this paper help to understand possible effects of laser irradiation of modern tattoos and possible influencing parameters on the release of toxins. Since most common structures of organic pigments are covered, we here extend the knowledge on laser induced pigment decomposition upon tattoo laser removal.

The chemical decomposition of organic pigments in general must be included in future tattoo risk assessments. The data and method we provide with this study could lay the foundation for these estimations. The increase in lifetime cancer risk should be estimated for worst-case scenarios with the

quantities given for all carcinogenic substances found after pigment decomposition in this investigation. In terms of regulatory actions, it must be kept in mind that the tattoo community will not relinquish all of these color brilliant pigments. A complete ban would lead to the use of other pigments, with unknown toxicological properties or the purchase of uncontrolled inks via the internet. It is therefore necessary to distinguish between pigments with a potentially high release of toxic substances upon laser irradiation and those with the ability to release these when exposed to sunlight or during sterilization procedures. In future studies, we plan to investigate the sensitization potential of decomposition products from laser irradiation and sunlight exposure.

Acknowledgements

This work was supported by the intramural research project (SFP #1322-604) at the German Federal Institute for Risk Assessment (BfR). Dr. Christian Seim is acknowledged for the design of the skin graphics.

Author contributions

A.L., C.H., I.S., H.-P.B. and P.L. designed and supervised the study. I.S., N.R., M.G. and H.-P.B. carried out the laser experiments and I.S., N.R. and M.G. analyzed the samples by means of GC-MS. I.S., A.L., C.H. and P.L. critically reviewed the data and drafted the manuscript.

Materials and Methods

Chemicals and pigments

All chemicals, analytical standards and solvents used were of analytical or LC-MS grade.

2-Aminobenzonitrile, 4-aminobenzamide, aniline, benzamide, benzene, benzene-D₆ (isotope purity 97%), 1,2-benzenedicarbonitrile, benzonitrile, biphenyl, 4-bromobenzonitrile, 3-chlorobenzamide, chlorobenzene, chlorobenzene-D₅, 3-chlorobenzonitrile, 4-chlorobenzonitrile, 2-chloroaniline, 1-cyanonaphthalene, 4,4'-dibromobiphenyl, DCBD, 3,3'-dichlorobiphenyl, HCB, naphthalene-D₈, o-phenetidine, phenylisocyanate, potassium cyanide-¹³C-¹⁵N (isotope purity 99% and 98%, respectively)(K¹³C¹⁵N), sodium cyanide (NaCN), sodium hydroxide (NaOH), 1,2,4,5-tetrabromobenzene, 1,2,3,4-tetrachlorobenzene, xylene, and *m*-xylene D₁₀ were purchased at Sigma Aldrich (Munich, Germany). Benzonitrile-D₅ and pentachlorobenzene were obtained from Biozol (Eching, Germany) and Sulpeco (Bellafonte, PA, USA), respectively. Dimethylsulfoxide (DMSO) and ethanol used in cell culture experiments were purchased at Carl Roth (Karlsruhe, Germany).

Pigments used in this investigation were PV Fast Blue BF (P.B.15, C.I. 74160), Paliotol Yellow DO960 (P.Y.138, C.I. 56300), Permanent-Rot FGR (P.R.112, C.I. 12370), Hansa-Brilliantgelb 5GX (P.Y.74, C.I. 11741), Hansa Yellow G 02 (P.Y.1, C.I. 11680) and PV-Echtviolett RL (P.V.23, C.I. 51319) from Clariant (Burgkirchen, Germany). Also, Irgalite Orange D2895 (P.O.13, C.I. 21110), Cinquasia Red L4100 HD (P.V.19, C.I. 73900), Graphotol-Rot F3RK 70-CN09 (P.R.170, C.I. 12475), Heliogen Grün D 8730 (P.G.7, C.I. 74260), Heliogen Grün D 9360 (P.G.36, C.I. 74265) and Irgazin Red L3660 HD (P.R.254, C.I. 56110) from BASF (Kaiserslautern, Switzerland) were investigated. P.R.5 (C.I. 12490) with trade name 22016 RED was purchased from Univar (Billericay, United Kingdom) and rutile TiO₂ unipure white LC987 from Sensient Cosmetic Technologies (Saint-Ouen-l'Aumône, France).

Sample preparation and laser irradiation

Aqueous suspensions were prepared as described previously with the following amendments¹⁵. Each 1 mg/ml pigment was mixed with ultrapure water (18.2 MΩ·cm at 25°C) and sonicated for 60 min. TiO₂ was mixed with the freshly prepared pigment suspensions to a final concentration of 1 mg/ml and sonicated for an additional 30 min. Temperature was kept below 30°C. 250 µl of each pigment suspension were transferred into semi-micro UV/VIS cuvettes (Brand, Wertheim, Germany) and closed with polypropylene caps (Ratiolab, Dreieich, Germany).

For the imitation of skin, abdominal pig skin was taken *postmortem* and stored at -20°C after hair removal by electrical razor blades. Thawed skin was tattooed with a Cheyenne hawk thunder tattoo machine and a 17 magnum long taper tattoo needle with 0.35 mm thickness (both from MT.Derm, Berlin, Germany) until a uniform color shade was achieved. Tattoo inks were prepared shortly before tattooing. For each ink,

8–10% pigment was suspended in a 40% 2-propanol ($\geq 99.5\%$, Sigma Aldrich, Munich, Germany) mix with ultrapure water ($18.2 \text{ M}\Omega\cdot\text{cm}$ at 25°C) and 1% polyvinylpyrrolidone (PVP) solution (K 60, 45% in H_2O , Sigma Aldrich, Munich, Germany). High molecular weight PVP was used as a dispersant to facilitate a homogeneous pigment suspension and to prevent its extraction in the following analysis. The ink mixture was mixed for 5 min at an amplitude of 10% with a probe sonifier (200 W Bandelin Sonopuls HD 2200, Bandelin Electronic, Berlin, Germany).

Samples were treated with multiple quantities of Q-switched ruby ($3\text{--}5 \text{ J}/\text{cm}^2$, spot size 4 mm, pulse duration 20 ns, 694 nm, Sinon, WaveLight, Erlangen, Germany) or Nd:YAG ($5 \text{ J}/\text{cm}^2$, spot size 4 mm, pulse duration >20 ns, at 1,064 nm or 532 nm, Revlight SI, Cynosure, Westford, MA, USA) laser pulses and either placed on ice until further processing or directly transferred into GC-vials and crimp-sealed. For each data point, at least three independent samples were processed.

GC-MS

If not stated otherwise, the Agilent 7890A gas chromatograph was coupled to an Agilent 5975C inert XL MSD with Triple-Axis Detector (Agilent Technologies, Santa Clara, CA, USA). Ionization was induced by an inert electron impact (EI) ion source at 70 eV and helium (purity of 99.999%) from Air Liquide (Düsseldorf, Germany) was used as carrier gas. Injection and pre-incubation were automatically executed by a multi-purpose sampler (Gerstel, Mülheim, Germany). For quantification and qualitative data analysis ChemStation Version E.02.02.1431 (Agilent Technologies, Santa Clara, CA, USA) was used.

Liquid injection GC-MS

From the irradiated cuvettes, 200 μl aqueous suspension were extracted with 200 μl ethyl acetate. The irradiated 4 mm diameter pig skin biopsies were extracted in 500 μl ethyl acetate. Ethyl acetate contained 5 $\mu\text{g}/\text{ml}$ of the corresponding internal standards and samples were extracted for 1 hour at room temperature while shaking. Extracts were transferred into a new glass vial and 1 μl of was injected into the GC-MS for quantification.

For analysis of liquid extracts, a DB-17MS (30 m, 0.25 mm, 0.25 μm i.d.) column (Agilent Technologies, Santa Clara, CA, USA) was used. The cold injection system (CIS) had an initial temperature of 15°C and was ramped with $2^\circ\text{C}/\text{s}$ to a final temperature of 250°C and held for 10 min. The final temperature of the CIS was chosen as a way of preventing thermal decomposition of possibly injected pigment residues. The initial oven temperature was set to 40°C and remained for 1 min followed by the first ramp with $30^\circ\text{C}/\text{min}$ to 80°C , the second ramp with $10^\circ\text{C}/\text{min}$ to 260°C , and the third ramp with $99^\circ\text{C}/\text{min}$ to 320°C , which was finally held for 3 min. Front inlet flow was 1.1 ml/min. The temperatures of the ion source and quadrupole were set to 230°C and 150°C , respectively. Data acquisition took place in a mixed scan/single

ion mode (SIM) approach. In scan mode, all m/z values from 30–430 were recorded. MS-SIM parameters are listed in Table 5. All analytes for the liquid extraction method are displayed with the respective quantifier and qualifier-ions in the time-dependent acquisition groups. Ion ratios were taken from the injections of the standard chemicals and a variance of 15% was allowed for quantification. Internal standards (IS) were chosen based on the similarity of their molecular weight, retention time, molecular structure and $\log K_{ow}$ to the respective analyte and linearity of the resulting calibrations.

Table 3: SIM parameters for liquid GC-MS.

Group	Start time [min]	Substance	Quantifier ion m/z	Qualifier ion m/z	Ion ratio	Internal standard
1	3.64	xylene	91	106	50	Xy-D ₁₀
		<i>m</i> -xylene-D ₁₀ (Xy-D ₁₀)	98	116	39	-
		chlorobenzene-D ₅ (CB-D ₅)	117	82	39.7	-
		chlorobenzene	112	114	30	CB-D ₅
2	5.5	phenylisocyanate	119	91	47	4-BrBCN
		aniline	93	66	40	BCN-D ₅
		benzotrile-D ₅ (BCN-D ₅)	108	80	30.1	-
		benzotrile	103	76	23	BCN-D ₅
3	7.5	3-chlorobenzotrile	137	139	31.8	4-BrBCN
		4-chlorobenzotrile	137	139	31.8	4-BrBCN
		<i>o</i> -phenetidine	80	137	81.5	BCN-D ₅
		naphthalene-D ₈ (Na-D ₈)	136	108	11.3	-
4	9.8	2-chloroaniline	127	129	31	BCN-D ₅
		4-bromobenzotrile (4-BrBCN)	181	183	95	-
		2-aminobenzotrile	118	91	32	BCN-D ₅
6	11	1,2,3,4-tetrachlorobenzene	216	214	80	4-BrB
		biphenyl	154	153	39	Na-D ₈
7	12.3	1,2-benzenedicarbonitrile	101	128	21.6	BCN-D ₅
		benzamide	105	121	81.9	BCN-D ₅
8		pentachlorobenzene	250	252	65.2	4-BrB
9	14	1-cyanonaphthalene	153	126	18	Na-D ₈
		3-chlorobenzamide	139	155	63.1	BCN-D ₅
10	15.75	HCB	284	286	80	4-BrB
		PCB No. 11	222	152	99	4-BrB
		1,2,4,5-tetrabromobenzene (4-BrB)	394	392	70	-
12	17.5	4-aminobenzamide	120	136	65.4	BCN-D ₅
13	19	4,4'-dibromobiphenyl (DBrBP)	152	312	83.3	-
		DCBD	252	254	64.5	DBrBP

HS-GC-MS method for HCN and benzene quantification

Directly after laser irradiation, 200 μl of the irradiated pigment suspension were transferred into a 10 ml ND18 brown glass vial (Neolab, Heidelberg, Germany) containing 740 μl of an aqueous 5×10^{-5} N NaOH solution and crimped immediately. Pig skin biopsies were added to 940 μl of the aqueous 5×10^{-5} N NaOH solution. In order to monitor evaporation until sample analysis, 50 μl of a stock solution of 100 $\mu\text{g/ml}$ $\text{K}^{13}\text{C}^{15}\text{N}$ and 10 μl of a 1 $\mu\text{g/ml}$ benzene- D_6 solution were added through the butyl-red septum as internal standard to a final volume of 1 ml. Before analysis, 30 μl of 30% phosphoric acid were added through the septum using a 100 μl Hamilton syringe (Neolab, Heidelberg, Germany). The last step guaranteed protonation of dissolved cyanide ions to form gaseous HCN.

For subsequent HS-GC-MS analysis of HCN and benzene an HP-Plot/Q column (Agilent Technologies, Santa Clara, CA, USA) was used. Samples were incubated for 4 min at 60°C with agitation. Injection of 1 ml was cryo-focused at -50°C by cooling with liquid nitrogen. After 12 s the temperature of the CIS was increased to 220°C which was held for 1 min. Transfer line was kept constant at 260°C. Injections were carried out in splitless mode. The initial oven temperature of 110°C was heated with 4°C/min up to 130°C and finally increased to 250°C with a rate of 99°C/min which was held for 5 more minutes.

The analysis was performed in the combined SIM/scan mode using a full scan mass range from m/z 10–250 in combination with Single Ion Monitoring (SIM) starting after solvent delay of 4 min. For SIM data acquisition, HCN was quantified with m/z 27 (qualifier ion 26, ratio 16.3) and the isotope standard potassium cyanide- ^{13}C - ^{15}N (m/z 29). Benzene was quantified with m/z 78 (qualifier ion 77, ratio 21.5) and the internal standard benzene- D_6 with m/z 84 (qualifier ion 82, ratio 21.5), each with a dwell time of 40 ms, respectively.

Benzene calibration standards were processed using freshly prepared standard solutions, transferred and diluted with Hamilton syringes through septa to prevent evaporation. NaCN and $\text{K}^{13}\text{C}^{15}\text{N}$ stock solutions (1 mg/ml) were dissolved in aqueous 0.02 N NaOH to prevent outgassing. The solution was stored at -20°C and freshly thawed right before usage. For further dilution, water containing 5×10^{-5} N NaOH was used to guarantee a pH value of 10.

Microscopy

Biopsies of tattooed pig skin were frozen in TissueTek O.C.T. matrix (Sakura Finetek, Staufen, Germany) for cryo-microtome sectioning. Thickness of sections were 7 μm for fluorescence light microscopy and were mounted in DAPI-Fluoromount G (Southern Biotech, Birmingham, AL, USA) for cell nucleus staining. Autofluorescence of pigments was excited with a 510–550 nm band-pass filter and recorded with a BX-51TF microscope (Olympus, Hamburg, Germany).

Inductively coupled plasma mass spectrometry (ICP-MS) analysis

Cu concentrations of 4 mm biopsies containing P.B.15 were quantified using a nitric acid microwave digestion (Ultraclave, MLS, Leutkirch, Germany) followed by ICP-MS analysis. Five milliliters of 69% nitric acid was added to each biopsy in Teflon vessels and heated in the microwave with the following steps: 20–80°C (3.5 min, 100 bar, 700 W); 80–130°C (10 min, 120 bar, 1,000 W); 130–200°C (6.5 min, 150 bar, 1,000 W), 200°C (30 min, 150 bar, 1,000 W). Nitric acid was purified using a duoPUR quartz sub-boiling distillation system (MLS, Leutkirch, Germany). Ultrapure water was obtained using a Milli-Q Advantage A10 water purification system equipped with a Millipore Q-POD Element Unit (both from Merck, Darmstadt, Germany). Standard elements for ICP were purchased either from Sigma Aldrich (Munich, Germany; i.e. Sc, Cu) or Merck (Darmstadt, Germany) in the case of In. A 20-fold dilution of each sample was prepared including 10 ppb of the elements In and Sc as internal standards. XSeries II ICP-MS (Thermo Fischer Scientific, Bremen, Germany) together with an ESI SC2 autosampler (Elemental Service & Instruments, Mainz, Germany) were used for sample analysis. Sample analysis was carried out in triplicate with 100 sweeps each. Resolution was set to 0.02 u and the dwell time for all elements was 10 ms. Measurements were carried out with collision cell in -3.0 V mode. H₂/He (7% v/v) was used as the collision gas with 5 ml/min flow rate. Data were processed with PlasmaLab 2.5.11.321 (Thermo Scientific, Bremen, Germany).

***In vivo* pig skin study**

The study was carried out together with medical laser training approved by local authorities (KLS Martin, Tuttlingen, Germany) at the IRCAD training center (Strasbourg, France). The tattooing procedure did not cause perceptible harm to the pig and caused substantially less trauma compared to the laser training. The pig was anaesthetized during the tattoo procedure until slaughter (after 3 h). After initiation of death, the corresponding skin was excised and stored at -80°C until laser treatment.

References

- 1 Laux, P. *et al.* A medical-toxicological view of tattooing. *The Lancet* **387**, 395–402, doi:10.1016/s0140-6736(15)60215-x (2016).
- 2 Bernstein, E. F. Laser tattoo removal. *Semin Plast Surg* **21**, 175–192, doi:10.1055/s-2007-991186 (2007).
- 3 Kirby, W., Kaur, R. R. & Desai, A. Paradoxical darkening and removal of pink tattoo ink. *J Cosmet Dermatol* **9**, 149–151 (2010).
- 4 Ross, E. V. *et al.* Tattoo darkening and nonresponse after laser treatment: a possible role for titanium dioxide. *Arch Dermatol* **137**, 33–37, doi:doi:10.1001/archderm.137.1.33 (2001).
- 5 Rüdlinger, R. Successful removal by ruby laser of darkened ink after ruby laser treatment of mismatched tattoos for acne scars. *J Cosmet Laser Ther* **2**, 37–39, doi:10.1080/14628830050516597 (2000).
- 6 Wenzel, S., Landthaler, M. & Bäuml, W. Recurring mistakes in tattoo removal. A case series. *Dermatology* **218**, 164–167, doi:10.1159/000182252 (2009).
- 7 Schreiver, I. & Luch, A. At the dark end of the rainbow: data gaps in tattoo toxicology. *Arch Toxicol* **90**, 1763–1765, doi:10.1007/s00204-016-1740-9 (2016).
- 8 Taylor, C. R., Anderson, R. R., Gange, R. W., Michaud, N. A. & Flotte, T. J. Light and electron microscopic analysis of tattoos treated by Q-switched ruby laser. *J Invest Dermatol* **97**, 131–136 (1991).
- 9 Ferguson, J. E., Andrew, S. M., Jones, C. J. P. & August, P. J. The Q-switched neodymium:YAG laser and tattoos: a microscopic analysis of laser-tattoo interactions. *Br J Dermatol* **137**, 405–410 (1997).
- 10 Anderson, R. R. & Parrish, J. A. Selective photothermolysis: precise microsurgery by selective absorption of pulsed radiation. *Science* **220**, 524–527 (1983).
- 11 Schreiver, I., Hutzler, C., Andree, S., Laux, P. & Luch, A. Identification and hazard prediction of tattoo pigments by means of pyrolysis—gas chromatography/mass spectrometry. *Arch Toxicol* **90**, 1639–1650, doi:10.1007/s00204-016-1739-2 (2016).
- 12 Vasold, R. *et al.* Tattoo pigments are cleaved by laser light—the chemical analysis *in vitro* provide evidence for hazardous compounds. *Photochem Photobiol* **80**, 185–190 (2004).
- 13 Cui, Y. *et al.* Photodecomposition of pigment yellow 74, a pigment used in tattoo inks. *Photochem Photobiol* **80**, 175–184, doi:10.1562/2004-04-06-ra-136.1 (2004).
- 14 Hauri, U. & Hohl, C. Photostability and breakdown products of pigments currently used in tattoo inks. *Curr Probl Dermatol* **48**, 164–169, doi:10.1159/000369225 (2015).
- 15 Schreiver, I., Hutzler, C., Laux, P., Berlien, H. P. & Luch, A. Formation of highly toxic hydrogen cyanide upon ruby laser irradiation of the tattoo pigment phthalocyanine blue. *Sci Rep* **5**, 12915, doi:10.1038/srep12915 (2015).
- 16 Ho, D. D., London, R., Zimmerman, G. B. & Young, D. A. Laser-tattoo removal—a study of the mechanism and the optimal treatment strategy via computer simulations. *Lasers Surg Med* **30**, 389–397, doi:10.1002/lsm.10065 (2002).

-
- 17 Güssregen, B., Schröfel, S., Nauck, M. & Arndt, T. Selective Reaction Monitoring (SRM) Daten von mehr als 900 Xenobiotika für Aufbau und Validierung von LC-MS/MS Analysen (article in German). *Toxichem Krimtech* **75**, 149–172 (2008).
- 18 Rettig, W. *Lichtabsorption und Photochemie organischer Moleküle, (Reihe: Physikalische organische Chemie, Bd. 3) (in German)*. (VCH-Verlagsgesellschaft, Weinheim, 1991).
- 19 Engel, E. *et al.* Modern tattoos cause high concentrations of hazardous pigments in skin. *Contact Dermatitis* **58**, 228–233 (2008).
- 20 Lawandy, N. M., Balachandran, R. M., Gomes, A. S. L. & Sauvain, E. Laser action in strongly scattering media. *Nature* **368**, 436–438 (1994).
- 21 *Sax's Dangerous Properties of Industrial Materials*. 11 edn, (Wiley & Sons, Hoboken, NJ, USA, 2004).
- 22 Beute, T. C., Miller, C. H., Timko, A. L. & Ross, E. V. *In vitro* spectral analysis of tattoo pigments. *Dermatol Surg* **34**, 508–516, doi:10.1111/j.1524-4725.2007.34096.x (2008).
- 23 Engel, E. *et al.* Tattooing of skin results in transportation and light-induced decomposition of tattoo pigments - a first quantification *in vivo* using a mouse model. *Exp Dermatol* **19**, 54–60, doi:10.1111/j.1600-0625.2009.00925.x (2010).
- 24 Wang, C. C. *et al.* Comparison of two Q-switched lasers and a short-pulse erbium-doped yttrium aluminum garnet laser for treatment of cosmetic tattoos containing titanium and iron in an animal model. *Dermatol Surg* **36**, 1656–1663, doi:10.1111/j.1524-4725.2010.01714.x (2010).
- 25 Kent, K. M. & Graber, E. M. Laser tattoo removal: a review. *Dermatol Surg* **38**, 1–13, doi:10.1111/j.1524-4725.2011.02187.x (2012).
- 26 Izikson, L., Farinelli, W., Sakamoto, F., Tannous, Z. & Anderson, R. R. Safety and effectiveness of black tattoo clearance in a pig model after a single treatment with a novel 758 nm 500 picosecond laser: a pilot study. *Lasers Surg Med* **42**, 640–646, doi:10.1002/lsm.20942 (2010).
- 27 Ho, S. G. & Goh, C. L. Laser tattoo removal: a clinical update. *J Cutan Aesthet Surg* **8**, 9–15, doi:10.4103/0974-2077.155066 (2015).

2.4. Synchrotron-based v-XRF mapping and μ -FTIR microscopy enable to look into the fate and effects of tattoo pigments in human skin

Ines Schreiver*, Bernhard Hesse*, Christian Seim, Hiram Castillo-Michel, Julie Villanova, Peter Laux, Nadine Drejack, Randolph Penning, Remi Tucoulou, Marine Cotte, Andreas Luch

*These authors contributed equally to this work

This chapter was published online on 12. September 2017 in:

Scientific Reports 7, 11395 (2017).

DOI: 10.1038/s41598-017-11721-z

Link: <https://doi.org/10.1038/s41598-017-11721-z>

Involvement of the author within this publication: Project planning (70%), project execution (60%), data analysis (50%), writing of the manuscript (50%).

Supplementary materials for the following publication are detailed in Annex III.

SCIENTIFIC REPORTS

OPEN Synchrotron-based ν -XRF mapping and μ -FTIR microscopy enable to look into the fate and effects of tattoo pigments in human skin

Ines Schreiver¹, Bernhard Hesse², Christian Seim^{3,4}, Hiram Castillo-Michel², Julie Villanova², Peter Laux¹, Nadine Dreiaek¹, Randolph Penning⁵, Remi Tucoulou², Marine Cotte² & Andreas Luch¹

The increasing prevalence of tattoos provoked safety concerns with respect to particle distribution and effects inside the human body. We used skin and lymphatic tissues from human corpses to address local biokinetics by means of synchrotron X-ray fluorescence (XRF) techniques at both the micro (μ) and nano (ν) scale. Additional advanced mass spectrometry-based methodology enabled to demonstrate simultaneous transport of organic pigments, heavy metals and titanium dioxide from skin to regional lymph nodes. Among these compounds, organic pigments displayed the broadest size range with smallest species preferentially reaching the lymph nodes. Using synchrotron μ -FTIR analysis we were also able to detect ultrastructural changes of the tissue adjacent to tattoo particles through altered amide I α -helix to β -sheet protein ratios and elevated lipid contents. Altogether we report strong evidence for both migration and long-term deposition of toxic elements and tattoo pigments as well as for conformational alterations of biomolecules that likely contribute to cutaneous inflammation and other adversities upon tattooing.

In recent years, the seemingly unstoppable trend for tattoos has brought safety concerns into the spotlight¹. Currently, basic toxicological aspects, from biokinetics to possible alterations of the pigments, are largely uncertain. The animal experiments which would be necessary to address these toxicological issues were rated unethical because tattoos are applied as a matter of choice and lack medical necessity, similar to cosmetics². Consequently, the hazards that potentially derive from tattoos were as yet only investigated by chemical analysis of the inks and their degradation products *in vitro*³⁻⁶. Even though toxicological data might be available for some ink ingredients individually, information on *in vivo* interactions of the ink's components and their fate within the body is rare.

Tattoos and permanent make-up work by depositing insoluble pigments into the dermal skin layer (Fig. 1). In conjunction with tattoos, pigmented and enlarged lymph nodes have been noticed in tattooed individuals for decades⁷. After the traumatic insertion of inks during the tattooing procedure, the body will excrete as many components as possible via the damaged epidermis. Other ways to clean the site of entrance are through active transport to lymph nodes by phagocytizing cells, or passively along the lymphatic vessels⁸⁻¹¹. In addition to observations in humans, an *in vivo* study in mice revealed colored lymph nodes after tattooing with an azo pigment¹². Even though this leaves little doubt that the pigment originates from corresponding tattoos, the origin and fate of pigments in human lymph nodes have never been analytically investigated so far. Lately, the only study analyzing human lymph nodes in tattooed individuals assessed its contents on carcinogenic polycyclic aromatic hydrocarbons deriving from carbon black particles¹³.

¹German Federal Institute for Risk Assessment (BfR), Department of Chemical and Product Safety, Max-Dohrn-Strasse 8-10, 10589, Berlin, Germany. ²European Synchrotron Radiation Facility (ESRF), 38043, Grenoble, Cedex 9, France. ³Physikalisch-Technische Bundesanstalt, Department of X-ray Spectrometry, Abbestr. 2-12, 10587, Berlin, Germany. ⁴Technische Universität Berlin, Institute for Optics and Atomic Physics, Hardenbergstrasse 36, 10623, Berlin, Germany. ⁵Institute of Forensic Medicine, Ludwig-Maximilians University, Munich, Germany. Ines Schreiver and Bernhard Hesse contributed equally to this work. Correspondence and requests for materials should be addressed to A.L. (email: andreas.luch@bfr.bund.de)

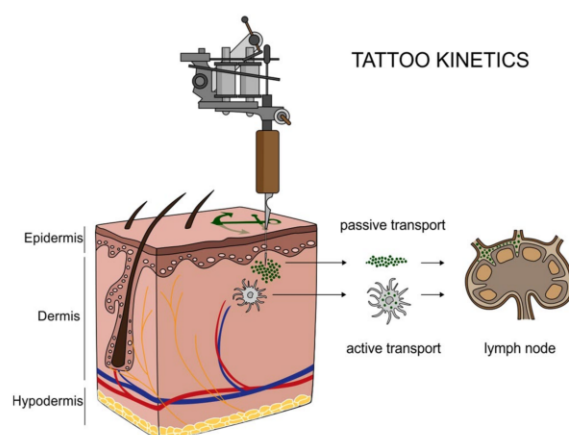


Figure 1. Translocation of tattoo particles from skin to lymph nodes. Upon injection of tattoo inks, particles can be either passively transported via blood and lymph fluids or phagocytized by immune cells and subsequently deposited in regional lymph nodes. After healing, particles are present in the dermis and in the sinusoids of the draining lymph nodes. The picture was drawn by the authors (i.e., C.S.).

Tattoo pigments consist of either inorganic colorful metals and its oxides, or of polyaromatic compounds, all of which are thought to be biologically inert. It can thus be expected to find a broad range of elements in tattooed human tissue—among them the sensitizers nickel (Ni), chromium (Cr), manganese (Mn), and cobalt (Co)—as parts of color-giving pigments or element contamination^{14–17}. Besides carbon black, the second most common used ingredient of tattoo inks is titanium dioxide (TiO₂), a white pigment usually applied to create certain shades when mixed with colorants. The toxicity of TiO₂ depends on its speciation (crystal structure) which can be either rutile or the more harmful photocatalytically active anatase¹⁸. The latter can lead to the formation of reactive oxygen species when exposed to sunlight. Delayed healing is thus often associated with white tattoos, along with skin elevation and itching¹⁹.

The contribution of tattoo inks to the overall body load on toxic elements, the speciation of TiO₂, and the identities and size ranges of pigment particles migrating from subepidermal skin layers towards lymph nodes have never been analytically investigated in humans before. The average particle size in tattoo inks may vary from <100 nm to >1 μm²⁰. Therefore most tattoo inks contain at least a small fraction of particles in the nano range.

Here, we analyzed tattooed human skin and regional lymph nodes originating from four donors (corpses). Inductively coupled plasma mass spectrometry (ICP-MS) was used to assess the general contents of elements in both tissues and tattoo inks after microwave digestion. Laser-desorption/ionization time-of-flight (LDI-ToF) MS facilitated the identification of organic pigments in enzyme-lysed samples. To precisely locate the different elements in the cutaneous and lymphatic microenvironments, to provide information on TiO₂ speciation and to assess primary particle sizes at the nanometric scale in particle mixtures, however, synchrotron-based X-ray fluorescence investigations have been performed at both the micro (μ-XRF) and nano (ν-XRF) range. Furthermore, we assessed biomolecular changes in the respective tissues at the micrometric scale and in the proximity of tattoo particles using synchrotron-based Fourier transform infrared (μ-FTIR) spectroscopy.

Results

Organic pigments translocate from skin to lymph nodes. Providing analytical evidence of tattoo particles being distributed inside the human body was a key objective of this investigation. To this end, tissue samples of four individuals tattooed with orange, red, green or black and two non-tattooed control donors were analyzed for the presence of organic pigments. Detection of the same pigment species in both skin and regional lymph nodes revealed the drainage of tattoo particles in two out of four tattooed donors (Fig. 2).

Identification of organic pigments using LDI-ToF-MS has mostly been described using inks^{21–23}. This technique is mainly based on isotope distributions and the molecular mass (see Supplementary Fig. S1). In the lysed tissues presented here, color-giving pigments were found to be copper phthalocyanines with either hydrogen, chlorine or bromine residues in three out of four skin samples. Reddish parts of the tattoos contained the azo group-containing pigments red 170 and orange 13 (Fig. 2).

For donors 1 and 2, the absence of organic pigments in the lymph nodes suggests either concentrations below the limit of detection (approx. 0.1–1% w/w pigment per extract), possible metabolic decomposition or drainage to alternative lymph nodes. The general ability for azo pigment translocation to lymph nodes was proven in additional skin and lymph node samples of donor 2 (Supplementary Table 1). On the other hand, carbon black particles possibly responsible for the black color in skin and lymph nodes (Fig. 2) were not accessible with the analytical methods used in this investigation. No xenobiotic pigment particles were detected in either skin or lymph tissue of the control samples.

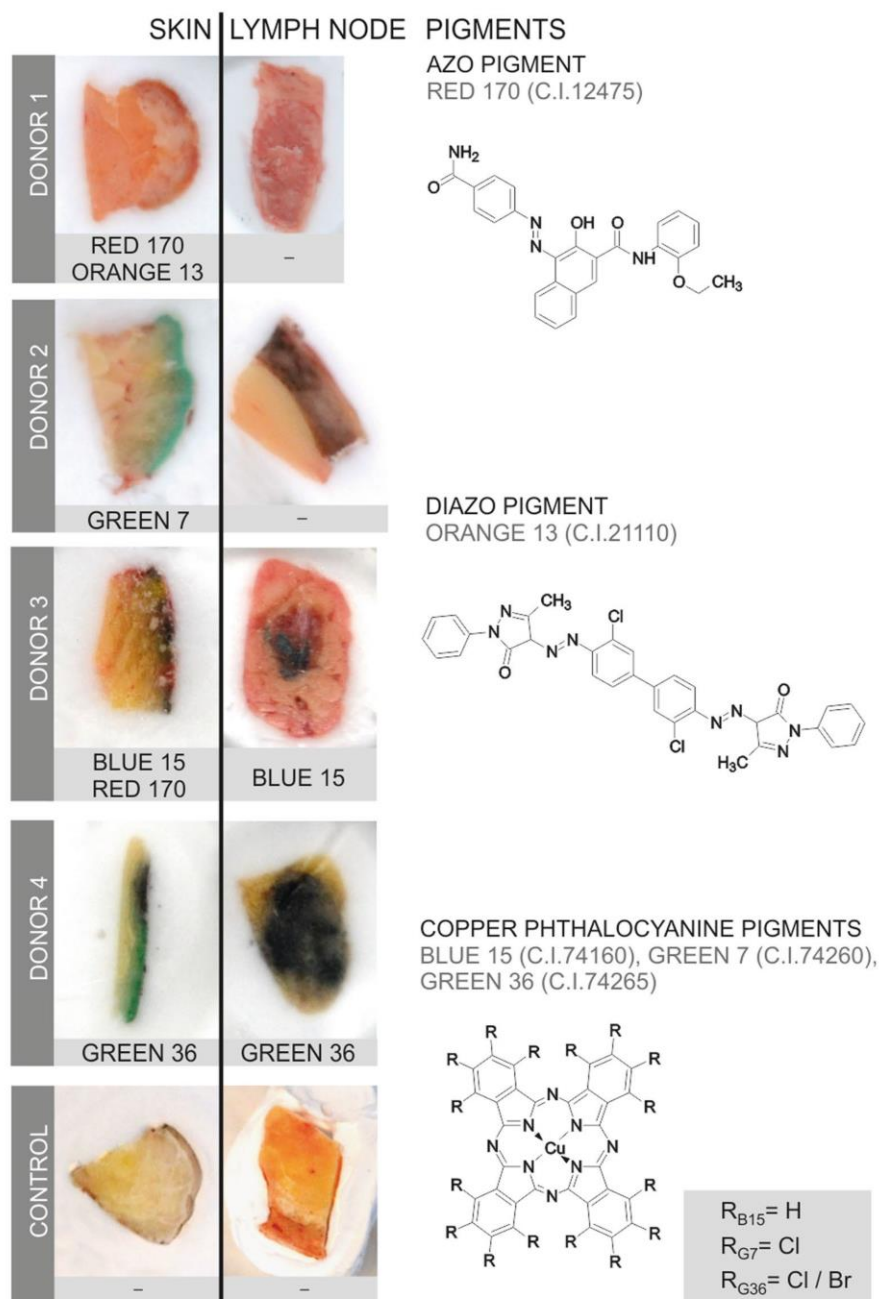


Figure 2. Organic pigments translocate from skin to lymph nodes. Organic pigments in lysed skin and lymph nodes were identified by means of LDI-ToF-MS. Adjacent skin and lymph tissue specimens (about 5–10 mm) are displayed in cryo-matrix after preparing thin sections for μ -FTIR and μ -XRF analyses. Skin specimens are oriented with its surface on the right side. Identified organic pigments are indicated below each sample. Chemical structures of the organic pigments identified in the samples are displayed on the right.

Tattoos contribute to the elemental load of lymph nodes. A central aim of this study was to assess to what extent tattooing increases the proportion of toxic elements in the body. We found Al, Cr, Fe, Ni and Cu quantitatively elevated in skin and lymph node specimens using ICP-MS analysis (Table 1 and Supplementary Table S2). For donor 4, Cd and Hg concentrations were found increased only in the lymph nodes, but not in the

Donor	Tissue	Location	Al	Cr	Fe	Ni	Cu	Cd	other ^a
1	Skin	dorsal	0.92	0.74	64.7	0.59	2.51	0.15	Ti
	LN	left axillary	1.97	0.43	125	0.28	2.98	0.35	Zn, Rb
2	Skin	right leg	7.29	5.54	51.1	2.51	18.8	0.23	Ti
	LN	right inguinal	9.06	22.5	235	10.1	118	1.23	Ti, Mn
3	Skin	right arm	3.39	2.73	84.7	1.61	67.5	0.17	Ti, I
	LN	right axillary	5.08	13.9	221	6.74	28.7	0.28	Ti, Mn, Zn, Rb, I
4	Skin	left arm	15.4	4.07	120	0.45	199	0.52	Ti, Br
	LN	left axillary	4.16	0.67	138	0.30	15.3	146	Ti, Br, Ba, Mn, W, Rb, Hg
Control 1	Skin	proximal	0.75	0.16	35.6	0.08	1.44	0.12	Pb
	LN	axillary	1.11	0.31	64.4	1.09	12.9	0.47	
Control 2	Skin	proximal	0.76	0.60	37.6	0.15	1.41	0.25	
	LN	axillary	0.24	0.14	74.7	0.09	2.48	0.83	Zn, Rb
Literature values	Skin						0.35/0.42 ^a	0.05/0.02 ^a	
	LN		2000 ^c	8.2 ^c	1800 ^c	0.28 ^b 3.7 ^c	2.94/ 5.89 ^a 7.6 ^c	0.24/ 0.20 ^a 2.5 ^c	

Table 1. Element concentrations per tissue weight (ppm) in human skin and lymph node samples analyzed by ICP-MS. Abbreviations: LN = lymph node. Elements measured (non-specified oxidation states): aluminum (Al), barium (Ba), bromine (Br), cadmium (Cd), chromium (Cr), copper (Cu), iodine (I), iron (Fe), lead (Pd), manganese (Mn), mercury (Hg), nickel (Ni), rubidium (Rb), titanium (Ti), tungsten (W), and zinc (Zn). ^aNon-quantitatively identified elements (elements marked in bold are associated with tattoo pigments). ^aWet basis, average from 21 male/female cadavers²⁴. ^bTissue dry weight, average in hilar lymph nodes from 3 cadavers²⁹. ^cTissue dry weight, average in hilar lymph nodes from 12 male cadavers³².

analyzed skin sections. These elements probably result from other tattoos that were not part of this study or other routes of exposure drained through the same lymphatic tissue. Non-quantitative evaluation of the survey scans revealed the presence of Ti, presumably derived from TiO₂, in all tattooed skin samples but not in controls.

The microwave digestion used in this investigation is not suitable to fully dissolve Fe and Ti, although no residual particles were visible. Therefore Fe concentrations might not represent the total amount in the samples, but they enable the distinction between physiological concentrations in controls and samples containing extrinsic Fe. The elevated levels of Fe found in the skin and lymph nodes of donor 4 imply an additional use of iron-based pigments. In donors 1, 2 and 3, Fe concentrations were only increased in adjacent lymph nodes and not in the corresponding skin samples (Table 1). Fe concentrations can also be affected by residual blood within the tissue samples.

In donor 4, the use of pigment copper phthalocyanine green 36, as identified with LDI-ToF-MS, is reflected by high amounts of Cu in skin and lymph nodes as well as the non-quantitative detection of Br (Table 1). By contrast, although pigment copper phthalocyanine green 7 was well detectable with our LDI-ToF-MS approach in the skin of donor 2, it was not in the corresponding regional lymph node. Increased Cu levels measured by ICP-MS in this adjacent sample, however, suggest the presence of this copper phthalocyanine pigment. In light of the other two copper phthalocyanines applied in donor 2 (green 7) and 3 (blue 15) elevated Cu levels in skin came without surprise (Table 1). In donor 2, Cu levels in lymph nodes are strongly increased despite the fact that green 7 could not be detected with LDI-ToF-MS. However, adjacent samples of tissue were used for each analysis. Given the nature of the samples, pigment deposition within skin and lymph nodes is not homogeneous and therefore explaining the different findings. Interestingly, the non-tattooed control donor 1 also had slightly elevated levels of about 13 ppm Cu in the lymph nodes which is still in the range of the average 5.89 ± 8.03 ppm of Cu detectable in lymph nodes of female cadavers (Table 1)²⁴.

Additionally, Ni and Cr were found in the human specimens. Since Ni levels were increased in the skin and lymph nodes of donor 2 and 3, the likely source is the tattoo. In different studies, both elements were linked to adverse reactions occurring in tattooed patients^{25–28}. Ni and Cr are known to be allergenic as well as carcinogenic. Ni concentrations of 0.28–10.05 ppm total tissue weight found here are within the range of 0.8–3.7 ppm dry weight Ni in hilar lymph nodes in previous studies²⁹. Cd was drastically elevated only in the lymph node of donor 4. For all other samples, Cd tissue burdens lie within normal values²⁴.

Finally, Al was also present in skin and lymph node tissues of the three tattooed donors 2, 3 and 4 (Table 1). Since auxiliary lymph nodes have been investigated in the case of donor 2 and 3, co-exposure from antiperspirants containing various aluminum salts cannot be excluded, neither in tattooed nor control samples. However, Al concentrations in the controls were lower. The light metal Al has recently attracted attention because of its accumulation in breast cancer tissue³⁰. While its role in the emerging of neoplasia is currently highly disputed, its contribution to the occurrence of hypersensitivity granulomas associated with tattoos has been proven since decades³¹.

μ-XRF mapping links metallic elements to tattoo particles. In order to link elements found with ICP-MS in tattoo pigment particles and to locate them inside the tissues, μ-XRF imaging was carried out with

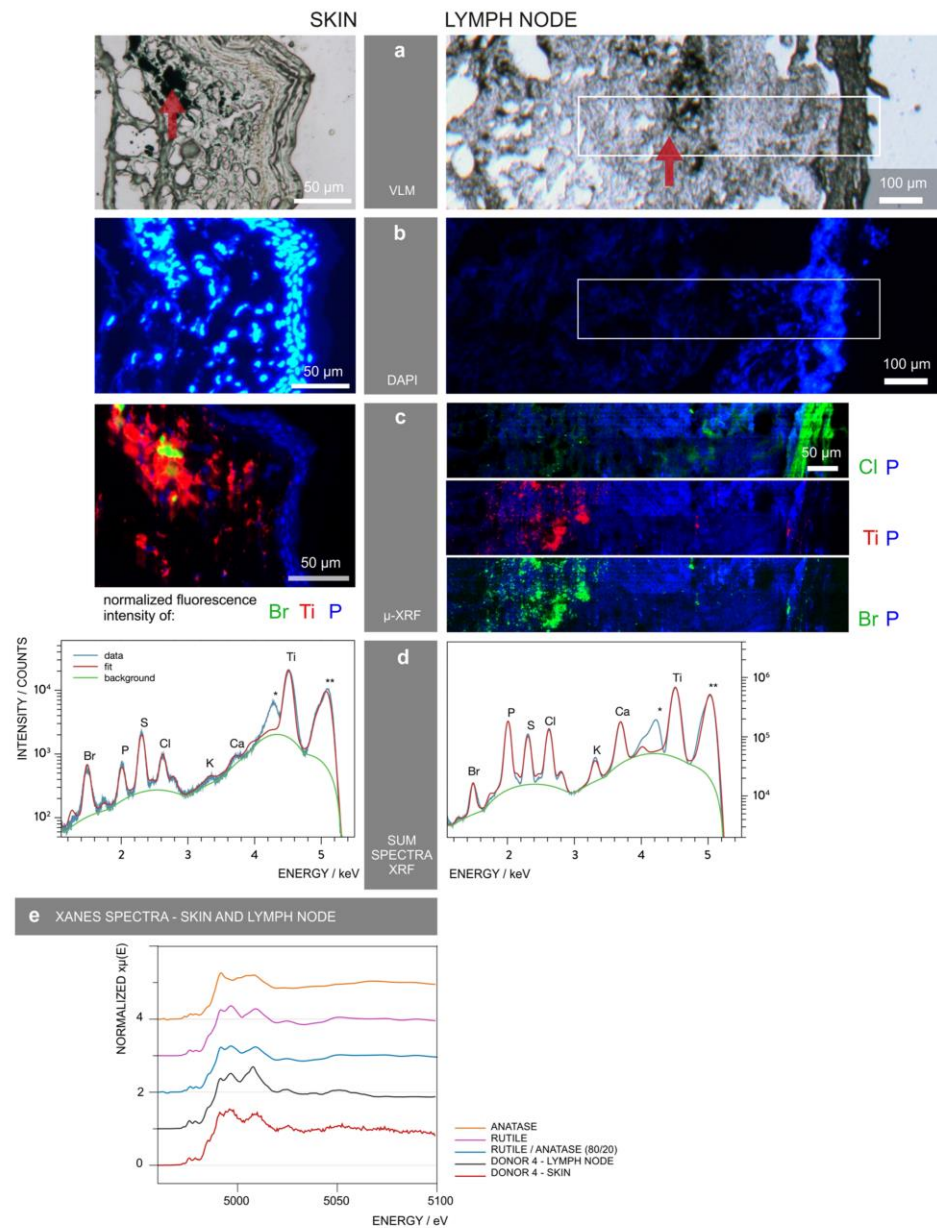


Figure 3. μ -XRF mapping identifies and locates tattoo particle elements in skin and lymph node tissue sections. Sections of skin and lymph node tissue from donor 4 were analyzed by means of synchrotron μ -XRF. (a) Visible light microscopy (VLM) images of the area mapped by μ -XRF. Tattoo pigments are indicated by a red arrow. (b) DAPI staining of adjacent sections showing the cell nuclei. (c) μ -XRF maps of P, Ti, Cl and/or Br. For the lymph node, areas of similar size are marked in (a) and (b). (d) Average μ -XRF spectra over the full area displayed in (c) *diffraction peak from sample support; **scatter peak of the incoming beam. (e) Ti K-edge μ -XANES spectra of skin and lymph node compared to transmission XANES spectra of reference material of rutile, anatase and an 80/20 rutile/anatase mixture calculation.

sub-micrometric probes over skin and lymph node sections (Fig. 3a–d). The location of particles can be altered by sample preparation. Since transversal sections were made by moving the knife parallel to the skin surface, the depth profile of the pigments should remain unaffected. Thin sections of skin and lymph nodes from donors 1, 3 and 4 were analyzed at the ESRF beamline ID21, with an exciting energy of 5.05 keV (Fig. 3a–d and Supplementary Fig. S2). Since the thin sections were deposited on BaF₂ windows for further μ -FTIR analyses, the

energy was chosen to avoid excitation of Ba L-lines (<5.24 keV). Results of donor 4 are displayed in Fig. 3 as an example.

The majority of particles in the skin tissue were surrounded by phosphor-rich nuclei visualized by DAPI staining in fluorescence light microscopy (Fig. 3b) and integration of the element P in μ -XRF analysis (Fig. 3c). It was previously shown that tattoo particles can primarily be found around vessels¹⁰ which might account for the high cell density in the dermis co-localized with the pigments.

Intensities of Ti K-lines and Br L-lines were extracted to map the distribution of TiO₂ and the highly brominated pigment copper phthalocyanine green 36 (Fig. 3c). Since the Br L-lines completely overlap with the Al K-lines, both may contribute to the intensity of the peak. However, LDI-ToF-MS analysis revealed the presence of pigment green 36 (Fig. 2) and the following ν -XRF results from ID16B acquired at 17.5 keV, i.e. above Br K-edge (13.47 keV) undermined the primarily Br-related contribution (see Supplementary Fig. S3).

Tattoo particles containing Ti and Br are adjacent to each other with only a slight overlap in skin and seem to be more evenly co-localized in lymph tissue (Fig. 3c). Both elements were found in the dermis of donor 4 directly beneath the cell nuclei-rich epidermis and up to a few hundred micrometers deep in the skin. In the lymph nodes, some particles were deposited in the stroma directly beneath the capsule. The bulk of Ti and Br containing particles, however, became visible as pigment agglomerates at a distance of about 250 μ m to the lymph node capsule. Conversely, Cl concentrations are highest in the lymph node capsule and lower concentrations can be found in the particle region as part of the pigment phthalocyanine green 36.

All analyzed samples from the tattooed donors contained Ti. It is unlikely that other sources, e.g. sun screens, would explain the high amounts found in this investigation. Elevated amounts of Ti are only expected in lung and hilar lymph nodes from respiratory exposure³². Other highly abundant elements are K and Ca as they are physiologically present in cells (Fig. 3d).

We also investigated if the Ti present is the expected white pigment TiO₂ and whether the stable rutile and/or the more photoreactive anatase crystal phases were used in tattoo inks. Micro X-ray absorption near edge structure (μ -XANES) spectra at the Ti K-edge were collected for the skin and lymph nodes of donors 1, 3 and 4. The spectra of donor 4 showed more qualitative correlation with the reference spectrum of rutile than with that of anatase (Fig. 3e). A clear switch of peak maxima between 4.99–5 keV occurs as a difference of both types of crystal structures. A calculated spectrum of 20% anatase and 80% rutile mixture is not clearly distinguishable from pure rutile, but shows a pre-edge at around 4.97 keV, similar to the μ -XANES spectra of the tattooed samples. Therefore, mostly rutile TiO₂ is present in all tattooed donors, with minor amounts of anatase (Fig. 3e and Supplementary Fig. S2).

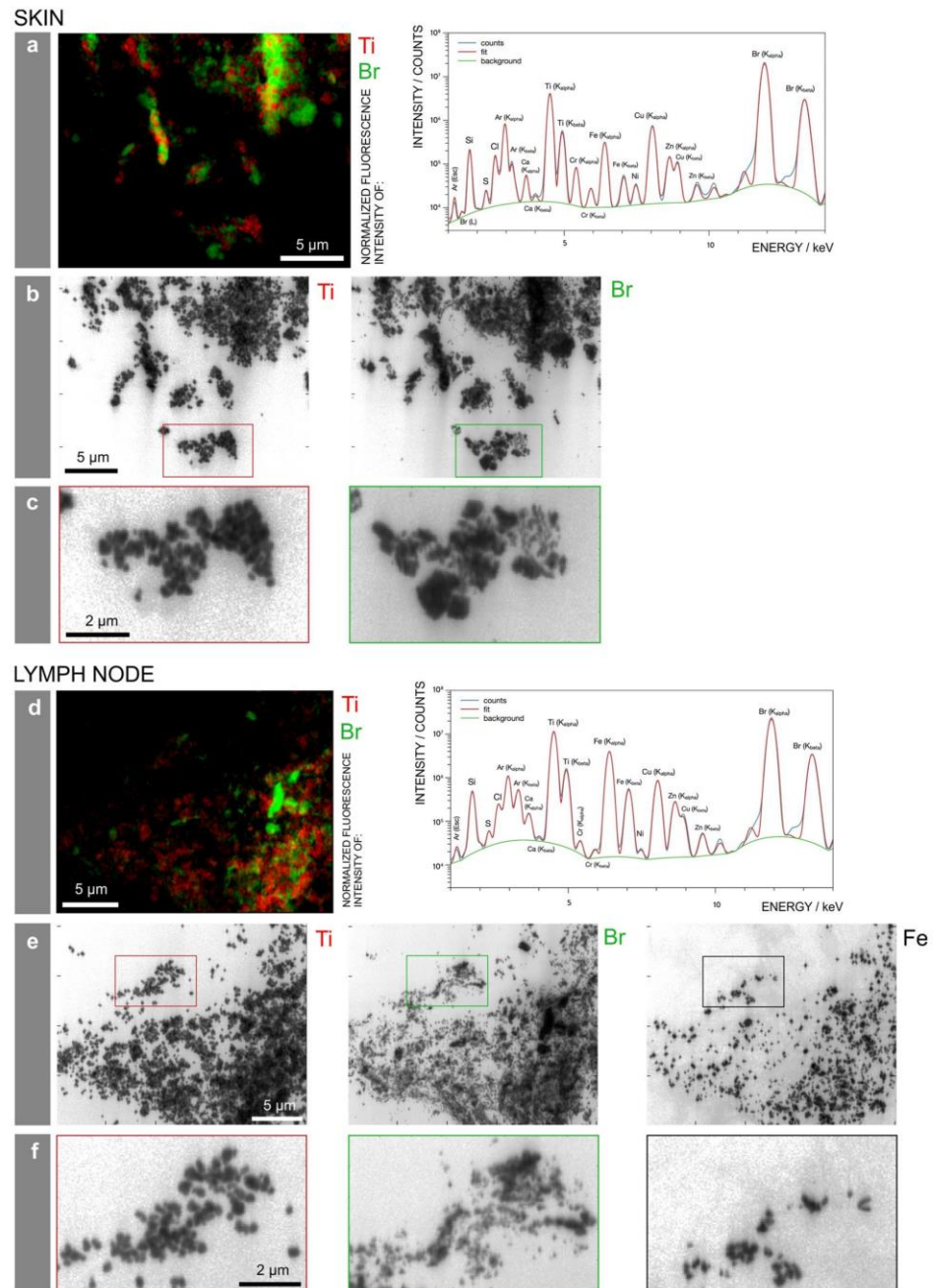
Particle size varies between pigment species. The obtained μ -XRF maps of skin and lymph node sections show large tattoo particle agglomerates up to several micrometers (Fig. 3c). However, it is known that small-sized particles are preferentially transported to lymph nodes. The $0.3 \times 0.7 \mu\text{m}^2$ beam size for μ -XRF mapping at ID21 was therefore a limiting factor for the determination of particle sizes. To assess the primary particle sizes, we additionally performed ν -XRF investigations by applying a beam of $50 \times 50 \text{ nm}^2$ at 17.5 keV in order to excite the Br K-lines. Experiments were carried out in adjacent sections of skin and lymph node from donor 4, prepared on ultralene foil (Fig. 4). We detected three different pigment particles, each showing a different elemental composition and distribution within the same area (Fig. 4b,e). The average particle size of TiO₂ in both skin and lymph nodes was 180 nm with a standard deviation of 23 nm and a standard error of 7 nm. Therefore this rather large particle size does not prevent distribution via the lymph fluid.

In contrast, the pigment phthalocyanine green 36 analyzed by ν -XRF mapping of Br was much more polydisperse, with particles presumably smaller than the resolution of 50 nm and up to the μm range in skin. In lymph node tissue, particles containing Br were smaller, with fewer particles of a larger size (Fig. 4c,f). Hence it can be assumed that the transport of smaller particles is preferential.

With the chosen energy, Br can be unequivocally identified from its K-lines emission. The skin and lymph node of donor 4 also contained Cu, related to the identified copper phthalocyanine pigments, and its maps show perfect co-localization with Br (see Supplementary Fig. S3). Additionally, Fe particles were present in the lymph node but not skin tissue and therefore possibly originate from another tattoo or route of exposure (Fig. 4c,f and Supplementary Fig. S3).

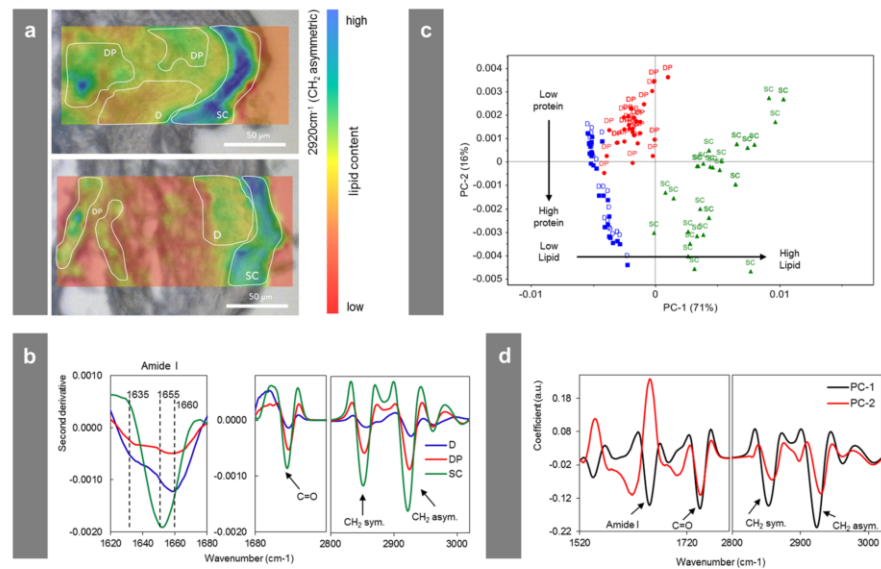
Tattoo particles induce biomolecular changes. The synchrotron-based μ -FTIR end-station at ID21 was used to monitor changes in protein conformation as well as in the overall protein and lipid contents in the proximity of tattoo particles. Synchrotron μ -FTIR analyses allow the assumption that tattoo pigments became located in a lipid-rich β -sheet protein environment.

The very same sections investigated by means of μ -XRF at ID21 were analyzed by means of μ -FTIR, prior to X-ray analyses, to facilitate exact site matching (cf. Figures 3 and 5). Thus, μ -FTIR results were not altered by μ -XRF radiation of the tissue sections. The high synchrotron photon flux allowed for high spatial resolution. Accordingly, the beam and pixel sizes were reduced to $10 \times 10 \mu\text{m}^2$ and $8 \times 8 \mu\text{m}^2$, respectively. This resolution is sufficient to distinguish regular dermis from pigment containing areas in the dermis, but remains insufficient to unambiguously separate the *stratum corneum* from the epidermis, which were analyzed here as a single domain (see below). Specific spectral changes related to the modification of biomolecule composition and conformation are displayed using donor 4 as an example, on the basis of two μ -FTIR maps obtained in a single section at two different locations, for the skin and regional lymph node (Fig. 5). The absorption band which peaks at 2920 cm^{-1} corresponds to the $-\text{CH}_2$ stretching mode, which is much more intense in lipids than in proteins. It can be used to qualitatively map the distribution of lipids over thin sections (Fig. 5a). It shows a higher intensity in the *stratum corneum*, as expected³³. These maps also qualitatively show a higher intensity in the areas of dermis containing tattoo pigments compared to pigment-free control regions. Based on the microscopic images and



the μ -XRF maps described earlier, three regions were selected on each map. For the skin section, we divided the obtained map into *stratum corneum* and epidermis (SC), dermis without pigment (D) and dermis around pigment particles (DP) (Fig. 5a). Spectra in the second derivative of these areas were statistically analyzed by means

SKIN



LYMPH NODE

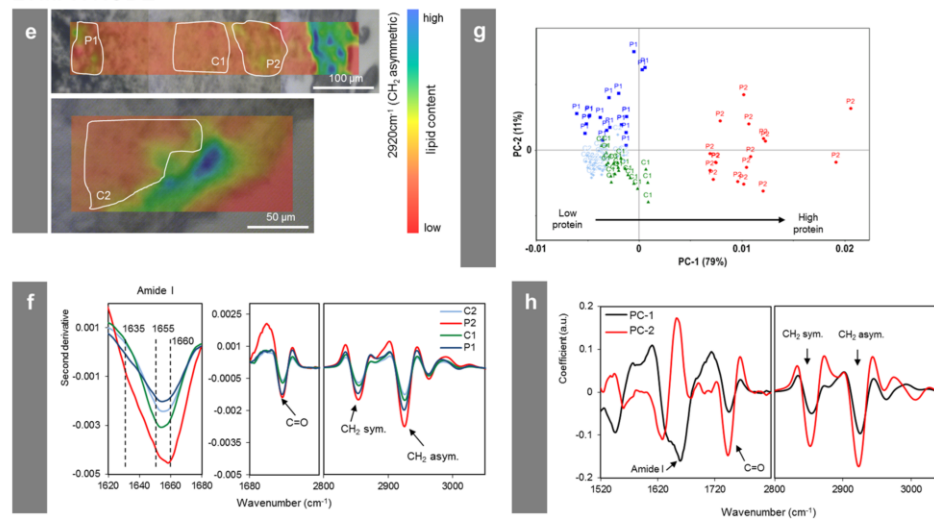


Figure 5. Changes of the biological composition and structure in the cellular proximity of tattoo pigment particles. Section of donor 4 analyzed by means of synchrotron μ -FTIR at ID21, ESRF. (a,e) Maps in second derivative obtained at 2920 cm^{-1} ($-\text{CH}_2$ asymmetric vibration) of two different areas in either the skin or lymph node of donor 4 in overlay with a visible light microscopy image. Single points for PCA analysis in (c) and (g) were picked from the indicated areas. (b,f) Mean spectra from each region marked in (a,e) in second derivative. (c,g) PCA score plot of PC-1 vs. PC-2. (d,h) Loading plots of PC-1 and PC-2. Abbreviations: SC = *stratum corneum* and epidermis; D = dermis; DP = dermis with particles; P1, P2 = particle-containing regions; C1, C2 = control regions without particles.

of Principal Component Analysis (PCA). Distribution of points along the PC-1 axis confirms that D and DP have fewer lipid-related long alkyl chains ($-\text{CH}_2$ stretching mode, asym. at 2920 cm^{-1} and $-\text{CH}_2$ sym. at 2854 cm^{-1}) and ester ($-\text{C}=\text{O}$ stretching mode, peak at 1745 cm^{-1}) vibrations than SC, and that DP regions contain higher levels of lipids than D (Fig. 5b–d). PC-2 separates DP from D and SC since the latter two have higher protein concentrations.

In addition to determining the component distribution, μ -FTIR can be used to identify and map the protein secondary structures across skin sections³³. In the epidermis, keratinocytes differentiate to finally form the dead, protein- and lipid-rich *stratum corneum*. In the designated SC area of our investigation—comprising also the epidermal layer—the amide I peak maximum at $\sim 1655\text{ cm}^{-1}$ (Fig. 5b) derives from α -helices present in keratin³³.

In the dermis, the peak maximum located at 1660 cm^{-1} corresponds to triple helices present in collagen, while the β -sheet shoulder at 1635 cm^{-1} can be assigned to crosslinked collagen fibers³³. In the proximity of the pigment particles (DP), the protein content is lower compared to other parts of the collagen-rich dermis. However, the β -sheet shoulder at 1635 cm^{-1} becomes more pronounced close to the particles (Fig. 5b). The $-\text{CH}_2$ and $-\text{C}=\text{O}$ vibrations related to lipids are also higher in the proximity of particles compared to other parts of the dermis. Both findings suggest the presence of denatured β -sheet-rich protein and lipid membranes surrounding the pigment particles. Other investigations have shown that when in contact with foreign surfaces, protein structures can be altered towards the formation of β -sheets³⁴. In the skin of donor 2, a similarly enhanced lipid content and the presence of β -sheet structures in the dermis around particles were also noticed (see Supplementary Fig. S4). A statistical comparison of particle-containing and particle-free areas in the lymph node tissue of donor 4 showed a similar increase of lipid contents in the former (Fig. 5e–h). However, no consistent differences in the kind of protein folding could be observed in lymph nodes.

Discussion

In this investigation, we found a broad range of tattoo pigment particles with up to several micrometers in size in human skin but only smaller (nano)particles transported to the lymph nodes. The exact size limit preventing this translocation is unknown yet. The deposit of particles leads to chronic enlargement of the respective lymph node and lifelong exposure. With the detection of the same organic pigments and inorganic TiO_2 in skin and lymph nodes, we provide strong analytical evidence for the migration of pigments from the skin towards regional lymph nodes in humans. So far, this only has been assumed to occur based on limited data from mice and visual observations in humans^{13,35}. We also were able to prove the presence of several toxic elements, such as Cr and Ni, derived from tattooing. However, elemental deposits in lymph nodes which were not found in the corresponding skin revealed that tattooing might not have been the only route of exposure in these particular individuals whose tissues were removed after their demise.

It is known that pigments reside in lysosomes or stay attached to membranes of dermal fibroblasts^{8,36}, an observation that supports our μ -FTIR findings of concentrated lipid levels in the proximity of pigment particles. Long alkyl chains and ester groups which we assigned to lipids may also derive from components of tattoo inks, e.g. thickening polymers, surfactants and pigment coatings. However, the frequently used polyethylene glycol³⁷ and polyvinyl pyrrolidone polymers below 20 kDa³⁸ are known to be metabolized and secreted. In addition, the strong lysosomal and reactive oxygen species-driven reaction of macrophages against foreign material was shown to alter even the highly stable polyurethane³⁹. We therefore assume these additives being biodegradable *in vivo* and thus not anymore present in healed tattooed skin. Since the initially used coatings and surfactants of the particles were unknown, interferences in μ -FTIR cannot be fully excluded though.

In cases where foreign hydrophobic material is introduced into the body, fibrinogen and other proteins are likely to become adsorbed and denatured at its surface, thus leading to the generation and presentation of pro-inflammatory matter and subsequent recruitment of immune cells as the initial step in the triggered foreign body reaction^{40,41}. This assumption becomes supported by our μ -FTIR data on β -sheet associated conformational changes of proteins in the proximity of hydrophobic, insoluble tattoo pigments. Foreign body reactions are known from subcutaneous injections of TiO_2 ⁴². Despite the hydrophobic nature of pigment surfaces and the here confirmed β -sheet protein conformation in the proximity of tattoo pigments in skin, most tattooed individuals including the donors analyzed here do not suffer from chronic inflammation though. Yet, granulomatous foreign material reactions are among the main non-infectious side effects occurring upon tattooing⁴³. Factors preventing the progression towards adverse foreign body reactions in most tattooed individuals despite a β -sheet conformation need to be further investigated.

In future experiments we will also look into the pigment and heavy metal burden of other, more distant internal organs and tissues in order to track any possible biodistribution of tattoo ink ingredients throughout the body. The outcome of these investigations not only will be helpful in the assessment of the health risks associated with tattooing but also in the judgment of other exposures such as, e.g., the entrance of TiO_2 nanoparticles present in cosmetics at the site of damaged skin.

Methods

Human sample preparation. Samples of tattooed skin and regional lymph nodes as well as skin and lymph node samples of two additional donors without any tattoos were taken *postmortem* at the Institute of Forensic Medicine at the Ludwig-Maximilians University of Munich (court-ordered autopsies without any additional cosmetic impairment to the skin). The experiments were performed according to the Helsinki Declaration of 1975. All samples were obtained anonymously without information on the patients disease status, causes of death or demographics. Ethical approval of human biopsy samples was granted by the Ethics committee of the Medical Faculty of the Ludwig-Maximilians University of Munich. We selected specimens with tattoos other than black and which are more likely to contain TiO_2 and organic pigments. The sample size was limited by the availability of specimens and the beamtime at ESRF. Tissue samples were stored in plastic bags at $-20\text{ }^\circ\text{C}$ directly after excision and further processed for analysis within a year. Subsamples were cut using a standard scalpel and frozen in TissueTek O.C.T. matrix (Sakura Finetek, Staufen, Germany) for cryo-microtome sectioning. Sections of 5 or 6 μm were obtained and mounted on BaF_2 substrates (Crystal GmbH, Berlin, Germany) for μ -FTIR and μ -XRF measurements at ID21. Sections for fluorescence light microscopy had a thickness of 6–10 μm and were deposited on standard glass slides, while ν -XRF analyses at ID16B were performed on 12–14 μm sections on 4 μm Ultralene window films (Spex Sample Prep, Metuchen, NJ, USA) mounted on Si_3N_4 windows. Sections were inactivated using 4% formaldehyde buffer for 10 min and subsequently washed with deionized water (2 times, 2–5 min). For μ -FTIR and μ -XRF analyses, samples were freeze-dried and stored in a dehydrated environment. Sections on

microscopic glass slides were mounted in DAPI-Fluoromount G (Southern Biotech, Birmingham, AL, USA) for cell nucleus staining.

ICP-MS analysis. Elemental compositions of in total 20 skin and 25 lymph node samples of tattooed donors as well as 2 skin and 2 lymph node samples of non-tattooed donors were analyzed using a nitric acid microwave digestion (Ultraclave, MLS, Leutkirch, Germany). Samples were directly adjacent to those used in other parts in this investigation. Five milliliter of 69% nitric acid was added to 50–200 mg tissue samples in Teflon vessels and heated in the microwave with the following steps: 20–80 °C (3.5 min, 100 bar, 700 W); 80–130 °C (10 min, 120 bar, 1000 W); 130–200 °C (6.5 min, 150 bar, 1000 W), 200 °C (30 min, 150 bar, 1000 W). Elemental concentrations given in ppm are calculated in relation to the weight of digested tissue. Nitric acid was purified using a duoPUR quartz sub-boiling distillation system (MLS, Leutkirch, Germany). Ultrapure water was obtained using a Milli-Q Advantage A10 water purification system equipped with a Millipore Q-POD Element Unit (both from Merck, Darmstadt, Germany). Standards for ICP were purchased either from Sigma Aldrich (Munich, Germany; i.e. Sc, Al, Cu, Ni, Hg) or Merck (Darmstadt, Germany) in the case of In. For Cr, Fe and Cd 1000 mg/l standard solutions in diluted nitric acid were obtained from VWR (Darmstadt, Germany).

A 20-fold dilution of each sample was prepared including 10 ppb of the elements In and Sc as internal standards. XSeries II ICP-MS (Thermo Fischer Scientific, Bremen, Germany) together with an ESI SC2 autosampler (Elemental Service & Instruments, Mainz, Germany) were used for sample analysis. Sample analysis was carried out in triplicate with 100 sweeps each. Resolution was set to 0.02 amu and the dwell time for all elements was 10 ms. Measurements were carried out with collision cell in either -3.0 V mode (In, Sc, Cr, Fe, Ni, Cu, Cd) or 0.0 V mode (Sc, Al). H_2/He (7% v/v) was used as the collision gas with 5 ml/min flow rate. Data were processed with PlasmaLab 2.5.11.321 (Thermo Scientific, Bremen, Germany).

LDI-ToF-MS identification of organic pigments. In total 8 skin and 8 lymph node samples of tattooed donors as well as 2 skin and 2 lymph node samples of non-tattooed donors were analyzed. Samples between 50–200 μ g were lysed using 1 mg/ml collagenase from *Clostridium histolyticum* Type IA (Sigma Aldrich, Munich, Germany) with an incubation time of at least 24 hours at 37 °C. Lysates were heat-inactivated at 90–95 °C for at least 12 hours. Precipitated pigment particles were washed twice with PBS. Centrifugation was carried out with 500 \times g for 10 min. Precipitates were applied as thin films to a ground steel target plate with a plastic pipette tip and measured using an UltrafleXtreme MALDI-ToF/ToF (Bruker Daltonik, Bremen, Germany). Spectra were obtained by averaging 3000 individual spectra, with a laser rate of 1000 Hz in positive reflector mode. The instrument was calibrated prior to each measurement with an external ProteoMass™ MALDI Calibration Kit (Sigma Aldrich, Munich, Germany). Data were processed using the flexControl 3.4 and flexAnalysis 3.4 software (Bruker Daltonik, Bremen, Germany).

Synchrotron FTIR microscopy. FTIR microscopy analyses were performed at beamline ID21 at the European Synchrotron Radiation Facility (ESRF) in Grenoble, France⁴⁴. The beamline is equipped with a Thermo Nicolet Continuum (Thermo Scientific, Madison, WI, USA) microscope coupled to a Thermo Nicolet Nexus FTIR spectrometer (Thermo Scientific, Madison, WI, USA) with a 32x objective, a motorized sample stage, and a liquid nitrogen-cooled 50 μ m HgCdTe detector. Maps were acquired in transmission mode using a 10 \times 10 μ m² beam, step size of 8 μ m. Spectra were recorded as an average of 64 scans per spectrum, over a range of 4000 to 850 cm^{-1} and with a spectral resolution of 4 cm^{-1} .

The OMNIC software was used to transform spectra from maps of skin and lymph node samples to second derivatives using Savitsky-Golay of second polynomial order with 21 smoothing points^{45,46}. Unscrambler X software (Version 10.3, CAMO Software, Oslo, Norway) was used for further statistical analysis. Principal component analysis (PCA) was performed on the mean-centered data using the spectral regions from: 1800 to 1350 cm^{-1} (related to proteins) and 3200 to 2800 cm^{-1} (related to lipids)^{47,48}. PCA was performed separately for skin and lymph node samples. Score plots and loading plots obtained by PCA analysis as well as mean values from the regions of interest were used for data interpretation.

Synchrotron μ -XRF and μ -XANES. μ -XRF and μ -XANES analyses were carried out at the beamline ID21⁴⁹. Here, X-rays were generated by an U42 undulator operated in “gap-tracking” mode, i.e. the gap value was optimized for each energy. A fixed exit double-crystal Si(111) Kohzu-monochromator was used in combination with a Ni-coated flat double-mirror rejecting high-energy harmonics and allowed for energy selection with about 0.4 eV resolution of the primary radiation at Ti K-edge (5.1 keV). Downstream of the monochromator, the beam was focused down to 0.4 \times 0.8 μ m² (vertical \times horizontal) using a fixed-curvature Kirkpatrick-Baez (KB) mirror system. The flux was 1.6 \times 10¹⁰ photons/s (~180 mA SR current in multi-bunch mode). A 30 μ m Al attenuator was used to reduce the photon flux by one order of magnitude to keep the XRF detector dead time within its linear range. A photodiode collecting the XRF from a thin Si₃N₄ membrane inserted in the beam path was used to continuously monitor the incoming beam intensity. XRF and scattered radiation were collected with a dispersive energy silicon drift detector with an active area of 80 mm² (Bruker Daltonik, Bremen, Germany). Acquisition time per point was 100 ms. The pixel size for collecting the XRF maps was adjusted to the regions of interest and varied from 0.5 μ m to 5 μ m. Scans were performed in continuous (zap) mode and an energy of 5.05 keV was selected for μ -XRF mapping. For collecting Ti XANES spectra, the energy of the incoming beam was scanned from 4.95 to 5.1 keV in increments of 0.5 eV, with acquisition times of 100 ms per energy. Depending on the concentration of the probed region, between 1 and 10 μ -XANES spectra were collected per point and subsequently averaged. Full-field XANES maps were also collected to total the XANES spectra over multiple pixels.

Synchrotron ν -XRF. The analysis on an adjacent section of skin and lymph node tissue from donor 4 was performed by means of ν -XRF at ID16B at the ESRF. The experimental set-up is described elsewhere⁵⁰. A pink

beam with an energy of 17.5 keV with $\Delta E/E = 1\%$ was focused down to $50 \times 50 \text{ nm}^2$ using KB mirrors. The flux of $>1 \times 10^{11}$ photons/s was subsequently reduced using gold and silicon attenuators to keep the dead time on the XRF detectors within the linear range. Two three-element silicon drift detector arrays (SGX Sensortech, Buckinghamshire, UK) were used. The two ν -XRF maps were recorded with a step size of $50 \times 50 \text{ nm}^2$ and 100 ms dwell time. In contrast to the set-up installed at ID21, ID16B operates in air. For estimating the particle size of TiO_2 , analysis was performed on 10 particles by computing the full width at half maximum of line profiles through the particles.

Availability of materials and data. XRF and FTIR data sets can be provided by the authors upon individual request.

Ethical approval of human biopsy samples. Samples of tattooed skin and regional lymph nodes were taken *postmortem* and anonymously at the Institute of Forensic Medicine at the Ludwig-Maximilians University of Munich in the frame of court-ordered autopsies without information on the patients disease status, causes of death or demographics. Experiments were performed according to the Helsinki Declaration of 1975 (see: <http://www.wma.net/en/30publications/10policies/b3/17c.pdf>). Ethical approval of human biopsy retrieval was granted by the Ethics committee of the Medical Faculty of the Ludwig-Maximilians University of Munich, Germany (confirmation by R.P., member of the ethics committee).

References

1. Laux, P. *et al.* A medical-toxicological view of tattooing. *The Lancet* **387**, 395–402 (2016).
2. Schreiber, I. & Luch, A. At the dark end of the rainbow: data gaps in tattoo toxicology. *Arch. Toxicol.* **90**, 1763–1765 (2016).
3. Schreiber, I., Hutzler, C., Laux, P., Berlien, H. P. & Luch, A. Formation of highly toxic hydrogen cyanide upon ruby laser irradiation of the tattoo pigment phthalocyanine blue. *Sci. Rep.* **5**, 12915 (2015).
4. Hauri, U. Inks for tattoos and permanent make-up – pigments, preservatives, aromatic amines, polyaromatic hydrocarbons and nitrosamines. http://www.kantonslabor.bs.ch/dms/kantonslabor/download/berichte/berichte-2014/Tattoo_PMU_2014_EN-UK-/Tattoo_PMU_2014_EN%28UK%29.pdf (2014).
5. Schreiber, I., Hutzler, C., Andree, S., Laux, P. & Luch, A. Identification and hazard prediction of tattoo pigments by means of pyrolysis—gas chromatography/mass spectrometry. *Arch. Toxicol.* **90**, 1639–1650 (2016).
6. Vasold, R. *et al.* Tattoo pigments are cleaved by laser light—the chemical analysis *in vitro* provide evidence for hazardous compounds. *Photochem. Photobiol.* **80**, 185–190 (2004).
7. Anderson, L. L., Cardone, J. S., McCollough, M. L. & Grabski, W. J. Tattoo pigment mimicking metastatic malignant melanoma. *Dermatol. Surg.* **22**, 92–94 (1996).
8. Taylor, C. R., Anderson, R. R., Gange, R. W., Michaud, N. A. & Flotte, T. J. Light and electron microscopic analysis of tattoos treated by Q-switched ruby laser. *J. Invest. Dermatol.* **97**, 131–136 (1991).
9. Zelickson, B. D. *et al.* Clinical, histologic, and ultrastructural evaluation of tattoos treated with three laser systems. *Lasers Surg. Med.* **15**, 364–372 (1994).
10. Ferguson, J. E., Andrew, S. M., Jones, C. J. P. & August, P. J. The Q-switched neodymium: YAG laser and tattoos: a microscopic analysis of laser-tattoo interactions. *Br. J. Dermatol.* **137**, 405–410 (1997).
11. Nopajaroonsri, C. & Simon, G. Phagocytosis of colloidal carbon in a lymph node. *Amer. J. Path.* **65**, 25–42 (1971).
12. Gopee, N. V. *et al.* Response of mouse skin to tattooing: use of SKH-1 mice as a surrogate model for human tattooing. *Toxicol. Appl. Pharmacol.* **209**, 145–158 (2005).
13. Lehner, K. *et al.* Black tattoos entail substantial uptake of genotoxic polycyclic aromatic hydrocarbons (PAH) in human skin and regional lymph nodes. *PLoS One* **9**, e92787 (2014).
14. Timko, A. L., Miller, C. H., Johnson, F. B. & Ross, V. *In vitro* quantitative chemical analysis of tattoo pigments. *Arch. Dermatol.* **137**, 143–147 (2004).
15. Forte, G., Petrucci, F., Cristaudo, A. & Bocca, B. Market survey on toxic metals contained in tattoo inks. *Sci. Total Environ.* **407**, 5997–6002 (2009).
16. Davis, M. D. *et al.* Patch testing with a large series of metal allergens: findings from more than 1,000 patients in one decade at Mayo Clinic. *Dermatitis* **22**, 256–271 (2011).
17. Yoshihisa, Y. & Shimizu, T. Metal allergy and systemic contact dermatitis: an overview. *Dermatol. Res. Pract.* **2012**, 749561 (2012).
18. Dirks, M. Making innovative tattoo ink products with improved safety: possible and impossible ingredients in practical usage. *Curr. Probl. Dermatol.* **48**, 118–127 (2015).
19. Brady, B. G., Gold, H., Leger, E. A. & Leger, M. C. Self-reported adverse tattoo reactions: a New York City Central Park study. *Contact Dermatitis* **73**, 91–99 (2015).
20. Hogsberg, T., Loeschner, K., Löf, D. & Serup, J. Tattoo inks in general usage contain nanoparticles. *Br. J. Dermatol.* **165**, 1210–1218 (2011).
21. Soltzberg, L. J., Hagar, A., Kridaratikorn, S., Mattson, A. & Newman, R. MALDI-TOF mass spectrometric identification of dyes and pigments. *J. Am. Soc. Mass. Spectrom.* **18**, 2001–2006 (2007).
22. Boon, J. J. & Learner, T. Analytical mass spectrometry of artists' acrylic emulsion paints by direct temperature resolved mass spectrometry and laser desorption ionisation mass spectrometry. *J. Anal. Appl. Pyrolysis* **64**, 327–344 (2002).
23. Hauri, U. Inks for tattoos and PMU (permanent make-up)/Organic pigments, preservatives and impurities such as primary aromatic amines and nitrosamines. www.kantonslabor.bs.ch/dms/kantonslabor/download/berichte/berichte-2011/JB_Tattoo_PMU_2011_EN.pdf (2011).
24. Saltzman, B. E., Gross, S. B., Yeager, D. W., Meiners, B. G. & Gartside, P. S. Total body burdens and tissue concentrations of lead, cadmium, copper, zinc, and ash in 55 human cadavers. *Environ. Res.* **52**, 126–145 (1990).
25. Sowden, J. *et al.* Red tattoo reactions: X-Ray microanalysis and patch-test studies. *Br. J. Dermatol.* **124**, 576–589 (1991).
26. Bagnato, G. F. *et al.* Urticaria in tattooed patient. *Allergol. Immunopathol.* **27**, 32–33 (1999).
27. Eun, H. C. & Kim, K. H. Allergic granuloma from cosmetic eyebrow tattooing. *Contact Dermatitis* **21**, 276–278 (1989).
28. Morales-Callaghan, A. M. Jr., Aguilar-Bernier, M. Jr., Martinez-Garcia, G. & Miranda-Romero, A. Sarcoid granuloma on black tattoo. *J. Am. Acad. Dermatol.* **55**, 71–73 (2006).
29. Rezuke, W. N., Knight, J. A. & Sunderman, F. W. Reference values for nickel concentrations in human tissues and bile. *Am. J. Ind. Med.* **11**, 419–426 (1987).
30. Darbre, P. D. Aluminium, antiperspirants and breast cancer. *J. Inorg. Biochem.* **99**, 1912–1919 (2005).
31. McFadden, N., Lyberg, T. & Hensten-Petersen, A. Aluminum-induced granulomas in a tattoo. *J. Am. Acad. Dermatol.* **20**, 903–908 (1989).
32. Teraoka, H. Distribution of 24 elements in the internal organs of normal males and the metallic workers in Japan. *Arch. Environ. Health* **36**, 155–165 (1981).

33. Gross, N. *et al.* High spatial resolution study of human skin using synchrotron infrared microscopy: application to the penetration of external agents. *IFSCC Magazine* **7**, 1–8 (2004).
34. Lenk, T. J., Horbett, T. A., Ratner, B. D. & Chittur, K. K. Infrared spectroscopic studies of time-dependent changes in fibrinogen adsorbed to polyurethanes. *Langmuir* **7**, 1755–1764 (1991).
35. Engel, E. *et al.* Tattooing of skin results in transportation and light-induced decomposition of tattoo pigments—a first quantification *in vivo* using a mouse model. *Experim. Dermatol.* **19**, 54–60 (2010).
36. Ross, E. V. *et al.* Tattoo darkening and nonresponse after laser treatment. *Arch. Dermatol.* **137**, 33–37 (2001).
37. Value, M. A. K. Documentation, 1998. Polyethylene glycol. *The MAK Collection for Occupational Health and Safety* **10**, 248–270 (2012).
38. Chi, C.-C., Wang, S. H. & Kuo, T. Localized cutaneous polyvinylpyrrolidone storage disease mimicking cheilitis granulomatosa. *J. Cutan. Pathol.* **33**, 454–457 (2006).
39. Zhao, Q. *et al.* Foreign-body giant cells and polyurethane biostability: *in vitro* correlation of cell adhesion and surface cracking. *J. Biomed. Mater. Res.* **25**, 177–183 (1991).
40. Lu, D. R. & Park, K. Effect of surface hydrophobicity on the conformational changes of adsorbed fibrinogen. *J. Colloid Interfac. Sci.* **144**, 271–281 (1991).
41. Tang, L. & Eaton, J. W. Natural responses to unnatural materials: a molecular mechanism for foreign body reactions. *Mol. Med.* **5**, 351–358 (1999).
42. Umbreit, T. H. *et al.* Tissue distribution and histopathological effects of titanium dioxide nanoparticles after intravenous or subcutaneous injection in mice. *J. Appl. Toxicol.* **32**, 350–357 (2012).
43. Wenzel, S. M., Rittmann, I., Landthaler, M. & Bäuml, W. Adverse reactions after tattooing: review of the literature and comparison to results of a survey. *Dermatology* **226**, 138–147 (2013).
44. Susini, J. M. *et al.* Technical Report: The FTIR Spectro-Microscopy End-Station at the ESRF-ID21 Beamline. *Synchrotron Radiat. News* **20**, 13–16 (2007).
45. Martin, F. L. *et al.* Distinguishing cell types or populations based on the computational analysis of their infrared spectra. *Nat. Protocols* **5**, 1748–1760 (2010).
46. Benseny-Cases, N., Klementieva, O., Cotte, M., Ferrer, I. & Cladera, J. Microspectroscopy (μ FTIR) reveals co-localization of lipid oxidation and amyloid plaques in human Alzheimer disease brains. *Anal. Chem.* **86**, 12047–12054 (2014).
47. Chwiej, J. *et al.* Synchrotron FTIR micro-spectroscopy study of the rat hippocampal formation after pilocarpine-evoked seizures. *J. Chem. Neuroanat.* **40**, 140–147 (2010).
48. Petibois, C., Drogat, B., Bikfalvi, A., Deleris, G. & Moenner, M. Histological mapping of biochemical changes in solid tumors by FT-IR spectral imaging. *FEBS Lett.* **581**, 5469–5474 (2007).
49. Salomé, M. *et al.* The ID21 Scanning X-ray Microscope at ESRF. *J. Phys. Conf. Ser.* **425**, 182004 (2013).
50. Martínez-Criado, G. *et al.* ID16B: a hard X-ray nanoprobe beamline at the ESRF for nano-analysis. *J. Synchrotron Radiat.* **23**, 344–352 (2016).

Acknowledgements

The authors thank the ESRF for allocated beamtimes on ID21 and ID16B. N. Dommershausen is acknowledged for technical help with LDI-ToF-MS analyses. We are grateful to Prof. Dr. Bäuml for valuable discussions. This work was supported by the intramural research project (SFP #1322–604) at the German Federal Institute for Risk Assessment (BfR).

Author Contributions

A.L., M.C., R.T. and P.L. designed and supervised the study, including the interpretation of analytical data. I.S., B.H., H.C.-M. and C.S. planned the experiments. B.H., H.C.-M., I.S. and C.S. performed the experiments at ID21. J.V. performed the experiments at ID16B. I.S. analyzed the samples by means of LDI-ToF-MS. I.S. and N.D. carried out ICP-MS analysis. I.S., B.H., H.C.-M. and C.S. critically reviewed the data and drafted the manuscript. C.S. graphically designed the figures. R.P. selected and provided human specimens suitable for these experiments. A.L. and M.C. analyzed the overall results and finalized the manuscript.

Additional Information

Supplementary information accompanies this paper at doi:10.1038/s41598-017-11721-z

Competing Interests: The authors declare that they have no competing interests.

Publisher's note: Springer Nature remains neutral with regard to jurisdictional claims in published maps and institutional affiliations.

 **Open Access** This article is licensed under a Creative Commons Attribution 4.0 International License, which permits use, sharing, adaptation, distribution and reproduction in any medium or format, as long as you give appropriate credit to the original author(s) and the source, provide a link to the Creative Commons license, and indicate if changes were made. The images or other third party material in this article are included in the article's Creative Commons license, unless indicated otherwise in a credit line to the material. If material is not included in the article's Creative Commons license and your intended use is not permitted by statutory regulation or exceeds the permitted use, you will need to obtain permission directly from the copyright holder. To view a copy of this license, visit <http://creativecommons.org/licenses/by/4.0/>.

© The Author(s) 2017

3. Discussion

3.1. Photothermolysis of organic pigments

3.1.1 Extrapolation of decomposition patterns to other pigments and sunlight exposure

The results of this work demonstrated that photodecomposition of organic pigments by laser light can be mimicked by pyrolysis (cf. Chapter 2.1–2.3).

The heat generated inside the pigment particles can easily reach a few hundred to a thousand Kelvin during laser removal⁹⁸. This energy is sufficient to destroy the exposed compounds up to atomization and a wide range of secondary pyrolysis products might be formed from rearranged molecules. However, many of the substances identified were simple cleavage products which could have been predicted from the structure of the pigments. In 6 out of 8 pigments investigated in a non-quantitative analysis, the predicted cleavage compounds resulting from pyrolysis were indeed found after laser irradiation (Chapter 2.3, Table 2). In the remaining 2 pigments analyzed, no products that would result from pigment decomposition were found, thus indicating that little or no cleavage occurred. Also, for all six pigments where the amounts of decomposed fragments had been quantified, the main laser decomposition products and pyrolysis results matched (Chapter 2.3).

The data generated from 36 pyrolyzed pigments and 14 pigments irradiated with medical lasers, allow the extrapolation of laser-induced decomposition patterns to pigments that have, as yet, not been investigated. For example, the cleavage of weaker amine and amide bonds appears to be a general decay mechanism of azo pigments after laser irradiation and has also been reported in relevant literature. Examples include P.R.22 and P.R.9, where existing studies showed the decomposition of the azo bond with and without loss of N_2 ⁴⁶. In the case of P.R.112, decomposition products deriving from azo and amide cleavage were identified after laser irradiation⁴⁹.

Other susceptible cleavage sites include residues of aryl hydrocarbon groups such as halogens, methyl and ethyl groups resulting in corresponding phenyl rings with amine, isocyanate, nitrile and halogen residues (cf. Chapter 2.2 and 2.3). Also, neighboring heterocyclic systems of benzenes are frequently cleaved and lead to specific patterns in quinacridone, diketopyrrolopyrrole pigments, as well as pyrazolone-coupling groups of diazo pigments (cf. Chapter 2.2 and 2.3). Heterocyclic cleavage leads to the release of mono- and dicyanobenzenes upon laser irradiation of phthalocyanines (Chapter 2.1–2.3). Yet, the exposure to cleavage products from tattoo pigments after laser irradiation naturally only poses a risk to the 4.9% of persons opting for this kind of tattoo removal⁶⁶. Sunlight, however, presents a

potential risk of pigment cleavage for every tattooed person. It was shown that not only UVA and UVB radiation, but also visible light, can destroy organic pigments⁴⁹. The question raised is therefore, whether the data presented here also allows for extrapolation of decomposition patterns to sunlight exposure. If again the assumption is made that cleavage occurs at the amide and azo bonds, the predicted cleavage patterns can be compared with data from literature. In the case of P.R.112, the cleavage of azo and amide bonds seen upon laser irradiation was also found upon sunlight simulation⁴⁹. Cleavage of the azo bond was shown in P.R.22, P.R.170, P.O.14, P.O.34, P.O.16 and P.Y.14⁴⁹. In the case of P.Y.74, the only common compound found after pyrolysis and sunlight simulation was *N,N'*-bis-(2-methoxyphenyl)urea which is a dimer from the amide bond coupling group (cf. Chapter 2.1 and Cui *et al.*⁴⁷). Analyzing P.Y.74, Cui and colleagues used liquid chromatography coupled to mass spectrometry (LC-MS) and nuclear magnetic resonance (NMR) spectroscopy for structural determination of the cleavage products resulting from sunlight⁴⁷. The main decomposition products could not be identified in their investigation, which they put down to their chemical instability.

In contrast to most investigations of pigment decomposition in literature, we chose a gas chromatography (GC)-MS approach to identify the largest possible portion of decomposition products by spectral library search. LC-MS currently lacks the large spectral libraries necessary for identification of analytes.

In our pyrolysis (py)-GC-MS analysis of P.Y.74, the main decomposition products were primary aromatic amines with a smaller molecular weight than those reported in literature using the LC approach⁴⁷. Often investigations in literature seem to have targeted the azo cleavage products only. Hence, the differences between our pyrolysis data and the data from literature most likely derive from the different methods used to analyze the cleavage products. Also, since LC and GC are each suitable for compounds with different chemical properties, the corresponding less suitable compounds will be discriminated.

In general, sunlight will transfer significantly less energy to the pigments at any given time than laser irradiation. Rearrangement and cleavage of stronger bonds of atoms with similar electron negativity, as seen in pyrolysis and laser irradiation, might occur rarely. This may explain why decomposition products derived by cleavage of multiple bonds, such as benzene, have not yet been reported in tests exposing the pigments to sunlight. In order to properly compare the py-GC-MS prediction with cleavage upon sunlight exposure, the same methods have to be applied for substance identification (cf. Chapter 2.1 and 2.3). This type of comparative analysis of both scenarios could potentially facilitate the prediction of corresponding cleavage products.

In summary, we showed for the first time that cleavage patterns of pyrolyzed pigments give a good prediction of decomposition products that occur as a result of laser irradiation in aqueous solution and pig skin. The data generated in this work underlines the validity of an extrapolation of the cleavage patterns to non-tested pigments of similar chemical structure while assuming the cleavage of weak bonds as proposed in the above and in Chapter 2.3. However, transfer of cleavage patterns induced by sunlight can only be confirmed by literature in the case of azo cleavage. Other possible cleavage sites still need to be investigated.

3.1.2 Toxicological risks of major laser decomposition products

In order to achieve appropriate regulation of tattoo inks, a health-based risk assessment of all ingredients and decomposition products is needed. The laser induced decomposition products of pigments that were identified in this work include known carcinogens, allergens and other skin relevant toxins. Substances released in skin can be assumed to be fully bioavailable and in worst case scenarios might be extrapolated to the blood concentration using data from *in vivo* studies via computer modelling. In this way, safety margins might be established, e.g. based on the lowest-observed-adverse-effect level in animal models (LOAEL). Pigments releasing decomposition products able to exceed safe concentrations might well be banned from use in tattoo inks. In terms of carcinogenicity, safety margins might only be applicable with regard to compounds that have a non-genotoxic mode of action.

Regarding carcinogenicity and in view of the expected systemic distribution (cf. Chapter 3.1.3), the carcinogens found after laser irradiation might cause effects in peripheral target organs rather than skin cancer. One main argument is that skin cancer evolves from altered epidermal cells in the superficial skin layer, whereas tattoo pigments are deposited in the deeper dermis. Diffusion of the carcinogens to the epidermis competes with systemic distribution via the blood and lymph streams. Secondly, because the dermal fibroblasts have only a limited metabolism they display little of the enzymatic activity necessary to activate some carcinogenic compounds compared to the epidermal layer. For example, cytochrome P450 (CYP)1A1 and CYP1A2 are less expressed¹⁰⁴. CYP1A2 is believed to contribute most to DCBD activation⁴² and also seems to contribute to the non-genotoxic carcinogenicity of hexachlorobenzene (HCB)^{105,106}. Also, most CYP and flavin-containing monooxygenase activity in the dermis can be attributed to hair follicles and glands instead of the fibroblast cells^{104,107}.

All pigments investigated showed the release of HCN and benzene. However, in general all organic compounds bare the potential to release these combustion products upon laser irradiation, including laser ablative surgery not involving xenobiotic pigments¹⁰⁸. The question to be raised is therefore,

whether the amounts released by laser irradiation display an additional risk compared to naturally occurring exposure with HCN and benzene?

In terms of benzene, the median blood level of non-smokers is reported as 0.046 µg/l in a 1994 study¹⁰⁹. Peak values of workers in contact with mineral oil products, reach up to 13.58 µg/l¹¹⁰. In our investigations, maximum values of benzene were found in P.O.13 and P.R.170. P.Y.138 only showed a minimal release of benzene. Therefore, 117.5 ng (1.5 nmol) per pig skin biopsy is considered to be the worst case benzene release and 1.56 ng (0.02 nmol) as the lowest level of release after laser irradiation. Assuming an average size tattoo of 300 cm² and a biopsy size of 0.126 cm², the amount of benzene must be multiplied by 2380.85 to give the total quantity of benzene released. Again, divided by a median blood volume of 5 liter, this scenario would result in a benzene blood concentration range of between approximately 0.74 µg/l and 55.9 µg/l for the organic pigments investigated. However, these maximum possible concentrations do not consider possible excretion mechanisms such as exhaling, known to facilitate a rapid decrease of benzene¹¹¹. Whether the repeat exposure to benzene of 5–10 removal sessions by laser irradiation may increase the life-time cancer risks has yet to be calculated for risk assessment purposes.

In the case of HCN, average blood levels of smokers directly after finishing a cigarette are 8.12–21.6 µg/l and decrease to pre-cigarette concentrations of 1.6–5.4 µg/l within 15 min. The highest levels of 0.405 µg (150 nmol) of HCN per sample in aqueous suspensions and 0.027 µg (10 nmol) per skin biopsy were found upon laser irradiation of P.B.15. A worst-case scenario of a 300 cm² tattoo and 5 liters of blood would result in a HCN blood concentration of 192.75 µg/l and 12.85 µg/l, respectively. Lethal blood concentrations of HCN are in the range of 2–7 mg/l in blood¹¹². Therefore, the HCN evolving upon laser irradiation of organic pigments is not thought to pose a life-threatening risk but may harm the skin locally (cf. Chapter 2.2).

A third decomposition product often occurring after laser irradiation was the PAA aniline. Aniline is a known human skin sensitizer¹¹³ and listed under carcinogenicity category 2 (GHS). However, the mode of action of the carcinogenicity of aniline is attributed to its reactive metabolites, which lead to methemoglobin formation and erythrotoxicity, ultimately resulting in tumor formation in rat spleen during animal testing at high concentrations¹¹⁴. Mutagenicity tests of aniline are often equivocal and need metabolic activation⁵⁴. Genotoxicity tests are positive only at high concentrations and there is often a lack of data on cytotoxicity at the concentrations used¹¹⁴. Nonetheless, aniline is categorized as possible carcinogen with mutagenic effects and therefore classified as a non-threshold substance. The US EPA estimates a cancer risk of 1 in 1 000 000 at a drinking water concentration of 6 µg/l aniline⁵⁴.

Also, in a survey of chemical substances in tattoo inks by the Danish Environmental Protection Agency, the derived minimal effect level in terms of carcinogenicity of aniline was calculated to be 20 ng/kg bodyweight per day for this route of application¹¹⁵. Therefore, 1.4 µg aniline per day for a 70 kg person or 511 µg per year should be correlated with minimal risks of cancer. A maximal dose exposure of aniline of 117.6 µg (0.547 nmol in 0.126 cm²) in a treatment of a 300 cm² tattoo can be calculated from our results. With 5 laser treatments per year a maximum of 588 µg aniline might be released—not considering that the amount of pigment and therefore the chemicals released are likely to reduce with each treatment. Therefore, it has to be discussed whether repeated doses from laser tattoo irradiation significantly add to this risk.

Aniline was found readily in about 10% of tattoo inks of various color shades tested in a 2013 monitoring program in Germany. Here, an average of 1.5 mg/kg ink and a maximum level of 30.9 mg/kg were detected²⁹. Assuming 1 mg ink per cm² being injected for an average tattoo of 300 cm², 0.45-9.29 µg aniline might enter the body upon tattooing. However, a much higher amount of ink will be in contact with the skin surface during the tattooing process, which is subsequently wiped away. Hence, the impurities might cause contact dermatitis or lead to sensitization. Also, aniline is often reported to show para-group cross reactivity with other primary aromatic amines such as *p*-phenylenediamine¹¹⁴—the main sensitizer from black henna tattoos¹¹⁶. Whether later release by laser irradiation can cause an allergic reaction needs to be investigated in the future.

The biggest uncertainty surrounding the toxicological effects of laser tattoo removal exists in regard to compounds with unknown chemical structures, which were observed upon pyrolysis. Similarly, only limited or no toxicological data is available for some compounds. To cope with these limitations, an investigation of single substances, as well as whole extracts from laser or UV irradiation, should be used in future toxicity tests.

However, not only the patient is at risk of being exposed to potentially harmful substances during a laser tattoo removal. The person performing the procedure is also at risk of exposure. During the laser removal procedure, harmful vapors are released, which could be inhaled by the operator if no proper safety precautions are implemented and followed¹¹⁷. The responsibility for the elaboration and implementation of such safety precautions lies with the authorities for health and safety at work.

3.2. Biokinetics of tattoo ink ingredients

In toxicology, substance biokinetics are mostly followed in terms of administration, distribution, metabolism and excretion (ADME). The administration of tattoo pigments into the skin makes them fully bioavailable. Metabolism of the pigments is assumed not to occur in case of inorganic and most organic pigments since they are chemically inert³⁸. However, metabolism of one yellow organic azo pigment by liver enzymes has been shown⁵². Also, corrosion of pigments possibly plays an important role in tattoo toxicology by releasing metal ions which may then exhibit their toxicological effects¹¹⁸.

On the other hand, very little is known regarding the distribution and excretion of tattoo pigments. Experiments in mice showed that about one-third of pigment vanishes from the skin within weeks after tattooing¹⁵. Since the skin of mice is barely comparable with human skin, the data can only be roughly extrapolated to humans. As stated in the introduction, transportation of pigments to lymph nodes has only been reported from observations of visible colorization.

Using human tissue, we could show the accumulation of inorganic and organic tattoo pigments in skin and lymph nodes with smaller particles being preferentially transported (cf. section 2.4). We could also show the permanent deposit of toxic elements such as Cr and Ni with the tattoo pigments in skin and lymph nodes. Preliminary data showed no increase in tattoo related elements such as Ti, Ba, Fe and Cu in other organs such as the liver, spleen and kidneys, which were found in corresponding skin and lymph node tissue in our investigation (data not shown). Because the analyzed samples were part of a retrospective study, co-exposure from sources other than the tattoo ink and pigment species analyzed could not be predefined. Therefore, background levels of physiological elements such as Fe and Cu may prevent identification of low level pigment deposit in more distant organs. Naturally low occurring elements such as Ti would be most suitable to track tattoo pigments throughout the body. However, since TiO₂ is highly abundant in our environment deriving from cosmetics or paints, results derived from human specimen might never be fully conclusive and could be attributed to sources other than the tattoo. Also, the initially administrated quantity of pigments deposited in skin, which is a key factor in calculating biodistribution, is not known for our samples. However, permanently enlarged lymph nodes and the deposit of allergenic and carcinogenic elements in the lymph nodes documented here, constitute a life-long risk.

Since particle research is carried out for multiple fields of application, data on the biodistribution of other insoluble particles might be extrapolated to tattoo pigments. For example, TiO₂ is an intensively investigated particle species also used in tattoo inks. A large number of studies investigating the biodistribution after intravenous (i.v.), i.p. and s.c. injections can be found in literature.

As early as 1966, Huggins and Froehlich reported remnants of 0.2–0.4 μm anatase TiO_2 particles after i.v. injection still present in the body after one year in rats¹¹⁹. About 75% of the pigment was found in liver, followed by spleen, and liver-draining lymph nodes. Smaller TiO_2 particles of 25 nm in diameter were found in liver, lung, spleen and to a lesser extent in the kidneys, heart, lymph nodes and brain 26 weeks after i.v. administration in mice²³. When those particles were injected s.c. in mice they were mainly found in the lymph nodes followed by the liver, spleen and lung. Only minor amounts could be detected in the heart, kidneys and brain²³. However, this data was generated using light microscopic counts without verification that the particles were indeed TiO_2 .

Olmedo *et al.* used energy-dispersive X-ray spectroscopy (EDX) to verify the presence of 1 μm Ti particles after s.c. and i.p. administration in the liver and lungs in rats²¹. Also, radio-labelled 20 nm TiO_2 particles have been used to follow the path of their distribution *in vivo*¹²⁰. Here, the preferential excretion of particles via the renal over the fecal path could be tracked after i.v. injection. Recent studies on the biodistribution of the insoluble quantum dot CdSe after i.d. injection revealed accumulation already after 24 h in liver (6%), lymph nodes (1%) and kidney (0.5%) based on its fluorescence properties¹²¹.

To investigate the excretion of inert particles, Cho *et al.* injected fluorescence labelled silica-particles of 50, 100 and 200 nm in diameter i.v. into mice¹²². The particle concentration found in urine and bile was inversely proportional to the particle size.

In addition to the size, the particle coatings also influence their distribution and excretion *in vivo*. A study comparing PEG-coated and non-coated silica particles with a diameter of 80–360 nm showed that smaller PEG-coated particles stayed longer in the blood-circulation than non-coated particles and therefore had a lower excretion rate via urine¹²³.

Existing data on *in vivo* biodistribution and excretion of insoluble particles can be extrapolated to same-sized tattoo particles. Still, it should be considered that the well-defined particles have been investigated in the studies mentioned above. Tattoo ink particles are polydisperse with particle sizes that range from a few nanometers—especially with carbon black pigments—up to several micrometers¹²⁴. Macrophages phagocytize particles up to 10 μm and therefore possibly remove even larger agglomerates¹²⁵. Passive transport to the lymph nodes is thought to occur minutes after exposure¹²¹. Since blood vessels can also be harmed during the tattooing process, the distribution most likely follows a kinetic a pattern known from i.d., s.c., or i.v. injections, but more likely a mixture of all three. Depending on the size and coating of the pigments, a predominant deposit in the draining lymph nodes of the puncture site, but also in liver, lung, and spleen can be expected. To a lesser extent, pigment deposits might also be expected to be found in the kidneys, heart, brain and liver (and its draining lymph nodes). Excretion of small particles

could take place via urine or bile with the predominant way being dependent on the coating (cf. He *et al.*¹²³).

Nonetheless, the biological consequences of the depicted distribution need to be investigated. Not the fact that particles are distributed *in vivo* but the species of particles, their dissolution, tissue interaction and possible biotransformation will account for possible toxic effects. As an example of the severe side effects otherwise biologically inert particles may have, one should consider the endemic elephantiasis of the lower legs in East Africa¹²⁶. The mechanism currently thought to cause the disease is initiated by the affected patients walking barefoot on volcanic soil. Thereby, silicate particles enter the lymphatic tissue and lead to a fibrous enlargement. This results in a clogging of the lymph paths and finally in the enlargement of the lower legs¹²⁷. Similarly, tender and swollen lymph nodes near the puncture site are sometimes noticed weeks after tattooing⁷².

In contrast to pigments, soluble tattoo ink ingredients will be distributed depending on their partitioning coefficients. The same applies to soluble compounds from biodegradation or light decomposition. The partitioning coefficient is known for most of these compounds or otherwise can be calculated, thus allowing computer-based modelling of their distribution.

3.3. Tissue-particle interactions

One key aspect of tattoo safety is the tolerance of the foreign material inside the human body. We therefore studied biomolecular changes induced by pigment particles in human tissue. Our results showed protein misfolding towards a beta-sheet configuration of the amide I band in skin containing tattoo pigments (cf. Chapter 2.4). Misfolded proteins are often reported as an initial step in the onset of an adverse foreign body reaction¹²⁵. After injury leading to the deposit of foreign material, the initial recognition is triggered by host proteins adsorbed at its surface¹²⁸. These might be serum proteins, fibrinogen, complement proteins or antibodies which can serve as pro-inflammatory signals by conformational changes of their structure¹²⁵. This so-called acute phase is accompanied by the infiltration of inflammatory mast cells and neutrophils. In the following chronic phase, monocytes and lymphocytes are present leading to the formation of fused macrophages, the foreign body giant cells (FBGC). FBGC formation has been described as early as 1912¹²⁹. They recruit fibroblasts involved in the formation of granulation tissue. As a result, a fibrous capsule separating foreign material from the vital tissue is formed¹²⁸. Biocompatible material is designed to trigger a fast resolution of acute and chronic inflammatory responses at its surface. The extent of the inflammatory response is also dependent on the severity of the initial injury¹²⁸. However, FBGC are only formed when material exceeding a size of 10 μm is present, which cannot be phagocytized by macrophages^{37,125}. Therefore, these cells might only be formed upon agglomeration of tattoo pigments *in vivo* which especially occurs with carbon black based tattoos¹³⁰.

The recognition of foreign material and proteins adsorbed at its surface plays a crucial role in the foreign body response. In the case of gram-negative bacteria, lipopolysaccharides (LPS) are recognized by the TOLL-like receptor 4 (TLR4) at the macrophage cell surface¹²⁵. These receptors mostly identify exogenous organisms but also endogenous ligands such as apoptotic cells, fibrinogen and heat shock proteins. Also, scavenger receptors and integrins mediate the phagocytosis by macrophages. Therefore, foreign material with attached LPS or microbe-related DNA, RNA but also other antigens or allergens may trigger an inflammatory host response¹²⁵.

Granulomatous foreign body reactions display the second frequent, non-infectious side-effect occurring with tattoos and have been recognized for a while³⁶. In tattoos, 5 out of 13 adverse reactions biopsies showed foreign body reaction with FBGC formation⁸³. Most individuals, however, display normal healing after being tattooed. The general non-reactivity of the insoluble pigments might be influenced by the respective tattoo ink formulation, as well as by potential pigment coatings. To make nanomaterials and implants biocompatible, two main approaches are used. Either, hiding the material from recognition by

preventing adsorption of proteins by using special coatings (non-fouling) or adding bioactive-peptide motifs to their surface to simulate signaling properties of the cell membrane³⁷. Non-fouling surface coatings for nanocarriers might consist of albumin, polysaccharides like hyaluronic acid or hydrophilic self-assembled monolayers like PEG¹³¹. The latter is often used as a dispersant in tattoo inks and might therefore already serve as a mediator for biocompatibility in the initial phase before undergoing degradation³⁷. Other possible coatings used for nanoparticles in biomedical approaches are dextran, polyvinylpyrrolidone, fatty acids, polyvinyl alcohols, polyacrylic acid, polypeptides, polylactide and phosphorylcholine¹³¹.

Permanently implanted material with non-adherent / non-fouling properties can, however, increase the foreign body reaction. Adherence to surrounding material is necessary for cell survival. Detachment leads to anoikis, a form of apoptosis, induced by detachment from the outer matrix¹²⁸. Therefore, the foreign material needs to promote cell adhesion¹²⁸. Hence, polymers preventing the adsorption of pro-inflammatory proteins but facilitating cell attachment by non-covalently linked molecules with bioactive recognition peptides might display a high biocompatibility¹²⁸. Therefore, the most likely interpretation of the absence of a granuloma formation with most tattoos is that wettability mediating substances, such as polymeric or surfactant structures, may reduce the initial protein absorption of pro-inflammatory mediators. In later chronic stages of wound healing, particles are internalized and physically shielded from recognition by inflammatory cells. Other less-inflammatory peptides might take the place of the degraded or detached dispersants. Hence, the denatured proteins in the proximity of the particles found in our investigation of non-granulomatous skin specimens, indicate that the kind of proteins and the stage at which they are adsorbed, have a major impact on their biocompatibility.

However, other factors related to the surface chemistry of the particles might also play an important role. For example, ROS production induced by nanoparticles upon the depletion of the antioxidative defense system is a cause of inflammation and fibrosis in lungs¹³². Different kinds of ROS species such as superoxide radicals occur endogenously in the mitochondria of mammalian cells; often involved in signaling during wound healing or as pathogen defense¹³³. If the protein or nucleic acid damage by ROS exceeds the capacity of the defense system, apoptosis, senescence, general aging and dysfunction of the cell and hence a contribution to cancer development might occur¹³³. ROS can be generated especially due to exposure to ultrafine particles (large surface area) either by PAH adsorbed to their surface in combination with UV light,²⁰ or by inorganic transition metals deriving from the particle itself¹³². Also high doses of bio-persistent fibers are known to induce ROS formation¹³². ROS can lead to

conformational changes in proteins,¹³⁴ which might result in a change of their antigenicity and ultimately in the initiation of autoimmune responses^{134,135}.

However, the different mechanistical hypotheses leading to a foreign body granulomatous reaction are still presumptuous and have to be further investigated. Future research should focus on parameters assumed to cause this adverse outcome in only certain individuals with the aim to manufacture pigment particles with better biocompatibility.

3.4. “Whitelist” for tattoo ink regulation: Scrutiny of the six organic pigments investigated

The ultimate goal in the tattoo legislative process is the generation of a whitelist including pigments which are thought to cause no adverse effects in humans. Current legislation is based on the classification of pigments for cosmetics, which is not always based on toxicological data. For example, one of the most widely used pigments in tattoo inks, pigment blue (P.B.)15 (also known as C.I. 74160) is banned for use in tattoo inks in Germany upon strict interpretation of the current law. The TätV states that all ingredients listed in Annex II of the Cosmetics Regulation must not be used in tattoo inks. P.B.15 is listed under the constraint “when used as a substance in hair dye products”. This ban is historically derived since the manufacturers did not submit safety dossiers specifically for hair dye applications¹³⁶. Since an insoluble pigment is of no use in dyeing hair, the lack of interest in preparing a safety dossier is understandable. Therefore the ban is not based on a higher risk of P.B.15 compared to other pigments. When applying the constraint in Annex II to tattoo pigments, the pigments P.R.4 and P.R.5 would, amongst others, also be banned. Another issue with the absence of a whitelist, is that all non-prohibited pigments can essentially be used for tattooing. The dilemma becomes obvious with the chlorinated phthalocyanine pigment green (P.G.)7. It is banned under the Cosmetics Regulation in contrast to brominated and chlorinated phthalocyanine P.G.36 without any evidence that the latter exhibits any less risk when used as tattoo pigment¹³⁷.

Hence, the regulation of tattoo inks cannot completely rely on references to the Cosmetics Regulation without defining specific safety criteria for intradermal application. All toxicological data available for the various tattoo ink ingredients have to be taken into consideration to facilitate tattoo risk assessment—including data from other fields of application.

The Council of Europe defined criteria for the safety assessment of tattoo ink ingredients, which were further elaborated by the BfR in 2009^{24,26}. These criteria include physico-chemical characterization, standard toxicological data, as well as biokinetics and data from *in vivo* subcutaneous application. Especially for the two latter points, the decline of animal testing in Germany for tattoo inks (personal communication Dr. Schacht, Hannover) will prevent the collection of appropriate data.

In terms of the physico-chemical characterization, most properties of a variety of tattoo ink components are already known. Impurities and other ingredients have already been monitored for years^{29,138}. Cleavage products from UV and laser light might be deduced as proposed in Chapter 3.1.1. However, except for P.Y.74, no data on metabolism of the ingredients is available so far⁵².

Toxicological data such as corrosion, irritation, phototoxicity and genotoxicity can be established with standardized *in vitro* tests. For sensitization, a combination of multiple *in vitro* tests can predict the *in vivo* outcome¹³⁹. However, these tests were developed for soluble substances and might therefore need modifications with pigment particles.

For a vast majority of the substances used in tattoo inks and their corresponding cleavage products some toxicological data already exists. Also in terms of allergenic properties of pigments, a small number of case reports can be found in the literature. This data in combination with the extrapolated decomposition of pigments would suffice for a major improvement of the current tattoo ink regulation. As an initial step, a reevaluation of the blacklists of banned tattoo pigments should be carried out based on toxicological data. In a second step, a whitelist should be established for pigments or groups of pigments with sufficient data regarding the criteria mentioned above. In the following paragraphs, I will briefly discuss selected criteria proposed by the Council of Europe and BfR^{24,26} in relation to the six investigated pigments in laser decomposition (see Chapter 2.2 and 2.3).

3.4.1 Cu-phthalocyanine P.B.15

A detailed report on P.B.15 by OECD SIDS, which summarizes toxicological standard tests, concludes a limited toxicity with no other effects reported¹⁴⁰. This conclusion was based on reversible toxicity seen in one out of three long-term feeding studies at a concentration of 200 mg/ml. Since tattoo inks, however, are directly injected into the skin accompanied by blood and lymph fluid contact followed by long-term exposure, no barrier to systemic distribution is present. Thus, oral toxicity data can be used to support a risk assessment but cannot be seen as representative for the unique application route of tattooing.

Nonetheless, the Danish EPA calculated a Derived No-Effect Level (DNEL) of 2 mg/kg bodyweight per day for P.B.15, based on a reduction of red blood cells seen in a 28 day rat gavage study¹¹⁵. Since no effects were seen in a 13 weeks study, the DNEL is thought to be over estimated¹¹⁵. Still, the DNEL would allow for a 140 cm² tattoo per day assuming the use of 1 mg/cm² and a person weighing 70 kg.

UV decomposition has not been observed so far. The half-life of photochemical degradation for P.B.15 was estimated with $1.04 \cdot 10^{-2}$ years, but the test conditions were not reported by the authors¹⁴⁰. In terms of laser decomposition, benzene and hydrogen cyanide are the only evolving substances of concern and have already been discussed in Chapter 3.1.2. Both substances are decomposition products of all organic pigments subjected to laser irradiation.

Phthalocyanines are frequently used as photosensitizers in photodynamic therapy, for example, for treatment of skin conditions but also for targeting cancer cells. The photosensitizer produces singlet

oxygen upon irradiation in the treated tissue leading to local cell death¹⁴¹. However, phototoxic properties of phthalocyanines with Cu as the central element are not expected since its quantum yield for generation of the singlet oxygen is close to that of naturally occurring molecules such as aromatic amino acids¹⁴².

Allergic reactions to blue nitrile gloves have been traced to their color, which contains P.B.15⁷⁸. It is not clear whether pure pigment without Ni contamination or even a pre-dispersed pigment mixture with possible preservatives was used in the patch test in this case report. The actual formulation and mixture with other pigments and dyes is proprietary information of the manufacturer. Hence, actual proof has not been established by the authors who conducted the study to the best of their knowledge. A vast amount of people wear nitrile blue gloves worldwide and P.B.15 is the only organic pigment used in the tattoo market at the moment. Thus far no increase in allergic reactions has been reported. In light of this observation, the report by Weimann *et al.* needs to be further substantiated by additional data to establish or refute a causative relationship between exposure to P.B.15 and an allergic reaction.

In a 1988 report by the European Commission, further information on sensitization and genotoxicity was requested for P.B.15¹⁴³. Since B.P.15 was subsequently deemed suitable for use in all cosmetic products for long-term skin contact, this pigment is unlikely to cause adverse effects when applied to the skin surface. However, the safety dossiers potentially used to make this judgement are not open for public review.

In summary, P.B.15 is a highly stable, non-soluble pigment that is unlikely to decompose except during laser removal. Potential health risks associated with the release of HCN and benzene have to be discussed at a higher level and are no P.B.15 specific concern. Impurities can be prevented and allergenic properties seem unlikely. A number of toxicological *in vivo* tests prove no or only limited effects regarding this pigment. Therefore, the pigment represents a good candidate for a whitelist of less harmful pigments.

3.4.2 Quinophthalone P.Y.138

One main risk factor of P.Y.138 is its contamination with the carcinogen HCB. HCB is not thought to act through a genotoxic mechanism, therefore non-carcinogenic concentrations will exist. However, in the area of work place safety, a MAK value (maximal working place concentration) has not yet been established due to uncertainties in the amounts accumulated in humans¹⁴⁴.

There is no publicly available data on the photodecomposition properties of P.Y.138, but it belongs to the group of highly light-fast pigments. Upon laser irradiation, HCB is also released, even though only in

small amounts compared to the already present pigment contamination. The skin sensitizer tetrachlorophthalic anhydride has only been found after pigment pyrolysis (Chapter 2.1) and as an impurity in some bulk pigments¹⁴⁵. It should be further evaluated whether this impurity can be avoided as should its threshold for inducing skin reactions.

In terms of tattoo ink safety, a safety margin still needs to be defined for HCB. HCB and tetrachlorophthalic anhydride should be kept at minimum possible levels in raw pigments.

The limited data available including the lack of animal and *in vitro* data prevent an informed opinion on this pigment. Since there is no available data on basic toxicology tests on the pure pigment, there is no justification for a black- or whitelist entry either.

3.4.3 Quinacridone P.V.19

Common impurities of P.V.19 are not known. The pigment used in our investigation did not show contamination with PAAs before laser treatment. Due to its high light-fastness and its use in photovoltaic cells, light decomposition is also assumed to be marginal¹⁴⁶. Upon laser decomposition, only low amounts of the mild skin irritant 1-cyanonaphthalene and aniline were found. Aniline is a known human skin sensitizer and classified as category 2 carcinogen (cf. Chapter 3.1.2). However, the amounts found after laser irradiation of P.V.19 are lower compared to levels found in market surveys by order of magnitude²⁹. Hence, the exposure of aniline caused by P.V.19 is low and also dependent the ink quality. As yet, there have been no investigations regarding this pigment's ability to release aniline upon sunlight exposure.

P.V.19 is currently restricted to only short-term skin contact in the Cosmetics Regulation¹⁴⁷. The toxicological reasons for this restriction in cosmetics are crucial to whether use is restricted or permitted in tattoo inks, but they are not publicly available.

Case reports listing quinacridones as probable cause of tattoo reactions lack proper proof of causality (c.f. Chapter 1.6.2). Next to P.V.19, the chlorine or methyl substituted quinacridone pigments P.R.202 and P.R.122 are also often found in tattoo inks. If the cleavage patterns of quinacridones are taken into consideration, P.R.202 is expected to release 4-chloroaniline which is a category 1B carcinogen (GHS) as well as a weak skin sensitizer¹⁴⁸. Indeed, 4-chloroaniline was found after irradiation with various light sources but not after laser irradiation of P.R.202⁴⁹.

In extrapolation to P.R.122, 4-toluidine is expected to be released. 4-Toluidine is a category 2 carcinogen according to GHS and also a category 1 skin sensitizer. We did not find decomposition products in a non-targeted laser experiment (cf. Chapter 2.3). The presence of these PAAs from both P.R.202 and P.R.122

as pigment impurities or cleavage products should be further investigated, along with their sensitization properties.

Similarly to P.Y.138, lack of toxicological data prevents the proposal of P.V.19 for whitelist inclusion—despite its stability. Conversely, quinacridones are in danger to be added to a blacklist if evidence of its sensitizing properties can be verified and are not solely attributed to impurities.

3.4.4 Diketopyrrolopyrrole P.R.254

Common impurities of P.R.254 are not known and have not been observed in our investigations. In a study by Hauri and Hohl, no decomposition under sunlight exposure was seen⁴⁹. In our study, 3-chlorobenzamide was released upon irradiation with laser light. This substance has been categorized as a potential skin sensitizer using Quantitative Structure Activity Relationship (QSAR) methods¹⁴⁹.

Other cleavage products pose limited risks (cf. Chapter 2.3). In-depth tests for skin sensitization should still be carried out, especially under UV-exposure. Also, as with other pigments basic toxicological data needs to be presented for P.R.254 to be proposed for a whitelist.

3.4.5 Azo-naphthol pigment P.R.170

Common impurities of P.R.170 with PAAs have not been observed in the pigment sample used in our investigation. Benzamide, 4-hydroxybenzamide and 4-aminobenzamide are released under sunlight simulation⁴⁹. We found mainly benzamide, 4-aminobenzamide and aniline after laser irradiation—along with HCN and benzene. Aniline, as mentioned above, is a skin sensitizer. Benzamide is categorized as a germ cell mutagen. As a potent poly-(ADP-ribose)-polymerase, benzamide increases sister chromatid exchange rate *in vitro*¹⁵⁰. Also significantly increased micronuclei were found in mice erythrocytes after oral gavage¹⁵¹. Due to its weak amide and amino bonds, its light-fast properties are limited, leading to possible release of significant substances under UV and laser light.

Data gaps on possible allergenic and genotoxic properties have to be closed. Especially in view of the benzamide released, P.R.170 does not seem to be an ideal candidate for a whitelist of pigments for use in tattoo inks.

3.4.6 Diazo pigment P.O.13

Just as other pigments above, P.O.13, as used in our investigation, did not show contamination with PAAs before laser treatment.

P.O.13 is known to release DCBD and 3,3-dichlorobiphenyl upon sunlight exposure⁴⁹. In our investigation, we found mainly DCBD, phenylisocyanate, benzonitrile and aniline as well as traces of 3,3-dichlorobiphenyl after laser irradiation.

Aniline and DCBD are classified skin sensitizers. The same concerns regarding sensitizing potential and possible release of benzidine were raised by the European Commission in 1988, resulting in a demand for additional testing¹⁴³. Since the pigment is not referred to in later statements, it was probably deleted in all annexes of the Cosmetics Regulation.

DCBD is also a category 1B carcinogen (GHS). Since DCBD is a mutagenic carcinogen, no exposure threshold can be drawn¹⁵². Since DCBD can be released under UV light, it poses a risk to all individuals tattooed with P.O.13. The amounts of DCBD released from an average tattoo can increase the life-cancer risk¹⁵³. With this knowledge in mind, it is rather alarming that DCBD is frequently found in tattoo ink monitoring reports with mean concentrations of 0.294 mg/kg ink²⁹. With reductive cleavage pre-treatment of the tattoo inks a maximum of 710 mg/kg DCBD has been found²⁹. The reductive cleavage method is usually used to mimic bacterial decomposition of ingested azo dyes from cosmetics and food products¹⁵⁴. However, liver enzymes are also able to cleave the azo bond¹⁵⁴ and thereby display a third source of release of DCBD from tattoo pigments alongside laser and UV light. P.O.13 released by far the highest amount of benzene in laser irradiation compared to other pigments in our investigation. Upon laser irradiation of large areas tattooed with P.O.13, benzene blood levels might even exceed those found in workers with occupational exposure (cf. Chapter 3.1.2).

Therefore, all diazo pigments with DCBD as core building block and probable cleavage product, should not be used in tattoo inks and listed in a toxicology-based blacklist.

4. Conclusion and Outlook

A major task in improving the safety of tattoo inks is the detection of ingredients that are not compliant with current legislation. The analysis of pigments is especially challenging since they are insoluble in water and most organic solvents by definition. The py-GC-MS applied here represents a suitable method for identification of organic pigments with specific cleavage patterns; such as azo pigments. Shortcomings of this method occur with quinacridone and other non-specifically cleaved pigments and in mixtures of multiple pigments with similar cleavage sites. Pigment identification by Py-GC-MS should be used as part of an analytical test battery, e.g. together with matrix-assisted laser desorption/ionization time-of-flight (MALDI-ToF)-MS and LC approaches.

The specific cleavage patterns observed after pyrolysis and laser irradiation can also be used to extrapolate decomposition patterns common to other pigments from the same chemical class. In this way, the prediction of toxic decomposition products likely to form during laser removal seems to be within reach. However, the extrapolation of cleavage patterns to sunlight exposure has to be strengthened with more data on decomposition products.

The aqueous suspensions and *postmortem* tattooed pig skin used as models for laser irradiation showed clear analogy in terms of general decomposition patterns compared to the rare data from *in vivo* mouse studies. However, the quantities of the decomposition compounds, especially if highly volatile, are more difficult to compare. Evaporation and fast distribution in hypothetical *in vivo* investigations would also bear uncertainties regarding the exact amounts of compounds formed. Therefore, considering the maximal amounts found in the aqueous suspensions and pig skin models, the application of additional safety factors might already be sufficient for risk calculations.

Concerning the overall exposure with toxins deriving from tattooing, residual harmful substances from pigment synthesis might be present in higher amounts in the ink mixtures than quantities found after laser irradiation (e.g. HCB in P.Y.138). Toxicity studies involving hydrogen cyanide released by laser irradiation showed cytotoxic properties at the expected skin concentrations and might therefore impair healing of the disrupted tissue after laser irradiation. Carcinogenic substances will be distributed to their target organs, e.g. liver, due to the full bio-availability and might therefore contribute to an increased cancer risk.

Since some of the decomposition products are also listed as potential sensitizers, their release upon laser and UV irradiation is of additional concern. In future, a set of *in vitro* assays mimicking the key events necessary to develop allergic contact dermatitis such as peptide reactivity, keratinocyte activation and

dendritic cell activation should be adapted to investigate adverse effects seen with tattoo allergy. A “2 out of 3” strategy to identify contact allergens assessing the named key events was shown to possess a higher predictivity than standard *in vivo* animal tests such as local lymph node assay^{139,155}. It is therefore desirable to evaluate not only the sensitizing properties of the tattoo ink formulation, but also of the decomposition products. Since allergies are sometimes confused or accompanied by granulomatous foreign body reactions, surface properties of the pigment particles might also play a role in the observed side effects and should be part of future research.

The biokinetics of pure tattoo pigments could be extrapolated from animal experiments conducted with other inert pigments. Main pigment deposit is expected in lymph nodes, liver with minor amounts in lung, spleen and kidneys (cf. Chapter 3.2). The distribution of pigments as such, does not automatically imply adverse effects at their place of deposit. However, the co-transport with carcinogenic metal impurities, as seen in our investigation, points to the potential health risk associated with pigment distribution. Also, other effects induced by the particles, such as foreign body reactions, might pose a risk upon systemic distribution. For example, necrosis of lymph nodes in a patient with ulcero-necrotic reactions to tattoos has been described in the literature⁷². Additionally, since active transport of pigment particles is facilitated by phagocytizing cells, which also harbor these pigments in the lymph nodes¹⁶, pigment alteration by ROS inside the phagolysosomes cannot be excluded¹⁵⁶.

Given the variety of different toxicological end points for which no data is yet available, conducting an appropriate risk assessment is a mammoth task and should also include the evaluation of already banned pigments. It might be a more practical approach to refine current legislation step by step, as has been the approach with the first tattoo regulation. This would improve consumer safety immediately, instead of postponing the process until all requisite endpoints have been experimentally investigated—which might as well never happen. Today’s use of highly sensitizing preservatives such as isothiazolinones and formaldehyde due to the lack of their regulation for tattoo inks is a warning example. Apart from pigments, other hazardous ingredients should also be limited by clear maximum values. Therefore, a whitelist is needed for all ingredients used in the manufacture of tattoo inks.

Future research should focus on the main risks such as carcinogenicity and allergies. Pigment decomposition products, contaminations and auxiliary ingredients should also be addressed. Special emphasis should also be placed on surface effects as well as on the photocatalytic properties of TiO₂. By this, the main side effects accounted to pigment chemistry, such as allergies, light sensitivity and granuloma formation as well as the highly discussed impact of tattooing on cancer development will be addressed.

5. References

- 1 Samadelli, M., Melis, M., Miccoli, M., Vigl, E. E. & Zink, A. R. Complete mapping of the tattoos of the 5300-year-old Tyrolean Iceman. *J Cult Herit* **16**, 753–758 (2015).
- 2 Deter-Wolf, A., Robitaille, B., Krutak, L. & Galliot, S. The world's oldest tattoos. *J Archaeol Sci: Reports* **5**, 19–24 (2016).
- 3 Deter-Wolf, A. in *Tattoos and bodymodifications in antiquity: Proceedings of the sessions at the annual meetings of the European Association of Archaeologist in The Hague and Oslo, 2010/11*. Vol. 9 *Zurich Studies in Archaeology* (eds P. Philippe Della Casa & C. Witt) 15–26 (Chronos-Verlag, Zurich, 2013).
- 4 Trampisch, H. J. & Brandau, K. *GfK Studie: Tattoos und Piercings in Deutschland. Eine Querschnittsstudie (article in German)*, <<http://aktuell.ruhr-uni-bochum.de/mam/content/tattoo-studie.pdf>> (2014), (accessed 06 June 2017).
- 5 Kluger, N. Epidemiology of tattoos in industrialized countries. *Curr Probl Dermatol* **48**, 6–20 (2015).
- 6 Rush, J. *Spiritual Tattoo: a cultural history of tattooing, piercing, scarification, branding, and implants*. (North Atlantic Books, Berkeley, CA, USA, 2005).
- 7 Gilder, W. H. *Schwatka's Search: Sledging in the arctic in quest of the franklin records*. (Charles Scribner's Sons, New York, USA, 1881).
- 8 Rosenkilde, F. in *Tattooed skin and health*. Vol. 48 *Curr Probl Dermatol* (eds J. Serup, N. Kluger, & W. Bäumlner) 21–30 (Karger, Basel, 2015).
- 9 O'Reilly, S. F. Tattooing machine. USA patent US464801 A (1891).
- 10 De Cuyper, C. Permanent makeup: indications and complications. *Clin Dermatol* **26**, 30–34 (2008).
- 11 De Cuyper, C. in *Tattooed skin and health*. Vol. 48 *Curr Probl Dermatol* (eds J. Serup, N. Kluger, & W. Bäumlner) 61–70 (Karger, Basel, 2015).
- 12 Yang, A. S. & Creagh, T. A. Black sentinel lymph node and 'scary stickers'. *J Plast Reconstr Aesthet Surg* **66**, 558–560 (2013).
- 13 Soran, A., Kanbour-Shakir, A., Bas, O. & Bonaventura, M. A tattoo pigmented node and breast cancer. *Bratisl Lek Listy* **115**, 311–312 (2014).
- 14 Mentrikoski, M. J., Rochman, C. M. & Atkins, K. A. Tattoo ink within lymph nodes: a possible clinical mimicker of abnormal calcification. *Breast J* **20**, 314–315 (2014).
- 15 Engel, E. *et al.* Tattooing of skin results in transportation and light-induced decomposition of tattoo pigments - a first quantification *in vivo* using a mouse model. *Exp Dermatol* **19**, 54–60 (2010).
- 16 Nopajaroonsri, C. & Simon, G. Phagocytosis of colloidal carbon in a lymph node. *Amer J Path* **65**, 25–42 (1971).
- 17 Taylor, C. R., Anderson, R. R., Gange, R. W., Michaud, N. A. & Flotte, T. J. Light and electron microscopic analysis of tattoos treated by Q-switched ruby laser. *J Invest Dermatol* **97**, 131–136 (1991).

-
- 18 Ross, E. V. *et al.* Tattoo darkening and nonresponse after laser treatment: a possible role for titanium dioxide. *Arch Dermatol* **137**, 33–37 (2001).
- 19 Sowden, J. *et al.* Red tattoo reactions: x-Ray microanalysis and patch-test studies. *Br J Dermatol* **124**, 576–589 (1991).
- 20 Regensburger, J. *et al.* Tattoo inks contain polycyclic aromatic hydrocarbons that additionally generate deleterious singlet oxygen. *Exp Dermatol* **19**, e275–281 (2010).
- 21 Olmedo, D. G., Tasat, D. R., Guglielmotti, M. B. & Cabrini, R. L. Biodistribution of titanium dioxide from biologic compartments. *J Mat Sci: Materi Med* **19**, 3049–3056 (2008).
- 22 Patri, A. *et al.* Energy dispersive X-ray analysis of titanium dioxide nanoparticle distribution after intravenous and subcutaneous injection in mice. *J Appl Toxicol* **29**, 662–672 (2009).
- 23 Umbreit, T. H. *et al.* Tissue distribution and histopathological effects of titanium dioxide nanoparticles after intravenous or subcutaneous injection in mice. *J Appl Toxicol* **32**, 350–357 (2012).
- 24 Council of Europe Committee of Ministers. *Resolution ResAP(2008)1 on requirements and criteria for the safety of tattoos and permanent make-up* 20 February 2008 (2008).
- 25 Nakagawa, Y., Wakuri, S., Sakamoto, K. & Tanaka, N. The photogenotoxicity of titanium dioxide particles. *Mut Res* **394**, 125–132 (1997).
- 26 Bundesinstitut für Risikobewertung. *1. Sitzung des adhoc Ausschusses „Tätowiermittel“ der BfR-Kommission für Kosmetische Mittel. Protokoll vom 4. November 2009 (article in German)*.
- 27 Laux, P. *et al.* A medical-toxicological view of tattooing. *The Lancet* **387**, 395–402 (2016).
- 28 Daoud Ali, A. *et al.* UVB-induced apoptosis and DNA damaging potential of chrysene via reactive oxygen species in human keratinocytes. *Toxicol Lett* **204**, 199–207 (2011).
- 29 Bundesamt für Verbraucherschutz und Lebensmittelsicherheit. *BVL-Report 9.3. Berichte zur Lebensmittelsicherheit. Monitoring 2013 (article in German)* (2013).
- 30 Hauri, U. Inks for tattoos and PMU (permanent make-up) / Organic pigments, preservatives and impurities such as primary aromatic amines and nitrosamines. *State Laboratory of the Canton Basel City* (2011).
- 31 The European Commission. *Commission Decision 2010/15/EU, OJ L 22, 1–64*. 26 January 2010.
- 32 Krutak, L. *Tattooing and piercing among the Alaskan aleut*, <<http://www.larskrutak.com/tattooing-and-piercing-among-the-alaskan-aleut/>> (2006), (accessed 06 June 2017).
- 33 Pandya, V. B., Hooper, C. Y., Essex, R. W. & Cook, M. Tattoo-associated uveitis. *Am J Ophthalmol* **158**, 1355–1356 (2014).
- 34 Dirks, M. in *Tattooed Skin and Health*. Vol. 48 *Curr Probl Dermatol* (eds J. Serup, N. Kluger, & W. Bäuml) 118–127 (Karger, Basel, 2015).
- 35 Silberberg, I. & Leider, M. Studies of a red tattoo: appearances in electron microscope, and analysis by chemical means, laser microprobe and selected-area diffraction of tattooed material. *Arch Dermatol* **101**, 299–304 (1970).

- 36 Rorsman, H. *et al.* Tattoo granuloma and uveitis. *The Lancet* **295**, 27–28 (1969).
- 37 Meyers, S. R. & Grinstaff, M. W. Biocompatible and bioactive surface modifications for prolonged *in vivo* efficacy. *Chem Rev* **112**, 1615–1632 (2012).
- 38 Petersen, H. & Lewe, D. in *Tattooed skin and health*. Vol. 48 *Curr Probl Dermatol* (eds J. Serup, N. Kluger, & W. Bäumlner) 136–141 (Karger, Basel, 2015).
- 39 Forte, G., Petrucci, F., Cristaudo, A. & Bocca, B. Market survey on toxic metals contained in tattoo inks. *Sci Total Environ* **407**, 5997–6002 (2009).
- 40 Hostynek Jurij, J. Sensitization to Nickel: Etiology, Epidemiology, Immune Reactions, Prevention, and Therapy. *Rev Environ Health* **21**, 253–280 (2006).
- 41 Konformität von Tätowier- und Permanent-Make-up-Farben nicht zufriedenstellend (article in German). *Kantonales Laboratorium Basel Bulletin* **29** (2009).
- 42 U.S. department of health and human services. Public Health Service, Agency for Toxic Substances and Disease Registry. *Toxicological profile for 3,3'-dichlorobenzidine* (1998).
- 43 Shen, Y. *In vitro* cytotoxicity of BTEX metabolites in Hela cells. *Arch Environ Contam Toxicol* **34**, 229–234 (1998).
- 44 Bond, J. A. & Bolt, H. M. Review of the toxicology of styrene. *Crit Rev Toxicol* **19**, 227–249 (1989).
- 45 Lerche, C. M., Sepehri, M., Serup, J., Poulsen, T. & Wulf, H. C. Black tattoos protect against UVR-induced skin cancer in mice. *Photodermatol Photoimmunol Photomed* **31**, 261–268 (2015).
- 46 Vasold, R. *et al.* Tattoo pigments are cleaved by laser light—the chemical analysis *in vitro* provide evidence for hazardous compounds. *Photochem Photobiol* **80**, 185–190 (2004).
- 47 Cui, Y. *et al.* Photodecomposition of pigment yellow 74, a pigment used in tattoo inks. *Photochem Photobiol* **80**, 175–184 (2004).
- 48 Engel, E. *et al.* Photochemical cleavage of a tattoo pigment by UVB radiation or natural sunlight. *J Dtsch Dermatol Ges* **5**, 583–589 (2007).
- 49 Hauri, U. & Hohl, C. in *Tattooed skin and health*. Vol. 48 *Curr Probl Dermatol* (eds J. Serup, N. Kluger, & W. Bäumlner) 164–169 (Karger, Basel, 2015).
- 50 Wezel, K. *Examination of the behaviour of tattoo inks and pigments under the influence of light*. Master thesis, Justus-Liebig Universität Gießen, Germany (2013).
- 51 Gaugler, S. *Analysis of bioactive compounds in tattoo inks before and after irradiation with sunlight using HPTLC and in situ detection with vibrio fischeri*. Master equivalent (Staatsexamen) thesis, Universität Hohenheim, Germany (2011).
- 52 Cui, Y., Churchwell, M. I., Couch, L. H., Doerge, D. R. & Howard, P. C. Metabolism of pigment yellow 74 by rat and human microsomal proteins. *Drug Metab Dispos* **33**, 1459–1465 (2005).
- 53 Shaw, D. W. Allergic contact dermatitis from carmine. *Dermatitis* **20**, 292–295 (2009).

-
- 54 U.S. Environmental Protection Agency. National Center for Environmental Assessment. *Integrated Risk Information System (IRIS) Chemical Assessment Summary. Aniline; CASRN 62-53-3* 01 November 1990.
- 55 Parry, M. F. & Wallach, R. Ethylene glycol poisoning. *Am J Med* **57**, 143–150 (1974).
- 56 Montaudo, G., Samperi, F. & Montaudo, M. S. Characterization of synthetic polymers by MALDI-MS. *Progr Polym Sci* **31**, 277–357 (2006).
- 57 Lehner, K. *et al.* Black tattoo inks are a source of problematic substances such as dibutyl phthalate. *Contact Dermatitis* **65**, 231–238 (2011).
- 58 Armand, L. *et al.* Long-term exposure of A549 cells to titanium dioxide nanoparticles induces DNA damage and sensitizes cells towards genotoxic agents. *Nanotoxicology* **10**, 913–923 (2016).
- 59 Bettini, S. *et al.* Food-grade TiO₂ impairs intestinal and systemic immune homeostasis, initiates preneoplastic lesions and promotes aberrant crypt development in the rat colon. *Sci Rep* **7**, 40373 (2017).
- 60 Baan, R. A. Carcinogenic hazards from inhaled carbon black, titanium dioxide, and talc not containing asbestos or asbestiform fibers: recent evaluations by an IARC Monographs working group. *Inhal Toxicol* **19**, 213–228 (2007).
- 61 *Skinvoke UV tattoo ink info sheet*, <<http://www.razorbladeproducts.com/xcart/uv-ink-info.html>>, (accessed 06 June 2017).
- 62 *Glow in the dark tattoos the pros and cons*, <<http://blog.tat2x.com/glow-in-the-dark-tattoos-the-pros-and-cons/>> (2012), (accessed 06 June 2017).
- 63 Tsang, M. *et al.* A visible response to an invisible tattoo. *J Cutan Pathol* **39**, 877–880 (2012).
- 64 Wenzel, S. M., Rittmann, I., Landthaler, M. & Bäuml, W. Adverse reactions after tattooing: review of the literature and comparison to results of a survey. *Dermatology* **226**, 138–147 (2013).
- 65 Kluger, N. Self-reported tattoo reactions in a cohort of 448 French tattooists. *Int J Dermatol* **55**, 764–768 (2016).
- 66 Klügl, I., Hiller, K. A., Landthaler, M. & Bäuml, W. Incidence of health problems associated with tattooed skin: a nation-wide survey in German-speaking countries. *Dermatology* **221**, 43–50 (2010).
- 67 Brady, B. G., Gold, H., Leger, E. A. & Leger, M. C. Self-reported adverse tattoo reactions: a New York City Central Park study. *Contact Dermatitis* **73**, 91–99 (2015).
- 68 Klein, A., Rittmann, I., Hiller, K. A., Landthaler, M. & Bäuml, W. An Internet-based survey on characteristics of laser tattoo removal and associated side effects. *Lasers Med Sci* **29**, 729–738 (2014).
- 69 Høgsberg, T., Saunte, D. M., Frimodt-Møller, N. & Serup, J. Microbial status and product labelling of 58 original tattoo inks. *J Eur Acad Dermatol Venereol* **27**, 73–80 (2013).
- 70 Drage, L. A., Ecker, P. M., Orenstein, R., Phillips, P. K. & Edson, R. S. An outbreak of *Mycobacterium chelonae* infections in tattoos. *J Am Acad Dermatol* **62**, 501–506 (2010).
- 71 Guiliere, S. *et al.* Outbreak of *mycobacterium haemophilum* infections after permanent makeup of the eyebrows. *Clin Infect Dis* **52**, 488–491 (2011).
-

-
- 72 Serup, J., Hutton Carlsen, K. & Sepehri, M. in *Tattooed skin and health*. Vol. 48 *Curr Probl Dermatol* (eds J. Serup, N. Kluger, & W. Bäumlner) 48–60 (Karger, Basel, 2015).
- 73 Serup, J. in *Diagnosis and therapy of tattoo complications. With atlas of illustrative cases*. *Curr Probl Dermatol* (eds J. Serup & W. Bäumlner) Diagnostic tools for doctors' evaluation of tattoo complications Diagnostic tools for doctors' evaluation of tattoo complications, 42–57 (Karger, Basel, 2017).
- 74 Eun, H. C. & Kim, K. H. Allergic granuloma from cosmetic eyebrow tattooing. *Contact Dermatitis* **21**, 276–278 (1989).
- 75 Morales-Callaghan, A. M., Jr., Aguilar-Bernier, M., Jr., Martinez-Garcia, G. & Miranda-Romero, A. Sarcoid granuloma on black tattoo. *J Am Acad Dermatol* **55**, S71–73 (2006).
- 76 Greve, B., Chytry, R. & Raulin, C. Contact dermatitis from red tattoo pigment (quinacridone) with secondary spread. *Contact Dermatitis* **49**, 265–266 (2003).
- 77 Gaudron, S., Ferrier-Le Bouedec, M. C., Franck, F. & D'Incan, M. Azo pigments and quinacridones induce delayed hypersensitivity in red tattoos. *Contact Dermatitis* **72**, 97–105 (2015).
- 78 Weimann, S., Skudlik, C. & John, S. M. Allergic contact dermatitis caused by the blue pigment Vinamon(R) Blue BX FW - a phthalocyanine blue in a vinyl glove. *J Dtsch Dermatol Ges* **8**, 820–822 (2010).
- 79 Wenzel, S. M., Welzel, J., Hafner, C., Landthaler, M. & Bäumlner, W. Permanent make-up colorants may cause severe skin reactions. *Contact Dermatitis* **63**, 223–227 (2010).
- 80 Tammaro, A. *et al.* Heavy metal and tattoo: an allergy and legislative problem. *Eur Ann Allergy Clin Immunol* **48**, 153–155 (2016).
- 81 Serup, J. & Hutton Carlsen, K. Patch test study of 90 patients with tattoo reactions: negative outcome of allergy patch test to baseline batteries and culprit inks suggests allergen(s) are generated in the skin through haptenization. *Contact Dermatitis* **71**, 255–263 (2014).
- 82 Bernstein, E. F. Laser tattoo removal. *Semin Plast Surg* **21**, 175–192 (2007).
- 83 Körner, R., Pföhler, C., Vogt, T. & Müller, C. S. Histopathology of body art revisited - analysis and discussion of 19 cases. *J Dtsch Dermatol Ges* **11**, 1073–1080 (2013).
- 84 Tournalaki, A., Boneschi, V., Tosi, D., Pigatto, P. & Brambilla, L. Granulomatous tattoo reaction induced by intense pulse light treatment. *Photodermatol Photoimmunol Photomed* **26**, 275–276 (2010).
- 85 McFadden, N., Lyberg, T. & Hensten-Pettersen, A. Aluminum-induced granulomas in a tattoo. *J Am Acad Dermatol* **20**, 903–908 (1989).
- 86 Serup, J. in *Tattooed skin and health*. Vol. 48 *Curr Probl Dermatol* (eds J. Serup, N. Kluger, & W. Bäumlner) 236–247 (Karger, Basel, 2015).
- 87 Hutton Carlsen, K. & Serup, J. Photosensitivity and photodynamic events in black, red and blue tattoos are common: A 'Beach Study'. *J Eur Acad Dermatol Venereol* **28**, 133–262 (2013).
- 88 Wamer, W. G. & Yin, J. J. Photocytotoxicity in human dermal fibroblasts elicited by permanent makeup inks containing titanium dioxide. *J Cosmet Sci* **62**, 535–547 (2011).
-

-
- 89 Hutton Carlsen, K. & Serup, J. Patients with tattoo reactions have reduced quality of life and suffer from itch: Dermatology Life Quality Index and Itch Severity Score measurements. *Skin Res Technol* **21**, 101–107 (2015).
- 90 Kent, K. M. & Graber, E. M. Laser tattoo removal: a review. *Dermatol Surg* **38**, 1–13 (2012).
- 91 Sepehri, M., Jørgensen, B. & Serup, J. Introduction of dermatome shaving as first line treatment of chronic tattoo reactions. *J Dermatolog Treat* **26**, 451–555 (2015).
- 92 Bundesinstitut für Risikobewertung. *Gesundheitsgefahren durch Tätowierungen und Permanent Make-up. Aktualisierte Stellungnahme Nr. 019/2007 des BfR vom 22. März 2004 (article in German)* (2007).
- 93 Scutt, R. The chemical removal of tattoos. *Br J Plastic Surg* **25**, 189–194 (1972).
- 94 Bundesinstitut für Risikobewertung. *Stellungnahme Nr. 033/2011 des BfR vom 1. August 2011. Tattoo-Entfernung: Einsatz wässriger Milchsäure ist mit gesundheitlichen Risiken verbunden (article in German)* (2011).
- 95 Yim, G. H., Hemington-Gorse, S. J. & Dickson, W. A. Letter to the editor: the perils of do it yourself chemical tattoo removal. *J Plast Surg* **10**, 177–179 (2010).
- 96 Veysey, E. & Downs, A. M. R. Correspondence: adverse side-effects following attempted removal of tattoos using a non-laser method. *Br J Dermatol* **150**, 770–795 (2004).
- 97 Anderson, R. R. & Parrish, J. A. Selective photothermolysis: precise microsurgery by selective absorption of pulsed radiation. *Science* **220**, 524–527 (1983).
- 98 Ho, D. D., London, R., Zimmerman, G. B. & Young, D. A. Laser-tattoo removal—a study of the mechanism and the optimal treatment strategy via computer simulations. *Lasers Surg Med* **30**, 389–397 (2002).
- 99 Bernstein, E. F., Schomacker, K. T., Basilavecchio, L. D., Plugis, J. M. & Bhawalkar, J. D. A novel dual-wavelength, Nd:YAG, picosecond-domain laser safely and effectively removes multicolor tattoos. *Lasers Surg Med* **47**, 542–548 (2015).
- 100 Suchin, K. R. & Greenbaum, S. S. Successful treatment of a cosmetic tattoo using a combination of lasers. *Dermatol Surg* **30**, 105–107 (2004).
- 101 Beute, T. C., Miller, C. H., Timko, A. L. & Ross, E. V. *In vitro* spectral analysis of tattoo pigments. *Dermatol Surg* **34**, 508–516 (2008).
- 102 Eklund, Y. & Rubin, A. T. in *Tattooed skin and health*. Vol. 48 *Curr Probl Dermatol* (eds J. Serup, N. Kluger, & W. Bäuml) 88–96 (Karger, Basel, 2015).
- 103 Ferguson, J. E., Andrew, S. M., Jones, C. J. P. & August, P. J. The Q-switched neodymium:YAG laser and tattoos: a microscopic analysis of laser-tattoo interactions. *Br J Dermatol* **137**, 405–410 (1997).
- 104 Luu-The, V. *et al.* Expression profiles of phases 1 and 2 metabolizing enzymes in human skin and the reconstructed skin models Episkin and full thickness model from Episkin. *J Steroid Biochem Mol Biol* **116**, 178–186 (2009).

-
- 105 IARC. Hexachlorobenzene. *IARC Monographs on the Evaluation of Carcinogenic Risks to Humans* **79**, 493–568 (2001).
- 106 Health Council of the Netherlands. *Hexachlorobenzene. Health-based recommended occupational exposure limit. No. 2011/35* (2011).
- 107 Janmohamed, A., Dolphin, C. T., Philips, I. R. & Shepard, E. A. Quantification and cellular localization of expression in human skin of genes encoding flavin-containing monooxygenases and cytochromes P450. *Biochem Pharmacol* **62**, 777–786 (2001).
- 108 Lewin, J. M., Brauer, J. A. & Ostad, A. Surgical smoke and the dermatologist. *J Am Acad Dermatol* **65**, 636–641 (2011).
- 109 Ashley, D. L., Bonin, M. A., Cardinali, F. L., McCraw, J. M. & Wooten, J. V. Blood concentrations of volatile organic compounds in a nonoccupationally exposed US population and in groups with suspected exposure. *Clin Chem* **40**, 1401–1404 (1994).
- 110 Popp, W., Rauscher, D., Müller, G., Angerer, J. & Norpoth, K. Concentrations of benzene in blood and S-phenylmercapturic and *t,t*-muconic acid in urine in car mechanics. *Int Arch Occup Environ Health* **66**, 1–6 (1994).
- 111 Sherwood, R. J. Pharmacokinetics of benzene in a human after exposure at about the permissible limit. *Ann N Y Acad Sci* **534**, 635–647 (1988).
- 112 Ferrari, L. A., Arado, M. G., Giannuzzi, L., Mastrantonio, G. & Guatelli, M. A. Hydrogen cyanide and carbon monoxide in blood of convicted dead in a polyurethane combustion: a proposition for the data analysis. *Forensic Sci Int* **121**, 140–143 (2001).
- 113 Department of Health and Human Services, Centers for Disease Control and Prevention, National Institute for Occupational Safety and Health, DHHS (NIOSH). *Skin Notation (SK) Profile. Aniline. Publication No. 2015-192* (2015).
- 114 European Chemical Bureau (ECHA). Institute for Health and Consumer Protection. *European Union Risk Assessment Report. Aniline* (2004).
- 115 The Danish Environmental Protection Agency. *Chemical substances in tattoo ink. Survey of chemical substances in consumer products no. 116*. (2012).
- 116 Le Coz, C. J., Lefebvre, C., Keller, F. & Grosshans, É. Allergic contact dermatitis caused by skin painting (pseudotattooing) with black henna, a mixture of henna and p-phenylenediamine and its derivatives. *Arch Dermatol* **136**, 1515–1517 (2000).
- 117 Bargman, H. Laser-generated airborne contaminants. *Clin Aesthet Dermatol* **4**, 56–57 (2011).
- 118 Black, J. Systemic effects of biomaterials. *Biomaterials* **5**, 11–18 (1984).
- 119 Huggins, C. B. & Froehlich, J. P. High concentration of injected titanium dioxide in abdominal lymph nodes. *J Experim Med* **124**, 1099–1106 (1966).

-
- 120 Xie, G., Wang, C., Sun, J. & Zhong, G. Tissue distribution and excretion of intravenously administered titanium dioxide nanoparticles. *Toxicol Lett* **205**, 55–61 (2011).
- 121 Gopee, N. V. *et al.* Migration of intradermally injected quantum dots to sentinel organs in mice. *Toxicol Sci* **98**, 249–257 (2007).
- 122 Cho, M. *et al.* The impact of size on tissue distribution and elimination by single intravenous injection of silica nanoparticles. *Toxicol Lett* **189**, 177–183 (2009).
- 123 He, Q., Zhang, Z., Gao, F., Li, Y. & Shi, J. *In vivo* biodistribution and urinary excretion of mesoporous silica nanoparticles: effects of particle size and PEGylation. *Small* **7**, 271–280 (2011).
- 124 Høgsberg, T., Loeschner, K., Löf, D. & Serup, J. Tattoo inks in general usage contain nanoparticles. *Br J Dermatol* **165**, 1210–1218 (2011).
- 125 Xia, Z. & Triffitt, J. T. A review on macrophage responses to biomaterials. *Biomed Mater* **1**, R1–9 (2006).
- 126 Price, E. W. & Henderson, W. J. The elemental content of lymphatic tissues of barefooted people in Ethiopia, with reference to endemic elephantiasis of the lower legs. *Trans R Soc Trop Med Hyg* **72**, 132–136 (1978).
- 127 Price, E. W. The pathology of non-flarial elephantiasis of the lower legs. *Trans R Soc Trop Med Hyg* **66**, 150–159 (1972).
- 128 Anderson, J. M., Rodriguez, A. & Chang, D. T. Foreign body reaction to biomaterials. *Semin Immunol* **20**, 86–100 (2008).
- 129 Lambert, R. A. Variations in the character of growth in tissue cultures. *Anat Rec* **6**, 91–108 (1912).
- 130 Serup, J., Sepehri, M. & Hutton Carlsen, K. Classification of tattoo complications in a hospital material of 493 adverse events. *Dermatology* **232**, 668–678 (2016).
- 131 Gupta, A. K. & Gupta, M. Synthesis and surface engineering of iron oxide nanoparticles for biomedical applications. *Biomaterials* **26**, 3995–4021 (2005).
- 132 Nel, A., Xia, T., Mädler, L. & Li, N. Toxic Potential of Materials at the Nanolevel. *Science* **311**, 622–627 (2006).
- 133 Winterbourn, C. C. Reconciling the chemistry and biology of reactive oxygen species. *Nat Chem Biol* **4**, 278–286 (2008).
- 134 Venkatesh, S., Tomer, K. B. & Sharp, J. S. Rapid identification of oxidation-induced conformational changes by kinetic analysis. *Rapid Commun Mass Spectrom* **21**, 3927–3936 (2007).
- 135 Lynn, A. K., Yannas, I. V. & Bonfield, W. Antigenicity and immunogenicity of collagen. *J Biomed Mater Res B Appl Biomater* **71**, 343–354 (2004).
- 136 The Commission of the European Communities. *Commission directive 2008/88/EC* 23 September 2008 (2008).
- 137 Schreiber, I., Laux, P. & Luch, A. From tattooing to laser removal —risks of permanent skin decoration (article in German). *UMID* **1**, 5–10 (2016).
-

- 154 Chung, K. T., Stevens, S. E. & Cerniglia, C. E. The reduction of azo dyes by the intestinal microflora. *Crit Rev Microbiol* **18**, 175–190 (1992).
- 155 Reisinger, K. *et al.* Systematic evaluation of non-animal test methods for skin sensitisation safety assessment. *Toxicol In Vitro* **29**, 259–270 (2015).
- 156 Slauch, J. M. How does the oxidative burst of macrophages kill bacteria? Still an open question. *Mol Microbiol* **80**, 580–583 (2011).

6. List of publications

6.1 Publications integrated in the cumulative dissertation

1. **Schreiver, I.**, Hutzler, C., Andree, S., Laux, P. & Luch, A. Identification and hazard prediction of tattoo pigments by means of pyrolysis—gas chromatography/mass spectrometry. *Arch Toxicol* **90**, 1639–1650 (2016).
2. **Schreiver, I.**, Hutzler, C., Laux, P., Berlien, H.–P. & Luch, A. Formation of highly toxic hydrogen cyanide upon ruby laser irradiation of the tattoo pigment phthalocyanine blue. *Sci Rep* **5**, 12915 (2015).
3. **Schreiver, I.**, Hesse, B., Seim, C., Castillo–Michel, H., Villanova, J., Laux, P., Dreijack, N., Penning, R., Tucoulou, R., Cotte, M. & Luch, A. Synchrotron-based v-XRF mapping and μ -FTIR microscopy enable to look into the fate and effects of tattoo pigments in human skin. *Sci Rep* **7**, 11395 (2017).

6.2 Other publications

Review

1. Laux, P., Traulau, T., Tentschert, T., Blume, A., Al Dahouk, S., Bäumler, W., Bernstein, E., Bocca, B., Alimonti, A., Colebrook, H., De Cuyper, C., Dähne, L., Hauri, U., Howard, P., Janssen, P., Katz, L., Klitzman, B., Kluger, N., Krutak, L., Platzek, T., Scott-Lang, V., Serup, J., Teubner, W., **Schreiver, I.**, Wilkniß, E. & Luch, A. A medical-toxicological view of tattooing. *The Lancet* **387**, 395–402 (2016).

Articles

1. De Cuyper, C., Lodewick, E., **Schreiver, I.**, Hesse, B., Seim, C., Castillo–Michel, H., Laux, P. & Luch, A. Are metals involved in tattoo-related hypersensitivity reactions? A case report. *Contact Dermatitis* doi:10.1111/cod.12862 [epub ahead of print].
2. **Schreiver, I.**, Laux, P. & Luch, A. From tattooing to laser removal – risks of permanent skin decoration (article in German). *UMID* **1**, 5–10 (2016).

Editorial

1. **Schreiver, I.** & Luch, A. At the dark end of the rainbow: Data gaps in tattoo toxicology. *Arch Toxicol* **90**, 1763–1765 (2016).

Talks

1. 3rd European Congress on Tattoo and Pigment Research: Adverse tattoo reactions – analysis of human biopsies. 30 March 2017, Regensburg, Germany.
2. 3rd European Congress on Tattoo and Pigment Research: Distribution of tattoo particles in skin and local lymph nodes - analysis of human *postmortem* specimens. 30 March 2017, Regensburg, Germany.
3. Fortbildungsveranstaltung für den Öffentlichen Gesundheitsdienst: Tätowiermittel: Wo stehen wir derzeit in Bewertung und Forschung? 06 April 2016, Berlin, Germany.
4. German Pharm-Tox Summit: Emerging toxins in medical laser-irradiation of organic pigments. 03 March 2016, Berlin, Germany.
5. 2nd European Congress on Tattoo and Pigment Research: Tattoo pigment decomposition: From predictive pyrolysis to laser irradiation. 30 April 2015, Bruges, Belgium.
6. 1st European Congress on Tattoo and Pigment Research: Identification of pigments and tattoo ink ingredients by pyrolysis-gas chromatography/ mass spectrometry. 14 September 2013, Copenhagen, Denmark.

Poster

1. **Schreiver, I.**, Hesse, B., Seim, C., Michel-Castillo, H., Villanova, J., Penning, R., Laux, P., Tucoulou, R., Cotte, M., Luch, A. Imaging of tattoo pigment particles and biomolecular changes in the surrounding skin tissue. 28th Annual Conference of the European Society of Biomaterials (ESB), 04 - 08 September 2017, Athen, Greece.
2. **Schreiver, I.**, Serup, J., Sepehri, M., Drejack, N., Dommershausen, N., Eschner, L.-M., Laux, P. & Luch, A. Identification of potent allergens in 104 skin biopsies from allergic tattoo reactions. Joint European Academy of Allergy and Clinical Immunology and European Society for Contact Dermatitis Skin Allergy Meeting, 27 - 29 April 2017, Zurich, Switzerland.
3. **Schreiver, I.**, Röder, N., Gebhardt, M., Hutzler, C., Berlien, H.-P., Laux, P. & Luch, A. Emerging toxins during medical laser irradiation of organic tattoo pigments. 45. Deutscher Lebensmittelchemikertag, 12 - 14 September 2016, Freising-Weißenstephan, Germany.
4. **Schreiver, I.**, Hutzler, C., Röder, N., Laux, P., Berlien, H.-P. & Luch, A. The cyanide blues: Laser irradiation of the tattoo pigment phthalocyanine blue can cause formation of highly toxic

hydrogen cyanide in skin. Society of Toxicology 55th Annual Meeting and ToxExpo, 13 - 17 March 2016, New Orleans, Louisiana, USA.

5. **Schreiver, I.**, Gebhardt, M., Hutzler, C., Laux, P., Berlien, H.-P. & Luch, A. Laser-induced decomposition of light-fast organic tattoo pigments. German Pharm-Tox Summit, 29 February - 03 March 2015, Kiel, Germany.
6. **Schreiver, I.**, Hutzler, C., Laux, P. & Luch, A. Identification of pigments and tattoo ink ingredients by pyrolysis-gas chromatography / mass spectrometry. 80. Jahrestagung der Deutschen Gesellschaft für Experimentelle und Klinische Pharmakologie und Toxikologie e. V., 31 March - 03 April 2014, Hannover, Germany.

Annex I

Supplementary Data

Identification and hazard prediction of tattoo pigments by means of pyrolysis— gas chromatography/mass spectrometry

Ines Schreiver, Christoph Hutzler, Sarah Andree, Peter Laux, Andreas Luch

This chapter was published online on 21. May 2016 in:

Archives of Toxicology 90(7):1639–1650 (2016).

DOI: 10.1007/s00204-016-1739-2

Link: <https://doi.org/10.1007/s00204-016-1739-2>

Annex II

Supplementary Data

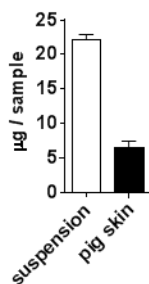
Tattoo laser removal releases carcinogens and sensitizers from organic pigments

Ines Schreiver, Nadine Röder, Maria Gebhardt, Christoph Hutzler, Hans-Peter Berlien, Peter
Laux, Andreas Luch

This chapter has not yet been submitted for publication.

Supplementary Figure 1: Cu content in P.B.15 aqueous suspensions and pig skin. Data is displayed as mean \pm SD of three replicates.

Copper content



Supplementary Table 1: Laser induced decomposition of P.Y.138 in pig skin, aqueous suspensions and as mixtures with TiO₂ using three different laser wavelengths. Data is displayed as mean \pm standard derivation (SD) of three replicates.

	*	unit	control	ruby (694 nm)	Nd:YAG (532 nm)	Nd:YAG (1064 nm)	Nd:YAG (532 nm) + TiO ₂
HCN	a	nmol	<LOQ		20.30 \pm 8.97		n.d.
	p	nmol	<LOQ	4.42 \pm 2.21	9.24 \pm 6.64	2.58 \pm 1.63	
1,2,3,4-tetrachlorobenzene	a	nmol	<LOQ		0.10 \pm 0.01		0.06 \pm 0.01
	p	nmol	<LOQ	0.01 \pm 0.01	0.10 \pm 0.05	<LOQ	
Pentachlorobenzene	a	nmol	<LOQ		0.14 \pm 0.01		0.09 \pm 0.01
	p	nmol	<LOQ	<LOQ	0.07 \pm 0.03	<LOQ	
Xylene	a	nmol	0.27 \pm 0.02		0.21 \pm 0.09		0.17 \pm 0.07
	p	nmol	0.13 \pm 0.02	0.17 \pm 0.07	0.18 \pm 0.06	0.14 \pm 0.05	
Hexachlorobenzene	a	pmol	24.00 \pm 3.00		47.00 \pm 6.00		32.00 \pm 5.00
	p	pmol	10.00 \pm 3.00	10.00 \pm 4.00	17.00 \pm 5.00	9.00 \pm 3.00	
Benzonitrile	a	pmol	0.20 \pm 0.20		4.00 \pm 1.00		<LOQ
	p	pmol	1.00 \pm 1.00	6.00 \pm 2.00	4.00 \pm 3.00	1.00 \pm 1.00	
Benzene	a	pmol	<LOQ		5.00 \pm 2.00		n.d.
	p	pmol	<LOQ	17.00 \pm 7.00	23.00 \pm 3.00	18.00 \pm 3.00	

*a= aqueous suspension; p= pig skin.

Abbreviation: LOQ= limit of quantification; n.d.= not determined.

Supplementary Table 2: Laser induced decomposition of P.R.170 in pig skin, aqueous suspensions and as mixtures with TiO₂ using three different laser wavelengths. Data is displayed as mean ± SD of three replicates.

	*	unit	control	ruby (694 nm)	Nd:YAG (532 nm)	Nd:YAG (1064 nm)	Nd:YAG (532 nm) + TiO ₂
HCN	a	nmol	<LOQ		13.53 ± 7.59		n.d.
	p	nmol	<LOQ	1.10 ± 0.71	9.85 ± 2.51	1.31 ± 1.09	
benzamide	a	nmol	<LOQ		0.92 ± 0.72		<LOQ
	p	nmol	<LOQ	0.99 ± 0.34	5.04 ± 0.54	<LOQ	
4-aminobenzamide	a	nmol	<LOQ		0.10 ± 0.06		<LOQ
	p	nmol	<LOQ	0.31 ± 0.06	1.88 ± 0.83	<LOQ	
benzotrile	a	nmol	0.01 ± 0.00		0.76 ± 0.31		0.70 ± 0.06
	p	nmol	<LOQ	0.16 ± 0.04	0.36 ± 0.04	0.01 ± 0.00	
aniline	a	nmol	<LOQ		0.49 ± 0.22		0.49 ± 0.05
	p	nmol	<LOQ	0.12 ± 0.03	0.43 ± 0.03	<LOQ	
benzene	a	nmol	<LOQ		1.53 ± 0.78		n.d.
	p	nmol	<LOQ	0.03 ± 0.02	0.28 ± 0.04	<LOQ	
1-cyanonaphthalene	a	pmol	<LOQ		37.00 ± 17.00		<LOQ
	p	pmol	0.20 ± 0.00	5.30 ± 1.60	13.30 ± 0.50	0.10 ± 0.10	
<i>o</i> -phenetidine	a	nmol	0.17 ± 0.07		2.06 ± 0.51		0.96 ± 0.07

*a= aqueous suspension; p= pig skin.

Abbreviation: LOQ= limit of quantification; n.d.= not determined.

Supplementary Table 3: Laser induced decomposition of P.R.254 in pig skin, aqueous suspensions and as mixtures with TiO₂ using three different laser wavelengths. Data is displayed as mean ± SD of three replicates.

	*	unit	control	ruby (694 nm)	Nd:YAG (532 nm)	Nd:YAG (1064 nm)	Nd:YAG (532 nm) + TiO ₂
4-chlorobenzotrile	a	nmol	0.02 ± 0.00		11.96 ± 0.79		29.93 ± 1.70
	p	nmol	0.02 ± 0.00	3.45 ± 0.54	8.90 ± 0.66	0.09 ± 0.01	
HCN	a	nmol	<LOQ		22.64 ± 5.69		n.d.
	p	nmol	0.07 ± 0.12	4.93 ± 0.76	20.46 ± 4.53	1.90 ± 1.27	
benzotrile	a	nmol	0.03 ± 0.01		0.55 ± 0.03		0.44 ± 0.03
	p	nmol	<LOQ	0.16 ± 0.03	0.34 ± 0.03	0.01 ± 0.00	
chlorobenzene	a	nmol	<LOQ		0.88 ± 0.37		0.37 ± 0.05
	p	nmol	<LOQ	0.51 ± 0.09	1.67 ± 0.14	0.01 ± 0.00	
3-chlorobenzamide	a	nmol	0.21 ± 0.01		0.39 ± 0.02		0.38 ± 0.01
	p	nmol	0.03 ± 0.00	0.11 ± 0.01	0.16 ± 0.06	0.06 ± 0.02	
3-chlorobenzotrile	a	nmol	0.01 ± 0.00		0.55 ± 0.04		0.36 ± 0.02
	p	nmol	<LOQ	0.06 ± 0.01	0.14 ± 0.01	<LOQ	
benzene	a	nmol	<LOQ		0.46 ± 0.07		n.d.
	p	nmol	<LOQ	0.02 ± 0.02	0.11 ± 0.01	0.01 ± 0.01	

*a= aqueous suspension; p= pig skin.

Abbreviation: LOQ= limit of quantification; n.d.= not determined.

Supplementary Table 4: Laser induced decomposition of P.O.13 in pig skin, aqueous suspensions and as mixtures with TiO₂ using three different laser wavelengths. Data is displayed as mean ± SD of three replicates.

	*	unit	control	ruby (694 nm)	Nd:YAG (532 nm)	Nd:YAG (1064 nm)	Nd:YAG (532 nm) + TiO ₂
HCN	a	nmol	<LOQ		36.59 ± 17.70		16.06 ± 7.36
	p	nmol	<LOQ	1.14 ± 0.21	15.51 ± 7.45	0.93 ± 1.79	
DCBD	a	nmol	<LOQ		0.67 ± 0.42		0.08 ± 0.01
	p	nmol	<LOQ	0.22 ± 0.10	0.82 ± 0.34	<LOQ	
benzointrile	a	nmol	<LOQ		0.48 ± 0.13		0.42 ± 0.08
	p	nmol	0.01 ± 0.00	0.17 ± 0.06	0.61 ± 0.20	0.01 ± 0.01	
aniline	a	nmol	<LOQ		1.68 ± 1.22		2.29 ± 0.40
	p	nmol	<LOQ	0.13 ± 0.04	0.55 ± 0.23	<LOQ	
phenylisocyanate	a	nmol	1.57 ± 0.90		71.35 ± 6.97		68.35 ± 7.42
	p	nmol	<LOQ	0.04 ± 0.06	0.68 ± 0.19	<LOQ	
benzene	a	nmol	<LOQ		1.24 ± 0.39		0.55 ± 0.15
	p	nmol	<LOQ	0.37 ± 0.04	1.05 ± 0.92	0.15 ± 0.04	
2-chloroaniline	a	nmol	<LOQ		0.04 ± 0.01		0.03 ± 0.00
	p	nmol	<LOQ	0.03 ± 0.01	0.10 ± 0.06	<LOQ	
2-aminobenzointrile	a	pmol	0.10 ± 0.00		34.50 ± 10.00		45.20 ± 13.00
	p	pmol	0.40 ± 0.40	6.20 ± 5.30	31.50 ± 11.50	0.40 ± 0.20	
biphenyl	a	pmol	0.40 ± 0.20		49.70 ± 9.30		38.40 ± 16.40
	p	pmol	0.40 ± 0.40	19.60 ± 7.80	82.50 ± 18.90	1.00 ± 1.00	
chlorobenzene	a	pmol	0.20 ± 0.10		18.00 ± 15.20		14.70 ± 3.70
	p	pmol	0.20 ± 0.20	14.50 ± 5.60	63.70 ± 20.60	0.40 ± 0.20	
PCB No.11	a	pmol	0.70 ± 0.10		28.20 ± 10.10		31.20 ± 5.40
	p	pmol	0.30 ± 0.30	24.10 ± 9.70	77.70 ± 18.80	1.50 ± 2.10	

*a= aqueous suspension; p= pig skin.

Abbreviation: LOQ= limit of quantification; n.d.= not determined.

Supplementary Table 5: Laser induced decomposition of P.B.15 in pig skin, aqueous suspensions and as mixtures with TiO₂ using three different laser wavelengths. Data is displayed as mean ± SD of three replicates.

	*	unit	control	ruby (694 nm)	Nd:YAG (532 nm)	Nd:YAG (1064 nm)	ruby (694 nm) + TiO ₂
HCN	a	nmol	<LOQ	169.75 ± 24.91	6.50 ± 1.52	18.50 ± 26.21	n.d.
	p	nmol	<LOQ	11.57 ± 4.13	2.31 ± 0.21	1.76 ± 0.37	
1,2-benzenedicarbonitrile	a	nmol	0.01 ± 0.01	4.87 ± 2.05	3.52 ± 2.09	0.03 ± 0.00	11.45 ± 0.88
	p	nmol	0.02 ± 0.01	4.15 ± 0.43	2.85 ± 1.26	1.24 ± 0.79	
benzointrile	a	nmol	0.01 ± 0.01	1.65 ± 0.71	0.56 ± 0.42	0.01 ± 0.00	3.29 ± 0.17
	p	nmol	0.02 ± 0.01	0.96 ± 0.14	0.43 ± 0.18	0.21 ± 0.12	
benzene	a	nmol	<LOQ	0.13 ± 0.01	0.01 ± 0.00	<LOQ	n.d.
	p	nmol	<LOQ	0.02 ± 0.00	0.01 ± 0.00	<LOQ	

*a= aqueous suspension; p= pig skin.

Abbreviation: LOQ= limit of quantification; n.d.= not determined.

Supplementary Table 6: Laser induced decomposition of P.V.19 in pig skin, aqueous suspensions and as mixtures with TiO₂ using three different laser wavelengths. Data is displayed as mean ± SD of three replicates.

	*	unit	control	ruby (694 nm)	Nd:YAG (532 nm)	Nd:YAG (1064 nm)	Nd:YAG (532 nm) + TiO ₂
HCN	a	nmol	<LOQ		27.16 ± 9.67		n.d.
	p	nmol	<LOQ	10.95 ± 2.60	11.16 ± 3.45	1.58 ± 1.21	
benzonitrile	a	nmol	<LOQ		0.40 ± 0.05		0.29 ± 0.04
	p	nmol	<LOQ	0.09 ± 0.01	0.12 ± 0.03	0.01 ± 0.00	
benzene	a	nmol	<LOQ		0.08 ± 0.02		n.d.
	p	nmol	<LOQ	0.07 ± 0.03	0.16 ± 0.04	0.01 ± 0.00	
biphenyl	a		<LOQ		<LOQ		<LOQ
	p	pmol	12.00 ± 2.00	11.00 ± 3.00	10.00 ± 1.00	7.00 ± 1.00	
1-cyanonaphthalene	a	pmol	0.50 ± 0.10		17.00 ± 0.40		16.00 ± 2.00
	p	pmol	<LOQ	6.00 ± 1.00	4.00 ± 1.00	1.00 ± 0.00	
aniline	a		<LOQ		<LOQ		<LOQ
	p	pmol	1.00 ± 1.00	8.00 ± 3.00	12.00 ± 2.00	1.00 ± 1.00	

*a= aqueous suspension; p= pig skin.

Abbreviation: LOQ= limit of quantification; n.d.= not determined.

Supplementary Table 7: Decomposition products of P.B.15 increase in a fluence-dependent manner with ruby laser irradiation of *postmortem* tattooed pig skin. Non-tattooed pig skin served as a control. Data is displayed as mean ± SD of three replicates.

	unit	control	ruby 3 J (694 nm)	ruby 4 J (694 nm)	ruby 5 J (694 nm)
HCN	nmol	<LOQ	4.08 ± 0.72	5.51 ± 0.82	7.25 ± 0.64
1,2-benzenedicarbonitrile	nmol	<LOQ	10.38 ± 8.96	12.99 ± 3.69	19.11 ± 3.30
benzonitrile	nmol	<LOQ	0.66 ± 0.07	1.03 ± 0.10	1.00 ± 0.13
benzene	pmol	<LOQ	1.70 ± 0.40	6.20 ± 4.50	2.20 ± 0.20

Annex III

Supplementary Data

Synchrotron-based v-XRF mapping and μ -FTIR microscopy enable to look into the fate and effects of tattoo pigments in human skin

Ines Schreiver*, Bernhard Hesse*, Christian Seim, Hiram Castillo-Michel, Julie Villanova, Peter Laux, Nadine Drejack, Randolph Penning, Remi Tucoulou, Marine Cotte, Andreas Luch

*These authors contributed equally to this work

This chapter was published online on 12. September 2017 in:

Scientific Reports 7, 11395 (2017).

DOI: 10.1038/s41598-017-11721-z

Link: <https://doi.org/10.1038/s41598-017-11721-z>

Supplementary Table S1. Organic pigments in human skin and lymph node samples from additional donors analyzed by LDI-ToF-MS.

Donor	Tissue	Location	Color	Pigment
Donor 2	Skin	left	black, red	red 170 (C.I.12475) , blue 15 (C.I.74160)
	LN	left		red 170 (C.I.12475) , blue 15 (C.I.74160)
Donor 5	Skin		black, red	green 7 (C.I.74260) , red 112 (C.I.12370), blue 15 (C.I.74160)
	LN	hilus	red	
	LN		black	blue 15 (C.I.74160)
Donor 6	Skin	left	green	blue 15 (C.I.74160), green 7 (C.I.74260)
	LN	left	green	green 7 (C.I.74260)
Control 2	Skin	proximal	-	-
	LN	axillary	-	-

Supplementary Table S2. Element concentrations per tissue weight (ppm) in human skin and lymph node samples from additional donors analyzed by ICP-MS.

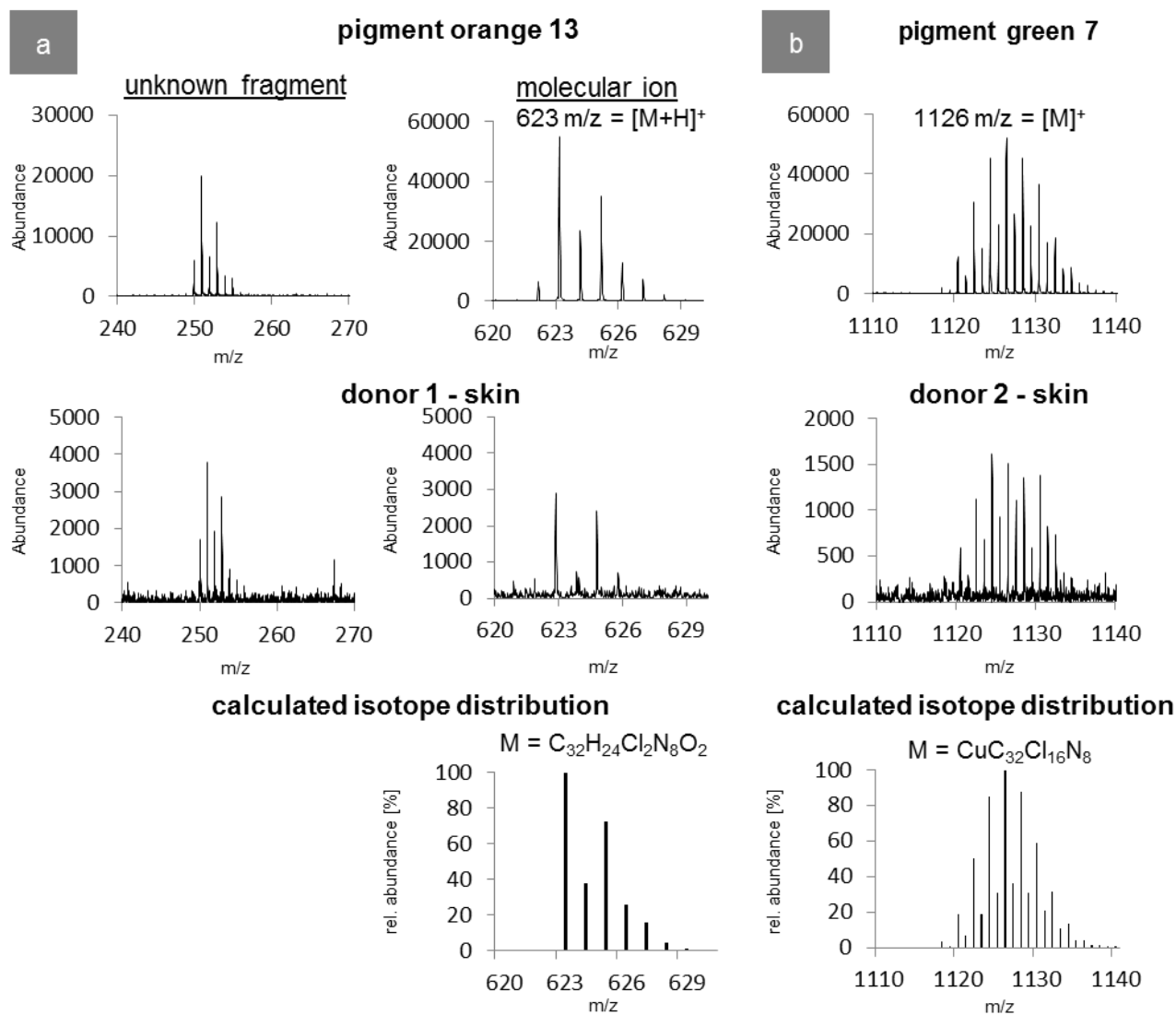
Donor	Tissue	Location	Color	Al	Cr	Fe	Ni	Cu	Cd	other [#]
2	Skin	left	black, red	2.49	9.34	95.4	0.33	6.54	< LOQ	
	LN	left		11.3	6.77	238	3.50	67.0	< LOQ	
5	Skin		black, red	0.62	0.36	138	< LOQ	1.72	< LOQ	Rb
	LN	hilus	red	1.12	0.36	758	0.90	2.33	< LOQ	Ti
	LN		black	0.88	< LOQ	193	< LOQ	4.33	0.69	Ti, Br, Rb, Hg
6	Skin	left	green	4.40	0.67	76.9	0.54	19.2	< LOQ	
	LN	left	green	6.19	9.29	735	5.09	84.2	0.83	
7	LN			3.66	0.65	123	0.23	3.52	< LOQ	Ti, Mn, Zn, Rb, Ba
	Skin		red, green, black	< LOQ	< LOQ	4.85	< LOQ	2.29	< LOQ	Ti
8	Skin	right leg	black	7.56	< LOQ	19.2	< LOQ	2.96	< LOQ	Zn
	LN	right inguinal	black	2.15	< LOQ	21.5	< LOQ	0.63	< LOQ	Zn
	Skin	left leg	black	< LOQ	< LOQ	8.73	< LOQ	< LOQ	< LOQ	Zn
	LN	left inguinal	black	0.16	0.06	4.65	< LOQ	0.10	< LOQ	Mn
	Skin	right arm	green	4.11	< LOQ	14.8	< LOQ	11.5	< LOQ	Ti, Ba
	Skin	right arm	red	38.5	< LOQ	10.1	< LOQ	< LOQ	< LOQ	Zn
	LN	right axillary	black	1.30	0.23	14.9	< LOQ	2.50	< LOQ	Ti
	Skin	left arm	red, yellow, orange	5.17	< LOQ	5.66	< LOQ	< LOQ	< LOQ	Zn
	LN	left axillary		1.75	< LOQ	14.5	< LOQ	0.51	0.15	Mn, Zn, Rb
	LN	trachea		20.8	< LOQ	63.0	< LOQ	1.28	< LOQ	Mn, Ba
9	Skin	left arm	green	6.49	< LOQ	3.29	< LOQ	2.03	< LOQ	Ti, Zr
	LN	left axillary	black	7.29	< LOQ	26.2	< LOQ	0.80	< LOQ	Ti, Mn, Zn, Rb, Ba
10	Skin	leg	red	8.24	< LOQ	4.26	< LOQ	< LOQ	< LOQ	I
	LN	inguinal		3.51	< LOQ	12.9	< LOQ	0.83	< LOQ	Ti, Mn, Zn, I
	LN	trachea		4.10	< LOQ	76.7	< LOQ	1.41	< LOQ	Mn, Zn, I
	LN	hilus		0.85	< LOQ	103	< LOQ	3.14	< LOQ	Mn, Zn, Rb, I, Ba, Pb
	LN	para aortic		4.20	< LOQ	37.7	< LOQ	1.23	< LOQ	Zn, I
11	Skin	right arm	green, blue	< LOQ	< LOQ	2.36	< LOQ	< LOQ	< LOQ	Zn, Ba
	LN	right axillary	black	7.55	4.68	89.4	< LOQ	5.33	36.4	Ti, Ba, Hg
12	Skin	left	red, green, black	< LOQ	< LOQ	49.5	< LOQ	1.66	< LOQ	
	Skin	left	red, green,	< LOQ	< LOQ	29.9	< LOQ	1.42	< LOQ	Zn

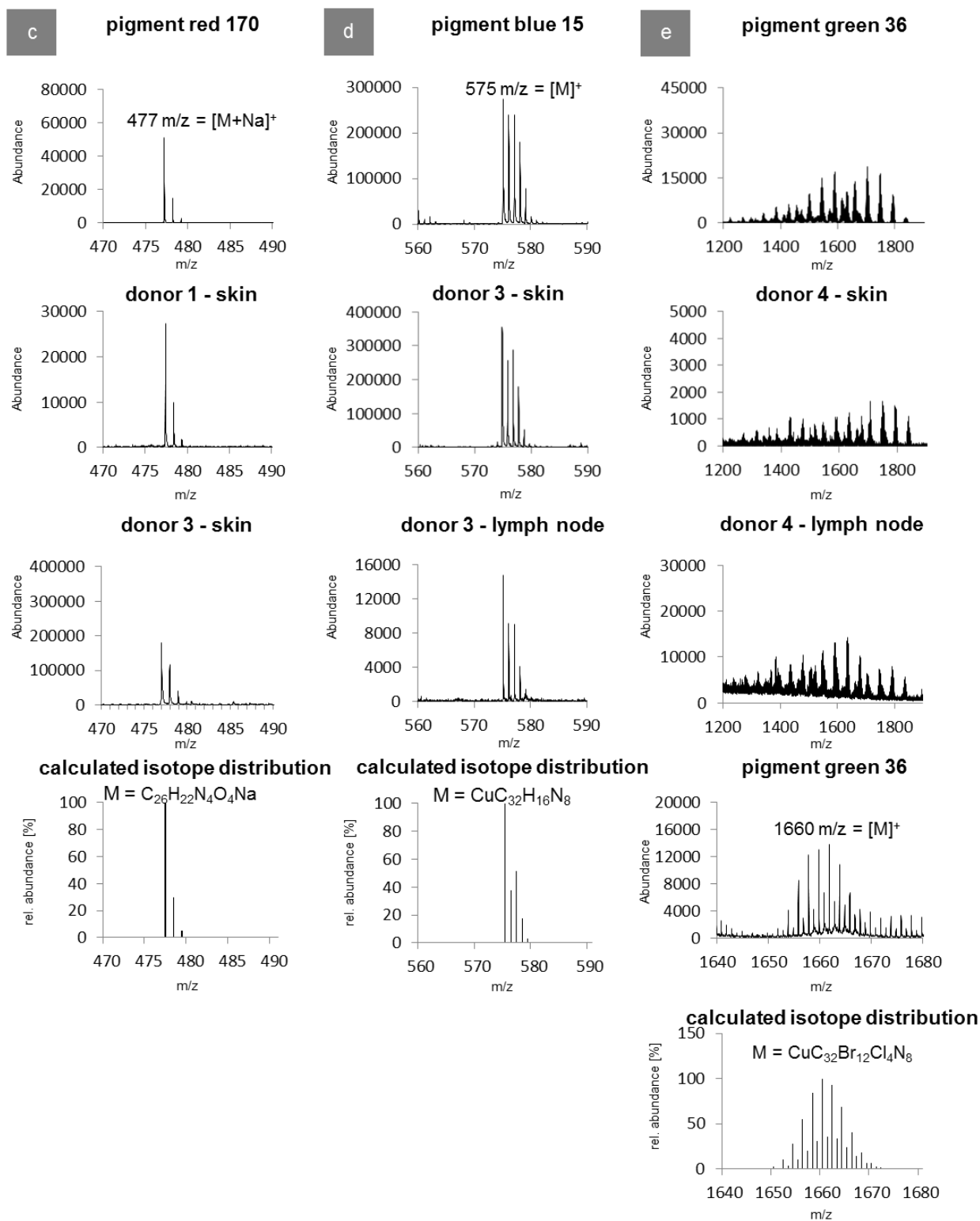
	LN	left	black	< LOQ	< LOQ	129	< LOQ	0.86	< LOQ	Zn
13	Skin	right leg	black, blue	38.6	1.76	94.6	0.73	28.1	< LOQ	Ti, Mn, Zn, Ba
	LN	right inguinal		5.80	0.71	200	0.37	12.5	< LOQ	Ti, Mn, Zn, Cd, Sn
	Skin	left arm	black, red	3.35	0.96	207	< LOQ	2.99	< LOQ	Mn, Zn
	LN	left axillary		1.43	1.56	279	0.72	3.75	< LOQ	Ti, Mn, Zn, Cd, Ba
	LN	coeliac		< LOQ	< LOQ	155	< LOQ	3.26	< LOQ	Ti, Mn, Zn, Cd
	LN	left para aortic		< LOQ	< LOQ	567	< LOQ	4.67	< LOQ	Ti, Mn, Zn, Cd
			Average	8.23	1.42	80.1	0.61	4.06	18.3	

Abbreviations: LN = lymph node; LOQ = limit of quantification. Elements measured (non-specified oxidation states): aluminum (Al), barium (Ba), bromine (Br), cadmium (Cd), chromium (Cr), copper (Cu), iodine (I), iron (Fe), lead (Pb), manganese (Mn), mercury (Hg), nickel (Ni), rubidium (Rb), selenium (Se), titanium (Ti), tungsten (W), and zinc (Zn).

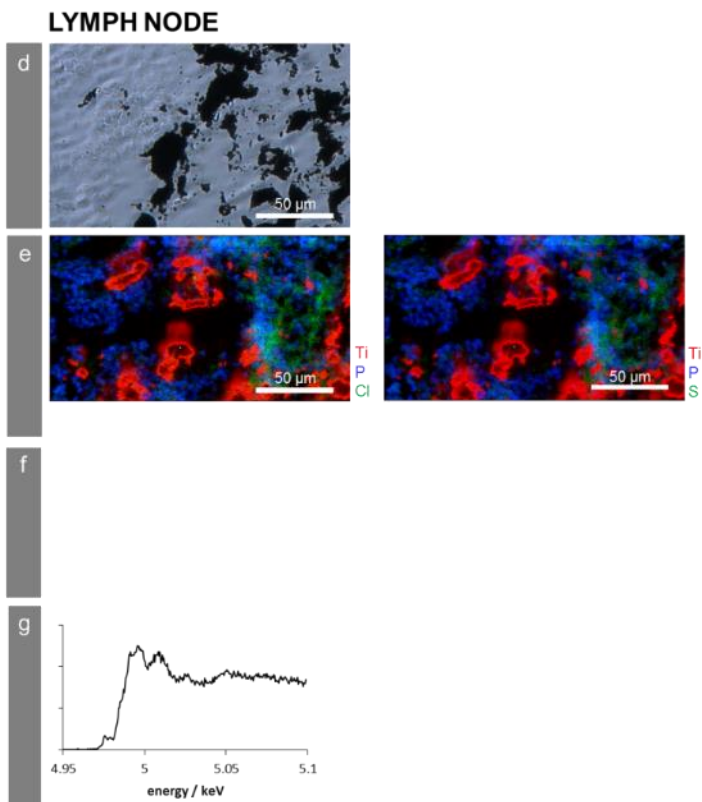
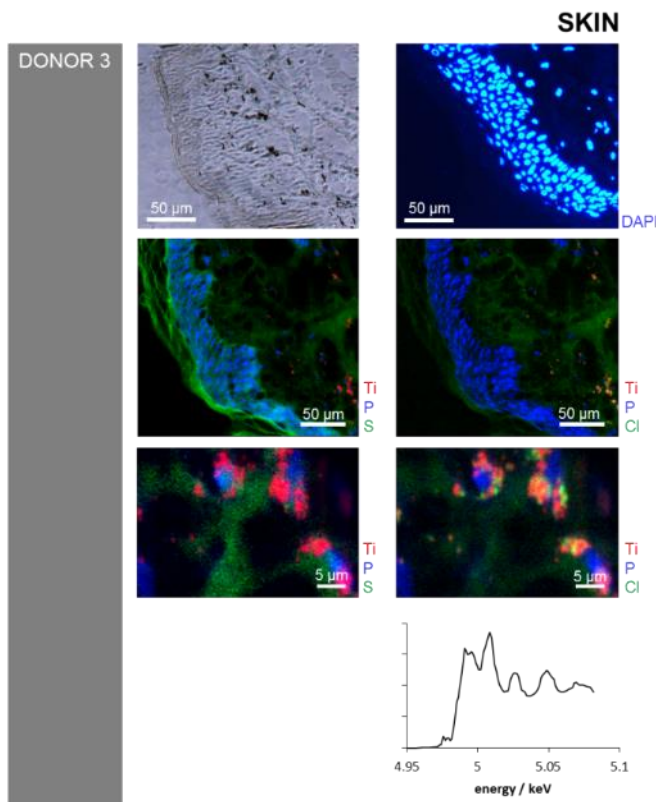
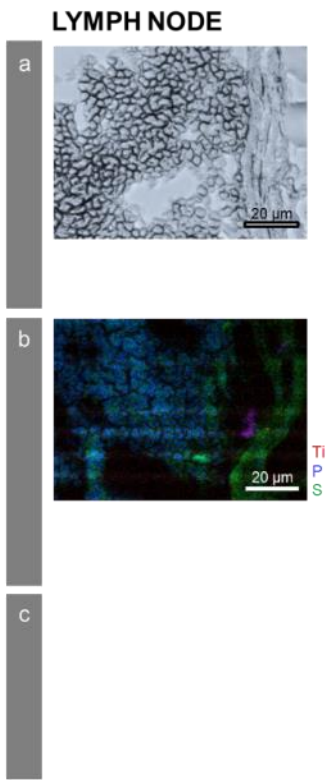
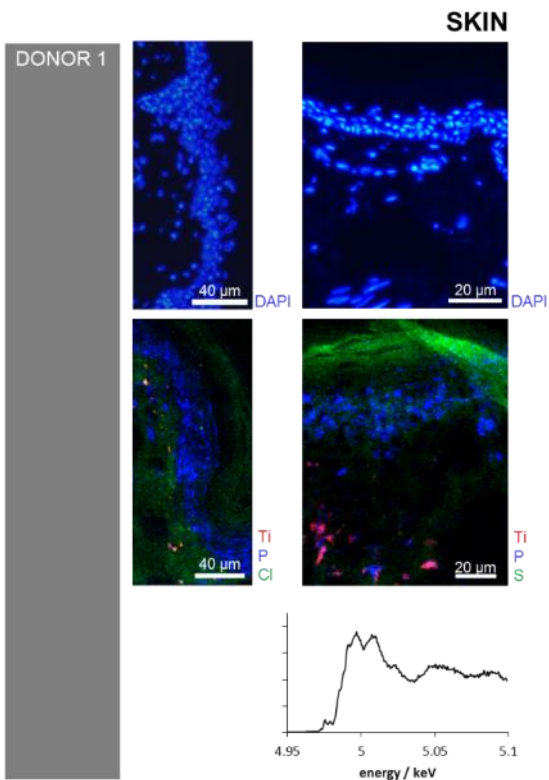
[#]Non-quantitatively identified elements.

Supplementary Figure S1. Identification of the used organic colorants by LDI-ToF-MS spectrometry. **a-e)** Mass spectra obtained from lysed skin or lymph node specimens are displayed next to spectra from pure reference pigments and their calculated isotope distribution (cf. Fig. 2).

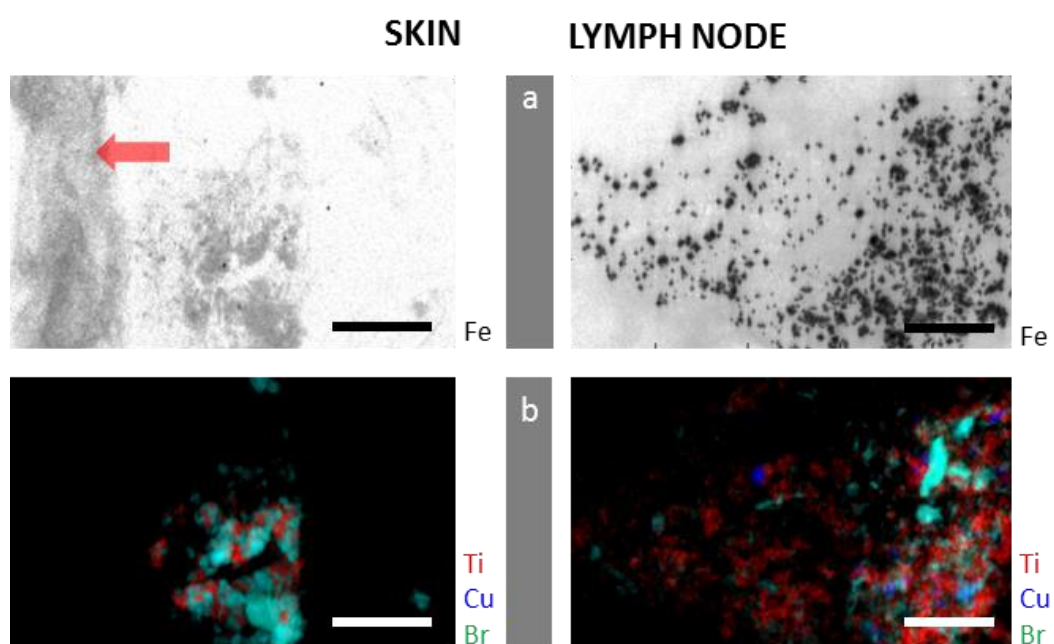




Supplementary Figure S2. μ -XRF mapping links elements to tattoo particles. Sections of skin and lymph node tissues of donors 1 and 3 were analyzed by μ -XRF at ID21, ESRF. **a, d)** Optical microscopy images of adjacent sections. **b, e)** μ -XRF maps of tissue sections. In skin, the epidermal layer is visualized by the elements P (cell nuclei, blue) and the *stratum corneum* by S (protein, green). The lymph node capsule of donor 1 shows also high S content (green layer, right). Cl (green) is increased in the proximity of Ti (red) in the dermal layer of donor 1 (left image) and 3 (right image). High Ti in the lymph node of donor 3 led to detector saturation. **f)** High resolution map of skin in e). Cl and Ti are in close proximity to P-rich cell nuclei. **c, g)** Ti K-edge μ -XANES spectra of skin (donors 1 and 3) and lymph node (donor 3) show mostly rutile TiO_2 (cf. Fig. 3). No μ -XANES was obtained for the lymph node of donor 1 since Ti concentrations were too low.



Supplementary Figure S3. Pigment particles in skin and lymph node tissues of donor 4 explored by using *v*-XRF at ID16B, ESRF. **a)** Fe elemental map (log scale). No Fe particles were detected in the skin of donor 4. Dissolved and protein-bound Fe concentrations are higher in cells when compared to the extracellular matrix, allowing the localization of the epidermal layer (arrow) and cells in the proximity of particles in the dermis. **b)** Ti, Cu, Br mapping in the exact same area as displayed in **a)**. Br (green) systematically overlays with Cu (blue) to give a turquoise shade in the images, thereby supporting the findings of the brominated copper phthalocyanine pigment green 36. Fe particles in the lymph node **a)** are co-localized to TiO₂ (red) and pigment green 36 (Cu, Br) particles. Scale bars = 5 μm.



Supplementary Figure S4. Changes of the biological structures in the cellular proximity of tattoo pigments. Skin section of donor 2 analyzed by means of synchrotron μ -FTIR at ID21, ESRF. **a)** Maps in second derivative obtained at 2920 cm^{-1} ($-\text{CH}_2$ asymmetric vibration in overlay with the FTIR visible light microscopic picture). Single points for PCA analysis in c) were picked from the indicated areas. **b)** Mean spectra from each region marked in a) in second derivative. Lipid and β -sheet related vibrations were increased in DP compared to D (see text). Similar to donor 4 (cf. Fig. 4), amide I band again separates DP (protein low) from D (protein high). In contrast to the skin of donor 4, the mean spectrum of the D area shows an amide I maximum at 1655 cm^{-1} comparable to the SC area. **c)** PCA score plot of PC-1 vs. PC-2. **d)** Loading plots of PC-1 and PC-2. Abbreviations: SC = *stratum corneum* and epidermis, D = dermis, DP = dermis with particles.

